UNIVERSIDADE DE LISBOA

FACULDADE DE CIÊNCIAS

DEPARTAMENTO DE BIOLOGIA VEGETAL

Assessment of *Erwinia amylovora* diversity and virulence: from strain molecular typing to immuno-flow cytometry of infected *Pyrus* fruits

Telma Patrícia Natário Guedes da Costa

Mestrado em Microbiologia Aplicada

Dissertação orientada por:
Ana Maria Gomes Moura Pires de Andrade Tenreiro
Maria Leonor Pato da Cruz

2020

This Dissertation was performed at Lab Bugworkers | M&B-BioISI, Biosystems & Integrative Sciences Institute, under the direct supervision of Principal Investigator Ana Maria Gomes Moura Pires de Andrade Tenreiro, and at Instituto Nacional de Investigação Agrária e Veterinária (INIAV), under the direct supervision of head of Phytobacteriology Lab Investigator Maria Leonor Pato da Cruz.

Professor Ana Maria Gomes Moura Pires de Andrade Tenreiro was the internal supervisor designated in the scope of the Master in Applied Microbiology of the Faculty of Sciences of the University of Lisbon

To my mother, who will always be with me

Acknowledgments

Thank you all for helping me ask the right questions.

First and foremost, I would like to thank Professor Ana Tenreiro, my supervisor at Bugworkers Laboratory | M&B – BioISI | Teclabs, for believing in me and making this experience possible. I am extremely grateful for the patience, empathy, knowledge, guidance and help through this year.

I am thankful to Dr. Leonor Cruz, my co-supervisor, head of the Phytobacteriology Labaratory (INIAV), for the opportunity to develop my work in another Lab, for the compassion and especially for her availability despite the busy schedule.

I want to thank Joana Cruz for her availability and motivation. Your understanding, patience and advises were fundamental to keep me going during this process. I wish you and your little baby girl much love and happiness.

To Professor Rogério Tenreiro, for the scientific input, different perspectives, availability and for helping me ~~significantly~~ considerably whenever I needed it.

To the entire team of the Phytobacteriology Lab (INIAV), Isaura, Lidia, Camila and Lina, and to Stefan: thank you for the warmly welcome, kind words, amazing food and particularly for making me feel part of the team.

To Filipa Silva, the CLO of Bugworkers Lab, not only for their professionalism and organization making the work easier, but also for the kind words and encouragement thorough the year.

To Professor Lélia Chambel, for the availability to help me when I needed it.

To Professor Lisete Fernandes, for the quick-witted comebacks which made me laugh many times and for the new gastronomic experiences, including the worst chocolate I have ever tasted in my life.

To the amazing people I met through this year.

Vanessa, thank you for the company, for putting up with all the "cascas", the ice creams and for always having a positive and understanding attitude.

Francisca, you are one of the sweetest and caring people I ever met. I am very grateful for all your maternal concern, attention and for taking care of all of us.

Maria, I want to thank you and your *actimel bubble*. Meeting you reminded me of the importance of seeing beyond the obvious. Your dark sense of humour, willingness to talk about numerous topics, your diverse knowledge and suggestions will be missed.

Sara, what I value the most about you is your unshakeable faith particularly in today's world. Despite our little disagreements, I want to thank you for your company, honesty and for being my dance buddy. Finally, I wanted to tell you that I fondly remember the sunset we saw together, particularly in the last few months.

To my father for giving me the opportunity and privilege to continue to learn.

To my long-time friend Diogo. There will never be enough words to describe the privilege, joy and blessing of walking beside you on this long-lasting journey. I've seen you grow, evolve and become what you are today, and I couldn't be prouder. Although you are the most gifted person I know, your ability to see a world full of infinite possibilities and the way you integrate everything never ceases to amaze me: for you the sky is not the limit only the beginning. Your humbleness and pure heart are extremely rare nowadays and are my favourite things about you. Never forget that you contain *multitudes* and you can be whatever you want. I will always be here every step of the way.

To my dear aunt, the strongest and kindest person I know and probably will ever meet. For you, I'll be eternally grateful. Thank you for always taking care of me and for accepting me as I am. Hopefully, one day I can be half of what you are and give you everything you deserve.

Abstract

Erwinia amylovora is a phytopathogenic bacterium and the causative agent of fire blight, a destructive disease that affects several members of the Rosaceae family. Pear and apple are particularly susceptible hosts of this bacterium, representing a major concern due to their socioeconomic value. The devasting nature of this disease has led to the classification of *E. amylovora* as a quarantine organism.

Although this bacterium is widespread throughout the world, its emergence in Portugal happened relatively recently when compared to other European countries. Since its first report in 2006 in Fundão region, the number of outbreaks has increased, leading Portugal to loss its statute of Integral Protected Area within the European Union, in 2019.

Factors such as the absence of a cure, false-negatives results and the need to understand unknown aspects about the life cycle of *E. amylovora*, lead to the interest in conducting characterization studies and developing alternative laboratory methods as an attempt to make preventive measures more effective.

A set of Portuguese and foreign *E. amylovora* isolates was characterized by molecular, pathogenicity and virulence studies. Molecular characterization used CRISPR-PCR and genomic fingerprintings, whereas pathogenicity and virulence were assessed by biological tests on immature fruitlets of *Pyrus communis* cv. "Rocha". In addition, a flow cytometry and an immuno-flow cytometry protocols were developed using pure and mixed bacterial cultures for the detection and cell viability assessment of *E. amylovora in planta*.

A total of two CRISPR genotypes, A and D, was observed revealing a low genetic diversity among the *E. amylovora* isolates tested. Genomic fingerprinting reinforced the high homogeneity of this species. In contrast, a wide diversity in virulence was displayed. Flow cytometry and immuno-flow cytometry protocols were validated, revealing the capacity to detect and distinguish different viability states of *E. amylovora* artificially inoculated in pear fruitlets.

In the future, the established protocols may help shed some light over previously undiscovered aspects of *E. amylovora* life cycle.

Key-words: fire blight, CRISPR-PCR, genomic profiles, virulence assays, flow cytometry, immuno-flow cytometry.

Resumo

Erwinia amylovora é uma bactéria fitopatogénica Gram-negativa responsável pela doença comummente denominada por fogo bacteriano. A designação desta doença está relacionada com o desenvolvimento de necroses de cor castanha a preta no hospedeiro durante o processo de infeção, cuja aparência se assemelha a uma queima. Outros sintomas típicos incluem o surgimento de lesões, exsudado bacteriano, cancros nos ramos e tronco, bem como de mumificação dos frutos.

Originalmente nativa da América do Norte, *E. amylovora* foi detetada pela primeira vez no final do século 18. Atualmente, por consequência da ação humana, a doença está amplamente disseminada pelo globo. Devido à elevada capacidade de propagação e ao efeito potencialmente devastador para os seus hospedeiros, *E. amylovora* foi classificada como um organismo de quarentena. Os hospedeiros desta bactéria pertencem à família Rosaceae, na qual estão inseridos géneros de plantas agrícolas importantes a nível socioeconómico, tais como *Malus* e *Pyrus*, Em Portugal, a presença de fogo bacteriano foi reportada pela primeira vez em 2006 no Fundão, data relativamente tardia aquando comparação do surgimento da doença nos restantes países da Europa. Desde então, a ocorrência de situações reportadas em várias regiões do país tem vindo a aumentar, fazendo com que o país perdesse o estatuto de Zona Integral Protegida na União Europeia em 2019.

Alguns fatores que tornam esta doença preocupante são a inexistência de cura e o desconhecimento de alguns aspetos do ciclo de vida de *E. amylovora*. Assim, são aplicadas estratégias de controlo que incluem abordagens complementares, tais como medidas preventivas, profiláticas e de erradicação. Outro fator preocupante é a ocorrência de resultados falso-negativos aquando aplicação dos métodos utilizados para o diagnóstico desta bactéria. Estes podem dever-se a uma concentração bacteriana insuficiente ou à indução do estado viável não cultivável em *E. amylovora*, o qual pode estar associado, por exemplo, a condições climáticas adversas e à utilização de compostos cúpricos como medida profilática. Um diagnóstico errado pode conduzir à falta de aplicação de medidas de controlo e, consequentemente, acarretar consequências catastróficas.

O presente trabalho teve dois objetivos. O primeiro consistiu na caracterização de um conjunto de isolados de *Erwinia amylovora* da Coleção Portuguesa de Bactérias Fitopatogénicas através de estudos genómicos, de patogenicidade e de virulência. O segundo compreendeu o desenvolvimento e validação de protocolos de citometria de fluxo e de imuno-citometria de fluxo, para servirem como método de diagnóstico alternativo na deteção e avaliação da viabilidade celular de populações de *E. amylovora* presentes em material infectado.

Um total de 48 isolados de *E. amylovora* foram caracterizados genotipicamente a partir da utilização CRISPR-PCR e de *fingerprintings* genómicos, nomeadamente rep- e MSP-PCR. A patogenicidade e virulência destes isolados foram caracterizadas a partir da utilização de frutos imaturos de *Pyrus communis* cv. “Rocha”, os quais foram artificialmente infetados por um subconjunto dos 48 isolados. Após 6 e 12 dias de infeção, foram registados o tamanho da lesão necrótica e a presença/ausência de exsudado bacteriano, respetivamente.

Para avaliação da viabilidade celular de *E. amylovora* por citometria de fluxo, foram testados três fluoróforos diferentes, nomeadamente Syto9, PI e $DIBAC_4(3)$. Estes foram aplicados em células tratadas por calor e em células não tratadas. A aplicação do protocolo de imuno-citometria de fluxo compreendeu o uso do anticorpo monoclonal Ea7A IVIA e de um anticorpo secundário conjugado com FITC. Ambos os protocolos foram testados primeiramente numa cultura pura de *E. amylovora* e posteriormente em

culturas mistas. Por fim, os dois protocolos foram implementados na deteção e avaliação de viabilidade celular de *E. amylovora* presente em peras imaturas cv. "Rocha" infetadas artificialmente.

A técnica CRISPR-PCR permitiu diferenciar os isolados em dois grupos consoante a presença ou ausência da duplicação do *spacer* 1029, nomeadamente em genótipo A e genótipo D, respetivamente. A análise dos isolados Portugueses permitiu verificar que ambos os genótipos estão presentes no país desde 2010 e que existe uma ligeira predominância do genótipo D, o qual foi registado em 17 dos 31 isolados. Em termos de distribuição, observou-se que o genótipo A e D estão presentes nas regiões Centro e Oeste de Portugal, contudo no Alentejo só se verificou a presença do genótipo A. Aquando análise conjunta de resultados de estudos prévios com os que foram obtidos no presente trabalho, verificou-se que o genótipo A é o genótipo mais distribuído na Europa, possivelmente devido à introdução mais precoce do mesmo no continente Europeu.

As técnicas de *fingerprinting* genómico utilizadas, nomeadamente rep- e MSP-PCR, permitiram a obtenção de perfis genómicos complexos, mas muito homogéneos entre si. Desta forma, os mesmos mostraram não ter poder discriminatório suficiente para a diferenciação dos isolados de *E. amylovora* a nível infraespecífico. Estes resultados são o reflexo de uma variedade genómica limitada característica desta espécie bacteriana, que culmina numa elevada homogeneidade entre os isolados.

Os ensaios em peras imaturas revelaram que, à excepção dos isolados CPBF 142 e CPBF 544, 43 isolados são patogénicos, uma vez que possuíram a capacidade de induzir o aparecimento de pelo menos um dos sintomas típicos do fogo bacteriano no hospedeiro. Todos os isolados patogénicos provocaram lesão necrótica de cor castanha a preta, contudo apenas 28 isolados produziram exsudado bacteriano. A análise destes sintomas permitiu observar variabilidade na virulência, de tal modo que os isolados foram distribuídos em três categorias de virulência, nomeadamente baixa, média e alta. Estas categorias tiveram em consideração o tamanho da lesão necrótica provocada no hospedeiro. Adicionalmente, observou-se a existência de correlação entre a categoria de virulência baixa e o genótipo D.

Os dados de CRISPR-PCR, patogenicidade, virulência e presença/ausência de exsudado bacteriano foram agrupados para uma análise polifásica de modo a adquirir mais informação acerca dos isolados. Os dados obtidos por *fingerprinting* genómico não foram considerados, uma vez que não tiveram o poder discriminatório adequado. A utilização desta abordagem permitiu separar os isolados em 11 grupos de estirpes distintos. Contudo, não foi possível fazer uma associação entre estes grupos e o hospedeiro original a partir do qual cada isolado foi obtido.

Relativamente à citometria de fluxo, a utilização dos fluoróforos permitiu a distinção de diferentes populações relativamente à integridade celular e potencial membranar presentes na cultura pura de *E. amylovora*. De facto, esta técnica apresentou uma boa correlação entre a viabilidade esperada e a observada, o que significa que os três fluoróforos se mostraram apropriados para serem utilizados em estudos de viabilidade celular nesta bactéria. O estudo de viabilidade celular de *E.* amylovora em cultura mista ficou comprometido devido ao comportamento semelhante que as bactérias podem ter face aos fluoróforos.

O protocolo de imuno-citometria de fluxo permitiu detetar *E. amylovora* em cultura pura a partir da observação de uma elevada intensidade de fluorescência verde. Em cultura mista, para além da intensidade de fluorescência verde característica de *E. amylovora*, verificou-se também a ocorrência de uma emissão de fluorescência verde menor que se supõe que resulte de ligações inespecíficas entre o anticorpo secundário e outros alvos que não o anticorpo monoclonal Ea7A IVIA. Contudo, uma vez que

a intensidade da emissão de fluorescência verde adicional foi reduzida, a mesma não impossibilitou a detecção de *E. amylovora*.

O presente estudo reforçou a paradoxalidade existente entre a homogeneidade genómica e a heterogeneidade de virulência em *Erwinia amylovora*. Adicionalmente, o mesmo mostrou que o desenvolvimento de um potencial método alternativo para a detecção desta bactéria, nomeadamente com recurso a citometria de fluxo e técnicas afins, pode significar uma melhoria considerável no processo de diagnóstico, bem como abrir portas para descobertas futuras relacionadas com o ciclo de vida de *E. amylovora*.

Palavras-chave: fogo bacteriano, CRISPR-PCR, perfis genómicos, ensaios de virulência, citometria de fluxo, imuno-citometria de fluxo.

Table of Contents

List of Tables

List of Figures

List of Abbreviations

ams	Amylovora Synthesis
CRISPR-PCR	Clustered Regularly Interspaced Short Palindromic Repeats-PCR
CPBF	Coleção Portuguesa de Bactérias Fitopatogénicas
CRR	CRISPR Repeat Region
DAI	Days After Inoculation
$DIBAC_4(3)$	Bis-(1,3-Dibutylbarbituric Acid) Trimethine Oxonol
dsp	Disease Specific
EPS	Exopolysaccharide
ERIC-PCR	Enterobacterial Repetitive Intergenic Consensus-PCR
FCM	Flow Cytometry
FITC	Fluorescein Isothiocyanate
hrp	Hypersensitive Reaction and Pathogenicity
IIF	Indirect Immunofluorescence
IFCM	Immuno-Flow Cytometry
mAB	Monoclonal Antibody
MSP-PCR	Microsatellite-Primed-PCR
PI	Propidium Iodide
rep-PCR	Repetitive Element Sequence-Based-PCR
REP-PCR	Repetitive Extragenic Palindromic-PCR
T3SS	Type III Secretion System
UPGMA	Unweighted Pair Group Method With Arithmetic Mean
VBNC	Viable But Nonculturable

1. Introduction

1.1. Fire blight disease

1.1.1. Distribution, host range and importance

Since its discovery in the late 18th century, fire blight, a bacterial plant disease caused by the phytopathogenic agent *Erwinia amylovora*, has been disseminated worldwide (fig. 1.1). From its native ecosystem in the Hudson Valley of New York State, United States of America (USA), where originally evolved together with native plants (e.g. *Crataegus*, *Malus*, and *Sorbus*), *E. amylovora* displayed the ability to colonize susceptible *Pyrus* sp. and *Malus* sp. introduced by the European colonisers (van der Zwet & Keil, 1979).

Until the 19th century fire blight was restricted to North America countries. However, in the beginning of the 1900's the disease was reported outside in New Zealand (1919) (Campbell, 1920; Cockayne, 1921 cit. in Bonn & van der Zwet, 2000; Cruz, 2010), related to the introduction of infected foreign plant material. In the 1950's fire blight was described for the first time in Europe and Africa. The United Kingdom (UK) was the first country to suffer from the disease in 1958, possibly due to the introduction of contaminated fruits (Crosse *et al.*, 1958 cit. in Bonn & van der Zwet, 2000). Since 1966 several European countries noticed the presence of fire blight (Netherlands Plant Protection Service, 1966; EPPO Global Database, 2019). Contrary to previous reports in which the contamination source was thought to be infected plant material, migratory birds may have contributed to the spread of the disease from the UK to western and northern European coastlines (Meijneke, 1972 cit. in Bonn & van der Zwet, 2000). Fire blight occurrence in some South-Eastern European and Middle East countries might resulted from the introduction of the disease in Egypt, reported near Alexandria, in 1964 (El-Helaly *et al.*, 1964 cit. in Bonn & van der Zwet, 2000).

Fire blight was reported for the first time in Portugal in 2006 affecting apple trees in Fundão, but the identification was only confirmed in 2010 with several outbreaks affecting pear orchards in the Alcobaça region, triggered by disease-favourable weather conditions (Cruz, 2010). Presently, Portugal lost already the statute of Integral Protected Area within the European Union (EU), due to the establishment of *E. amylovora* in the main production areas of pear and apple of the country (Regulamento de Execução (UE) 2019/2072).

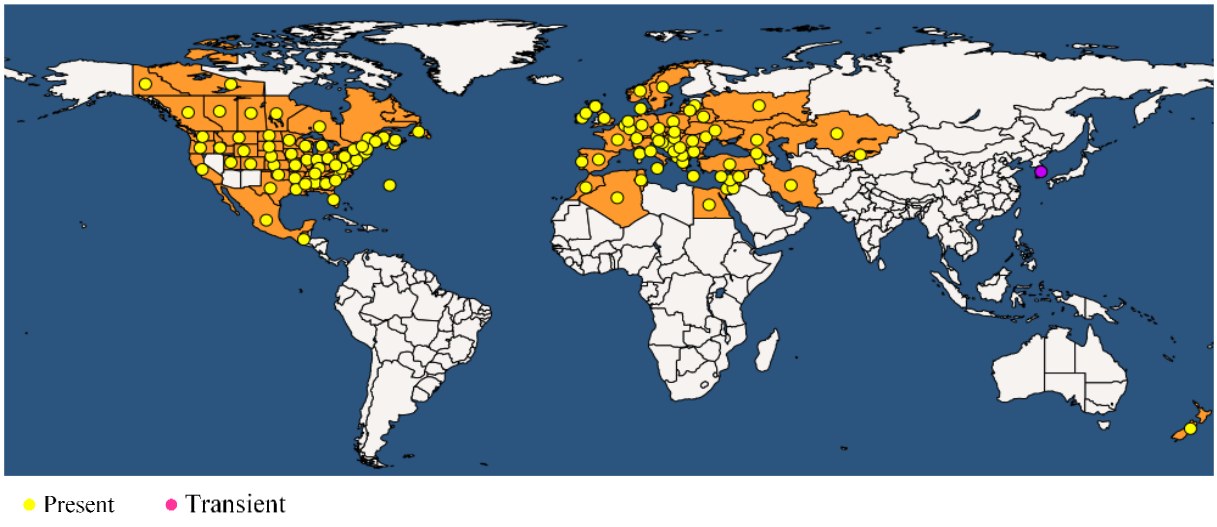

Figure 1.1 - Fire blight distribution (figure source: EPPO Global Database, 2019).

A pivotal factor for the successful dissemination of *E. amylovora*, is that most strains do not evidence a host specificity. *Erwinia amylovora* is able to infect a significant diversity of fruit and ornamental trees within the Rosaceae family, particularly of the Amygdaloideae subfamily. This subfamily comprises members with a relevant economic impact, particularly apples (*Malus* sp.) and pears (*Pyrus* sp.), which are highly susceptible to this harmful bacterium (Bonn & van der Zwet, 2000; Potter *et al.*, 2007; Hummer & Janick, 2009; Cruz, 2010; Xiang *et al.*, 2017). This causes an impact on fruit yield and, consequently, economic losses. According to Food and Agriculture Organization of the United Nations (FAOSTAT, 2019) and Instituto Nacional de Estatística (INE, 2019), several members of the Rosaceae family (apples, pears, quinces, peaches and nectarines) are included in the most produced fruits globally, corresponding to 15% of this production (fig. 1.2 A). In Portugal, the total fruit production between 2013 and 2017 reached approximately two million tons (FAOSTAT, 2019) meaning that in 2017 the production of apples, pears, quinces, peaches and nectarines reached nearly 580 thousand tons, representing closely to 29% of the total of fruit production (fig. 1.2 B). These data highlight the socio-economic role of pome fruit in Portugal and, consequently, offer an awareness to the potential consequences that may arise from fire blight disease.

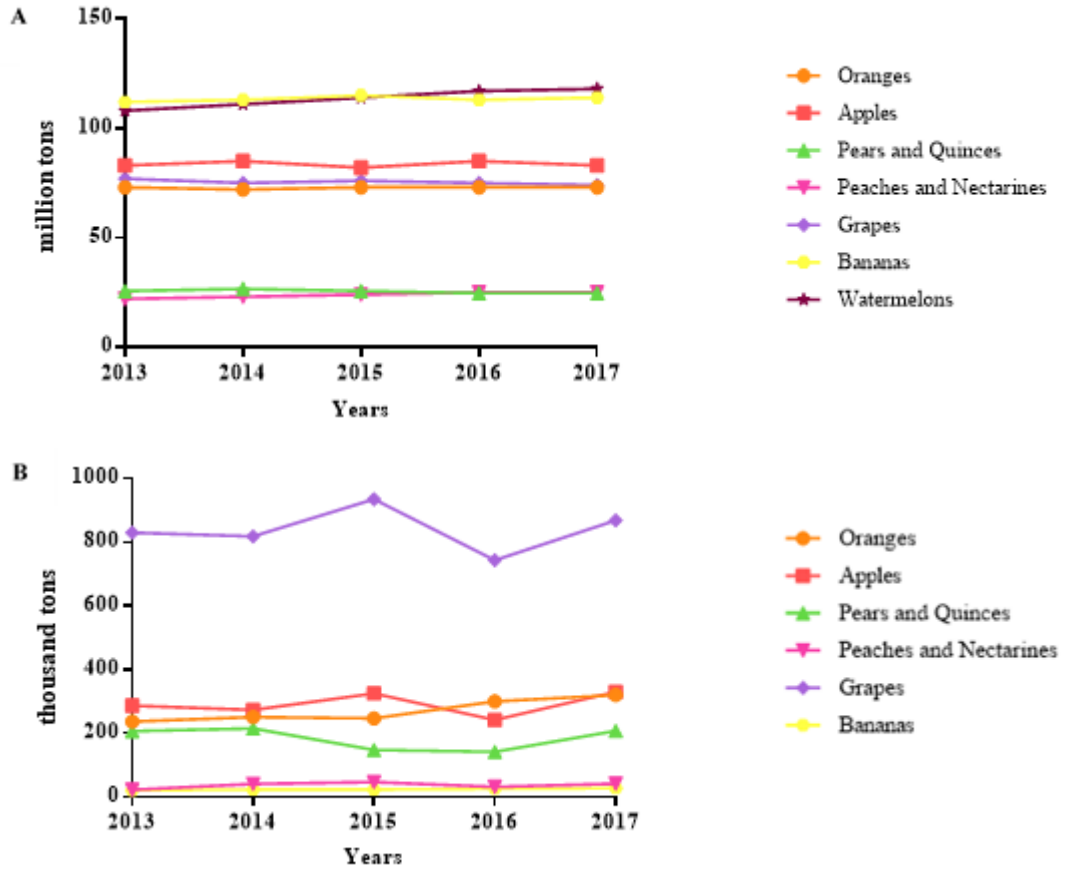

Figure 1.2 - Worldwide (A) and Portugal (B) fruit production between 2013 and 2017 (based on FAOSTAT, 2019; INE, 2019).

1.1.2. Epidemiological cycle and disease symptoms

The epidemiological cycle of *E. amylovora* is very complex and is not entirely known yet. To understand fire blight disease is crucial to analyse the different stages of disease evolution according to host phenological stages. Fire blight cycle is considered to start in the spring when the temperature and humidity conditions are favourable not only to blossoming but also to bacterial activity (Thomson, 2000; Luz, 2013). Active endophytic bacteria or bacterial ooze settled in overwintering cankers formed on

diseased branches from previous outbreaks (holdover cankers) preferentially spread to stigmas. A floral epiphytic phase occurs, in which there is bacterial multiplication on stigmas, forming the primary source of infection (Thomson, 2000; Cruz, 2010).

The primary infection also occurs when active bacterial cells invade specific organs by penetrating flowers, natural openings such as stomata or wounds. Flower stigmas are the preferential infection sites for *E. amylovora* multiplication and establishment. Under the right conditions this multiplication quickly develops, causing a downward movement into the pedicels, shoots, leaves and branches. As a result of the colonization some symptoms become visible. Firstly, blossom blight starts to be evident, giving flowers a water-soaked aspect evolving to a dark brown to black colour, resembling a flower burnt by fire. As infection progresses, twigs get darken, wilted and display a discrete shepherd's crook. Leaves may also develop necrotic areas and immature fruits mummify. Fire blight designation derives from the distinctive burned-like appearance by the plant presents in the symptomatic period of the disease (fig. 1.3 A and B) (Thomson, 2000; Cruz, 2010).

Secondary infections may occur throughout spring, summer and autumn due to formation of ooze droplets, consisting of intensive exudation of bacterial cells in an exopolysaccharide matrix produced on infected shoots, leaves, branches and fruits when relative humidity is high (fig. 1.3 C) (Thomson, 2000; Cruz, 2010).

At the end of the growing season (summer-autumn), when environmental conditions start to be less favourable, *E. amylovora* multiplication reduces or ceases. The colonized tissues in branches or trunks necrotize evidencing the presence of cankers, in which *E. amylovora* can overwinter until favourable conditions re-appear to begin a new cycle (Thomson, 2000).

Depending on the severity of the infection and host susceptibility, some trees and orchards may be completely destroyed in only a single season (fig. 1.3 D) (Bonn & van der Zwet, 2000).

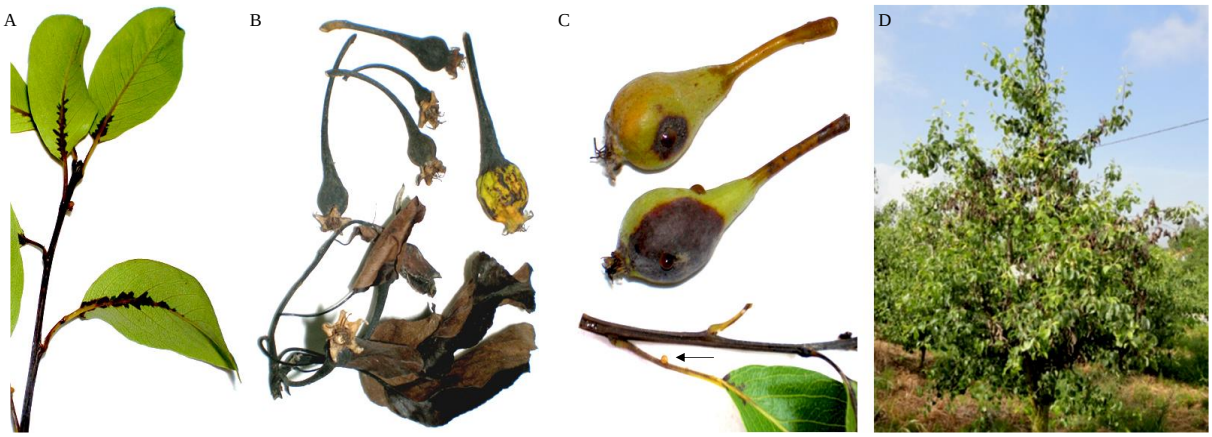

Figure 1.3 - Fire blight symptoms. A. Early necrosis on tree leaves. B. Necrosis on pear tree leaves and mummified immature pears. C. Bacterial exudate droplet on immature pears and branch (black arrow). D. General view of a tree with the disease. The images were provided by INIAV's Phytobacteriology Laboratory.

During the whole epidemiological cycle (fig. 1.4), short distance transmission of primary and secondary inoculum through the action of multiple agents, such as rain, pollinating insects, wind and birds must be taken into consideration, because these can greatly determine the extent of a fire blight outbreak in one region (van der Zwet, 1994; Thomson, 2000). The use of infected plant material is the major risk factor for long distance dissemination and for the introduction of the disease in new areas/countries (EPPO, 2004; Cruz, 2010).

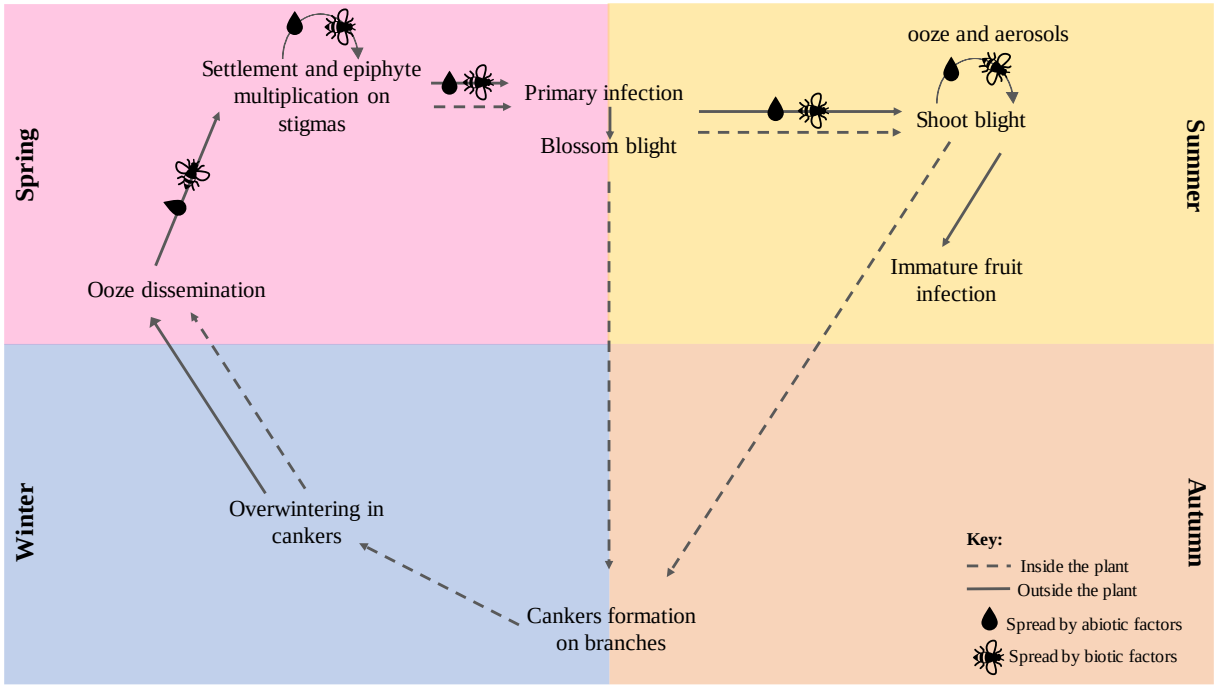

Figure 1.4 - Epidemiological cycle of *Erwinia amylovora* (adapted from Thomson, 2000).

1.1.3. Management and control

Due to the complex nature of fire blight, outbreak management and control have demonstrated to be quite challenging despite intensive efforts. The best alternative to a successful disease management comprise a combination of multiple and complementary approaches, such as predictive, prophylactic and eradication measures. Additionally, the temporal moment in which these tools are implemented has a direct influence in their efficacy against the disease. (Vanneste & Yu, 1996; Psallidas & Tsiantos, 2000; Billing, 2000; Prates & Cavaco, 2013).

Predictive computational models, such as MaryblytTM and Courgarblight software, were developed based on climatic factors (i.e. temperature, humidity, precipitation, frost, hail and strong wind) and on fruit phenological data. These algorithms are useful tools in the management and surveillance of diseases because they allow forecasting for blossom blight occurrence. The ability to predict the infection process in its early stages is crucial because some chemical control measures can only be used at specific times. Most of these predictive models were created with data collected in USA and UK, causing a loss of their predictive power when tested in other regions with different climatic conditions (Billing, 2000; Dewdney *et al.*, 2007*;* Gusberti, 2015).

Prophylactic measures aim to prevent or reduce the frequency of infections. Within these measures there is a panoply of methods that can be implemented, such as chemical, biological and cultural management (Steiner, 2000; Cruz, 2010).

Chemical measures may include bacteriostatic compounds (e.g. copper products) and disease resistance inducers. The use should occur during vegetative rest and before the flowering phase to increase the effectiveness of treatments and to prevent phytotoxicity. For instance, copper compounds are highly toxic to leaves and fruits. Consequently, chemical measures should not be applied on a regular basis (Psallidas & Tsiantos, 2000; Cruz, 2010).

The use of antibiotics as chemicals is quite controversial. In USA, the application of antimicrobial substances such as streptomycin is permitted. However, the continuous and abusive use in agriculture led to serious consequences, namely the emergence of antibiotic resistance (Psallidas & Tsiantos, 2000; McManus *et al.*, 2002; Prates & Cavaco, 2013). In EU, except in very particular conditions, the use of

antibiotics in agriculture is strictly prohibited by the phytosanitary legislation (EPPO, 2004; McManus *et al.*, 2002; Directive nº 2009/128/EC).

Due to the negative impact of these measures, biological control became an alternative against *E. amylovora*. Biocontrol requires the colonization of antagonistic agents, commonly bacteria, on the stigmatic surface disabling E. *amylovora* establishment. The interaction between epiphytic *E. amylovora* and antagonistic agents promotes the reduction of *E. amylovora* inoculum, preventing floral infection. Some of the antagonists of *E. amylovora* include *Pseudomonas fluorescens* and *Pantoea agglomerans* (Vanneste & Yu, 1996; Johnson & Stockwell, 2000; Psallidas & Tsiantos, 2000).

Cultural measures towards fire blight control include early pruning of symptomatic branches, wounds and tool disinfection, and to avoid planting susceptible cultivars (Cruz, 2010).

After disease establishment, eradication of the most affected trees is compulsory. In addition, sanitary pruning should be carried out on less affected trees, allowing the orchard a longer producing life (Cruz, 2010; Prates & Cavaco, 2013).

1.2. *Erwinia amylovora*

According to the Bergey's Manual of Systematic Bacteriology (Hauben & Swings, 2005) the causative agent of fire blight disease is the Gram-negative bacterium *Erwinia amylovora* which is included in the following taxonomic groups:

Phylum Proteobacteria
Class Gammaproteobacteria
Order Enterobacteriales
Family Enterobacteriaceae
Genus *Erwinia*

The genus *Erwinia* comprises pathogenic and epiphytic bacterial species associated to a wide variety of botanic families, including the Rosaceae members. Some non-pathogenetic species include *E. billingiae* and *E. tasmaniensis*, whereas pathogenic species include *E. amylovora*, *E. pyrifoliae*, *E. piriflorinigrans* and *E.* uzenensis (Palacio-Bielsa *et al.*, 2011). *Erwinia amylovora* is the type strain of this genus (Hauben & Swings, 2005). In 1882, Burril associated for the first time a plant disease – fire blight – to the bacterial pathogen – *Erwinia amylovora* (Winslow *et al.*, 1920 cit. in Hauben & Swings, 2005). Due to its destructive ability, *E. amylovora* is considered a quarantine organism by the European Union (Directive 2000/63/EU Annex II/A2).

1.2.1. Detection and identification

Fire blight diagnosis requires an integrated approach encompassing distinct identification methods, that may include isolation, biochemical, serological, molecular and pathogenicity tests. This polyphasic approach is advised, since fire blight symptoms may be confused with symptoms caused by other phytopathogenic organisms or by physiological reactions of host plants (López *et al.*, 2003, cit. in López *et al.*, 2009; Cruz & Sousa, 2013).

Different culture media can be used for isolation of *E. amylovora*, namely King B, levan and Crystal violet-Cycloheximide-Tergitol (CCT). Depending on the medium, bacterial colonies will display a distinct morphology (EPPO, 2013). There are several molecular tests available for the rapid detection of *E. amylovora* based on conventional PCR (Obradovic *et al.*, 2007) and real-time PCR (Pirc *et al.*, 2009). Concerning genomic diversity studies, several approaches can be used, such as, amplified fragment length polymorphism (AFLP) (Rico *et al.*, 2004), ribotyping (Donat *et al.*, 2007), pulse-field gel electrophoresis (PFGE) (Jock *et al.*, 2002), repetitive element sequence-based polymerase chain

reaction (rep-PCR) (Donat *et al.*, 2007) and clustered regularly interspaced short palindromic repeats (CRISPR)-PCR (Rezzonico *et al.*, 2011). Serological tests, such as the enzyme-linked immunosorbent assay (ELISA), can also be applied (Gorris *et al.*, 1996a).

All these approaches have limitations that should be carefully considered as they may compromise the diagnostic outcome. Serological techniques, as ELISA, when associated with a polyclonal antibody may present low sensitivity (10^5 to 10^6 cfu mL^{-1}) and especially low specificity (Gorris *et al.*, 1996b; EPPO, 2010). Molecular tests, such as PCR, are highly sensitive and specific, however its success depends on the DNA extraction, which can be compromised by the reagents used or by the presence of inhibitors in the sample (Fang & Ramasamy, 2015). Plating is one of the most used diagnostic methods. One of its limitations is the need for the pathogen to be in a culturable and viable state, otherwise false-negative results or underestimation of cell population may occur (Davey, 2011). Moreover, this procedure is time consuming as the results can take several days due to incubation period associated with cell growth (Kennedy & Wilkinson, 2017). The development of alternative diagnostic methods capable of overcoming these constraints would be extremely useful, such as flow cytometry (FCM) (Harkins & Harrigan, 2004; Kennedy & Wilkinson, 2017).

1.2.2. Genomic fingerprinting

Genomic fingerprinting is a molecular approach used for microbial genotypic characterization, frequently used due to its reproducibility and highly discriminatory power (Rademaker & De Bruijn, 1997).

One of the methods of genomic fingerprinting used is the rep-PCR, which uses DNA primers that target repetitive and conserved DNA sequences scattered throughout the genome in numerous copies of most Gram-negative and some Gram-positive bacteria (Rademaker & De Bruijn, 1997; Hiett & Seal, 2009). Three families of repetitive sequences are differentially located in intergenic positions, namely, the repetitive extragenic palindromic (REP) sequence with 35-40 bp, the enterobacterial repetitive intergenic consensus (ERIC) sequence with 124-127 bp and the BOX element with 154 bp. Besides genotypic characterization, rep-PCR is also used to study microbial evolution since it has a high taxonomic resolution, enabling differentiation of bacterial isolates (Martin *et al.*, 1992, Rademaker & De Bruijn, 1997; Hiett & Seal, 2009).

Alternatively, microsatellite-primed PCR (MSP-PCR) is a genomic fingerprinting technique that uses DNA primers complementary to microsatellite sequences located in several copies across the genome (Ryskov *et al.*, 1988; Martin *et al.*, 1998).

Both rep-PCR and MSP-PCR were already used for genomic characterization of *E. amylovora* isolates at intraspecific level (McManus & Jones, 1995; Donat *et al.*, 2007; Radunović *et al.*, 2017).

1.2.3. Clustered regularly interspaced short palindromic repeats (CRISPR) PCR

Clustered regularly interspaced short palindromic repeats (CRISPR) and CRISPR-associated proteins (Cas) are a bacterial adaptive immune system strategy against foreign genomic material that may compromise bacterial survival. CRISPR consist of a series of direct repeats (DR) with 23 to 55 bp separated by variable spacer sequences of 21 to 48 bp (fig. 1.5), whose variability results mostly from integrated bacteriophages or plasmid sequences (Horvath & Barrangou, 2010). Integration of exogenous material occurs with the addition of new spacers at the 5' end next to the leader sequence, which means these spacers possess newer information when compared with spacers positioned at the 3' end. This temporal discrepancy between ancient and recent spacers as well as internal spacer loss and duplication has proved to be quite useful in evolutionary and epidemiological studies of bacterial species, since it enables strain identification (Cui *et al.*, 2008; Fricke *et al.*, 2011; Rezzonico *et al.*, 2011;

McGhee & Sundin, 2012; Shariat & Dudley, 2014). Due to a low genetic diversity, CRISPR-PCR has been a valuable technique to assess *E. amylovora* strains variability (Jock *et al.*, 2002; Jock & Geider, 2004; Barionovi, 2006; Rico *et al.*, 2008).

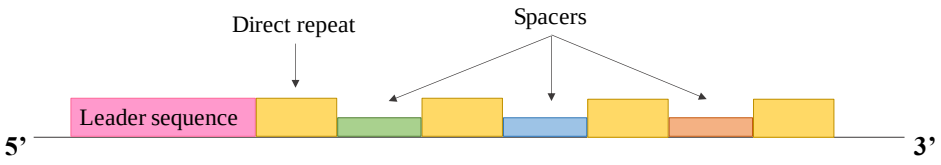

Figure 1.5 - CRISPR loci structure (adapted from Rezzonico *et al.*, 2014).

The genome of *E. amylovora* revealed the presence of three CRISPR repeat regions (CRR), namely CRR1, CCR2 and CCR4. While CRR1 and CRR2 are active and evolving regions, CRR4 conserved sequence indicated that this region is evolutionarily inactive (Rezzonico *et al.*, 2011). Sequence analysis of *E. amylovora* European isolates also demonstrated the presence of two main ancestral genotypes regarding CRR1, namely genotypes A and D, with differences on the presence or absence of a duplication in the spacer 1029, respectively (fig. 1.6) (Rezzonico *et al.*, 2011; Rezzonico, 2014).

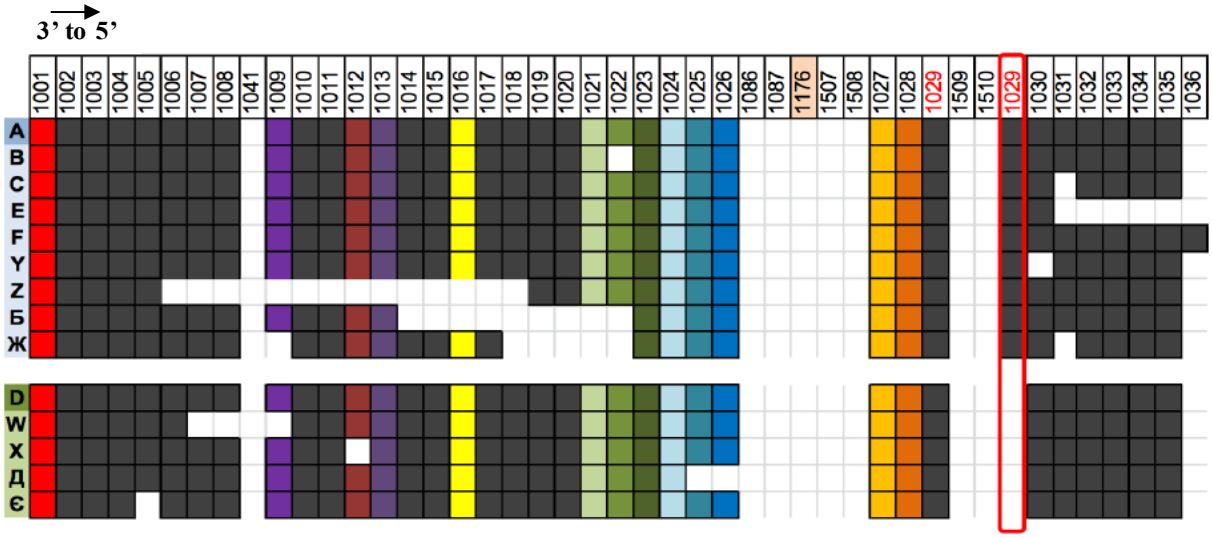

Figure 1.6 – CRISPR repeat region 1 genotypes of *Erwinia amylovora* strains. Each box represents a CRISPR spacer numbered at the top. Blocks with the same colour vertically represent identical spacers, except for white blocks, which indicate absence of that spacer in each genotype. The red border highlights the difference between genotypes A and D and their derivatives (adapted from Rezzonico, 2014).

1.2.4. Pathogenicity and virulence

Several virulence factors are involved in the successful infection by *E. amylovora*, including the production of siderophores, exopolysaccharide (EPS), biofilm formation, motility, and type III secretion system (T3SS) (Vrancken, 2013; Piqué *et al.*, 2015).

Exopolysaccharides constitute the matrix containing the viable bacteria present in exudates. These are considered the major virulence factor of *E. amylovora*, since they have a key role on the ability to produce biofilms, on overcoming the plant defence system by obstructing the vascular system, and protecting bacteria during dry environmental conditions (Vanneste, 1995; Vrancken *et al.*, 2013). Amylovoran is the main component of the polysaccharide matrix. It is a heteropolymer composed of a pentasaccharide repeating unit containing four galactose residues and one glucuronic acid molecule. Amylovoran biosynthetic genes are encoded by the *ams* operon, consisting of 12 *ams*-genes (*ams*A to *ams*L) (Bugert & Geider, 1995; Geider, 2000). *Erwinia amylovora* strains lacking amylovoran

production show no pathogenic effect and are incapable of colonizing the plant (Bellemann & Geider, 1992). *Erwinia amylovora* also produces levan, which is a homopolymer of fructose residues that is produced following the breakdown of sucrose (Geider, 2000). Although its function is not entirely understood, it is thought that its absence may lead to a slow development of symptoms (Geier & Geider, 1993).

Another major virulence factor is the highly conserved type III secretion system (T3SS). T3SS is a pilus-like structure whose function is to export and deliver effector proteins into the cytosol of the host plant cells. In *E. amylovora*, T3SS is mostly formed by hypersensitive reaction conserved (Hrc) and hypersensitive reaction and pathogenicity (Hrp) proteins, which are encoded in a pathogenicity island (Oh & Beer, 2005; Vrancken *et al.*, 2013). There are several proteins secreted by this T3SS, however the disease specific effector (DspA/E) seems to play an important function in bacterial pathogenicity, repressing host immune responses and enhancing bacterial growth post-infection (Vrancken *et al.*, 2013; Piqué, 2015).

1.3. Flow cytometry

Flow cytometry is a methodology that allows the analysis of morphological and physiological properties of isolated cells in motion in a flow. This methodology was developed in the 1960s and was primarily applied to mammalian cells for medical purposes. Nowadays, technical improvements have allowed its application to several areas, including veterinary, medical and microbiology (Wang *et al.*, 2010b; Kennedy & Wilkinson, 2017). FCM has numerous advantages, including multiparametric analysis, rapid data acquisition, cell sorting, single cell analysis, high sensitivity and accuracy, and statistical data acquisition. These have been useful in monitoring and characterization of cell physiology in real time, cell cycle assays, and quantification of intracellular compounds (Alvarez-Barrientos *et al.*, 2000).

The association of FCM with fluorescent-labelled antibodies, immuno-flow cytometry (IFCM), is an alternative method for the detection of pathogenic microorganisms. Immunofluorescence (IF) techniques take advantage of the synergistic effect from antibodies and fluorophores conjunction. The fluorescent-labelled antibody can turn visible the binding between the antibody and its antigen. Two IF procedures can be performed, namely direct or indirect IF, whose difference resides on whether the fluorophore is bound to a primary or secondary antibody, respectively. In indirect IF, the labelled secondary antibody will be bound to an unlabelled primary antibody that has been previously attached to its antigen (Aoki *et al.*, 2010; Babu *et al.*, 2013; Odell & Cook, 2013). IFCM is particularly helpful for the detection of pathogens in samples with low bacterial concentration, with non-viable cells or cells in a viable but non-culturable state (VBNC) (Wang *et al.*, 2010b; Kennedy & Wilkinson, 2017), since these situations can lead to false-negative diagnostic results. Copper compounds usage can promote the VBNC state in *E. amylovora* (Ordax *et al.*, 2009; Santander & Biosca, 2017), and may help the bacteria to go unnoticed in routine diagnostic tests. Consequently, management and control measures may not be properly employed, contributing to the survival and proliferation of bacterial inoculum (Ordax *et al.*, 2009; Kennedy & Wilkinson, 2017).

Flow cytometry has demonstrated to be a convenient and effective method for pathogens detection and viability assessment in environmental, clinical and food samples. In fact, FCM properly discriminated viable, non-viable and persistent VBNC cells (Bergervoet *et al.*, 2007). In aquatic microbiology, FCM expanded the understanding of physiological changes in microbial communities. Moreover, IFCM facilitated a fast and accurate detection of pathogens, like *Cryptosporidium parvum* and *Legionella pneumophila*, in low concentrations in water samples (Wang *et al.*, 2010b).

Concerning *E. amylovora*, FCM has already been used for cell enumeration, assessment of cell viability under stress conditions and expression of intracellular compounds (Bogs & Geider, 2000;

Ordax *et al.*, 2006; Cabrefiga & Montesinos, 2017; Santander & Biosca, 2017). Nonetheless, no literature was found regarding *E. amylovora* detection in environmental samples using IFCM. Concerning other phytopathogenic bacteria, an IFCM protocol was developed and successfully applied for the detection of *Xanthomonas campestris* in cabbage tissues and bean seeds (Chitarra *et al.*, 2002; Bergervoet *et al.*, 2007).

1.4. Dissertation objective

Erwinia amylovora is a phytopathogenic organism with a high destructive potential, threatening the Rosaceae crops production worldwide. The fact that fire blight is often difficult to control and eradicate makes this disease even more worrisome. Since the identification of *E. amylovora* in Portugal, several disease outbreaks were detected throughout the country, which led to the loss of the Integral Protected Area statute in 2019. The presence of this disease produced a negative impact in the economy by jeopardizing the most valuable Portuguese apple and pear crops, particularly the autochthonous *Pyrus communis* cv. "Rocha". Thus, characterization studies of Portuguese *E. amylovora* isolates becomes increasingly important to expand the knowledge of fire blight in Portugal.

The first objective of the present dissertation was to characterize a set of Portuguese and European *E. amylovora* isolates belonging to the Coleção Portuguesa de Bactérias Fitopatogénicas (CPBF) by conducting genomic, pathogenicity and virulence studies. Genomic characterization was implemented through CRISPR-PCR and distinct fingerprinting approaches. CRISPR-PCR was used to discriminate differences between isolates as well as to trace a possible geographical association between European and Portuguese isolates. Genomic fingerprinting was performed using BOX-, ERIC-, REP- and MSP-PCR, for the assessment of infraspecific diversity. Furthermore, biological tests on *Pyrus communis* fruitlets were implemented to study differences in pathogenicity and virulence for the whole set of isolates.

The second objective was to develop FCM and IFCM protocols for the detection and cell viability assessment of *E. amylovora* populations present in plant material during the infection process. The existence of an alternative diagnostic tool is advantageous to overcome false-negative results often associated with VBNC. Moreover, this would provide a deeper understanding about unclear aspects of the life cycle of *E. amylovora*, particularly during winter, when the bacterium is overwintering. The clear understanding of *E. amylovora* epidemiological behaviour may provide valuable data for the control of fire blight disease in Portugal. For this purpose, firstly a validation process using pure and mixed cultures was carried out to test whether the fluorophores and a monoclonal antibody were appropriate for further use. Then, FCM and IFCM analyses were performed on *P. communis* cv. "Rocha" fruitlets infected with *E. amylovora* isolates to assess if the established methodologies allowed the detection and cell viability assessment of these bacterial populations.

2. Materials and Methods

2.1. Bacterial isolates and growth conditions

In the present study, a set of 48 isolates belonging to CPBF, collected from rosaceous hosts and previously identified as *E. amylovora* by classical and molecular methods, were characterized (Table 2.1).

Table 2.1 - Collection of *Erwinia amylovora* isolates used.

CPBF Isolate ID	Original Collection ID	Host	Variety	Year of isolation	Country	County
142	SPV (Angers) 1558	*Crataegus* sp.			France	
360	BPic 841	*Pyrus communis*			Cyprus	
361	BPic 843	*P. communis*	Passe Crassane	1984	Greece	Arkadia
364	BPic 913	*P. communis*			Greece	Crete
365	BPic 917	*P. amygdaliformis*		1985	Greece	Cefalonia
366	BPic 928	*P. communis*			Greece	Mitilini
372	BPic 1624	*P. communis*		1990	Greece	Pella
373	BPic 1631	*Crataegus* sp.			Czech Republic	
387	SL2157	*Cotoneaster salicifolius*	Hybridus pendulus	1993	Ireland	
393	SL2163	*C. salicifolius*	Hybridus pendulus		Ireland	
410		*Crataegus* sp.			Poland	
411		*Crataegus* sp.			Poland	
412		*P. malus*			Poland	
450	SL2156	*Cotoneaster* sp.			Ireland	
544		Pomme tree		2015	Portugal	
564		Pomme tree		2015	Portugal	
593		*P. communis*		2015	Portugal	
849				2017	Portugal	
850				2017	Portugal	
851				2017	Portugal	
853				2017	Portugal	
855				2017	Portugal	
857				2017	Portugal	
884				2017	Portugal	
885				2017	Portugal	Lisboa
904		*P. communis*	Rocha	2017	Portugal	Alcobaça
905		*P. pyrifolia*	Nashi	2017	Portugal	Alcobaça
963^{T}	CFPB 1232	*P. communis*		1959	UK	
1137	SL2158	*Sorbus* sp.		1993	Ireland	
1276	SL2159	*Sorbus* sp.		1993	Ireland	
1307		*P. communis*	Rocha	2010	Portugal	Alcobaça
1310		*P. communis*	Rocha	2010	Portugal	Alcobaça
1311		*P. communis*	Rocha	2010	Portugal	Alcobaça
1312		*P. communis*	Rocha	2010	Portugal	Alcobaça
1313		*Mallus domestica*		2010	Portugal	Alcobaça
1314		*P. communis*	Rocha	2010	Portugal	Alcobaça
1315		*P. communis*	Rocha	2010	Portugal	Alcobaça
1316		*P. communis*	Rocha	2010	Portugal	Alcobaça
1317		*P. communis*	Rocha	2010	Portugal	Alcobaça
1318		*P. communis*	Rocha	2010	Portugal	Bombarral
1319					Portugal	

Table 2.2 - Continued.

CPBF Isolate ID	Original Collection ID	Host	Variety	Year of isolation	Country	County
1348		*M. domestica*	Tromba de Boi	2011	Portugal	Viseu
1349		*M. domestica*	Granny Smith	2011	Portugal	Guarda
1350		*M. domestica*	Ginger Gold	2011	Portugal	Ferreira do Alentejo
1351		*P. communis*	Rocha	2011	Portugal	
1352		*Cydonia oblonga*		2011	Portugal	Ferreira do Alentejo
1380		*C. oblonga*		2012	Portugal	Campo Maior
1404				2014	Portugal	

CPBF = Coleção Portuguesa de Bactérias Fitopatogénicas.
Empty cells, unknown information.

For molecular characterization studies, isolates were grown on King's medium B (KMB) (King *et al.*, 1954) and incubated at 27 °C for 48 h. For DNA extraction, a 1× phosphate saline buffer (PBS) 10 mM suspension of each isolate (optical density $(OD)_{600}$ = 0.1; 10^8 cfu mL^{-1}) was heated at 95 °C for 7 min. Nucleic acids suspensions were frozen at -20 °C until further use.

For biological assays, namely those to assess pathogenicity and virulence of *E. amylovora*, a set of isolates were grown on KMB and incubated at 27 °C for 48 h. Bacterial suspensions were made in 1x PBS 10 mM and adjusted to 10^8 cfu ml^{-1} ($(OD)_{600}$ = 0.1).

For FCM analyses, the following isolates were used: *E. amylovora* 365, *E. amylovora* 412 and *E. amylovora* 885 belonging to CPBF, presumptive *Aeromonas veronii* BBC016 and presumptive *Staphylococcus cohnii* BBC077 belonging to Coleção Bacteriana Lab Bugworkers (BBC).

Erwinia amylovora 885, *A. veronii* BBC016 and *S. cohnii* BBC077 were used in FCM validation assays. For this, 10 µL of *E. amylovora* CPBF 885 grown in KMB was transferred to 35 mL of liquid KMB and incubated at 25 °C for 24 h. Thereafter, 500 µL of this bacterial suspension were added to 35 mL of liquid KMB and incubated at 25 °C for 48 h. *S. cohnii* and *A. veronii* were grown in tryptone-soy broth (TSB) (Biokar Diagnostics, France) and incubated at 25 °C for 48 h. Cells were harvested from liquid KMB or TSB by centrifugation at 4 000 rpm at 20 °C for 20 min and washed twice in 1× PBS (Invitrogen, UK). Cells were heat-treated by incubation at 60 °C for 30 minutes.

2.2. Molecular identification and characterization of *Erwinia amylovora* isolates

2.2.1. *Erwinia amylovora* detection and identification

Identification of all isolates as *E. amylovora* was confirmed by conventional PCR using FER1-F (5'- AGCAGCAATTAATGGCAAGTATAG TCA - 3') and rgER2R (5′ - AAA AGA GAC ATC TGG ATT CAGACA AT - 3′) primers, according to Obradovic *et al.*(2007) modified by Gottsberger (EPPO, 2013). Reactions were carried out in a final volume of 25 µL containing 1× PCR Buffer, 1.5 mM $MgCl_2$, 0.1 mM of each dNTP (Solis Biodyne, Estonia), 0.4 µM FER1-F primer, 0.4 µM rgER2R, 1 U Taq DNA polymerase and 5 µL of genomic DNA. Except for dNTP, all reagents were obtained from Invitrogen (S.A., United Kingdom). Amplification was performed with initial denaturation at 94 °C for 3 min, followed by 41 cycles of 94 °C for 10 s, 60 °C for 10 s, 72 °C for 30 s and a final extension of 72 °C for 5 min. PCR reactions were performed in PTC100 MJ Research Thermocycler (Ecogen, United Kingdom). PCR products were separated by 1% agarose gel electrophoresis in 1× SGTB (w/v) at 38 V cm^{-1} for 45 min and stained with 2.5 µg mL^{-1} SYBR SAFE DNA Stain Gel (Invitrogen, United

Kingdom). Agarose gels were visualized under UV light (312 nm) and photographed using the digital camera Kodak EDAS 290 equipped with 1D LE 3.6 (Kodak Scientific Imaging Systems) software.

2.2.2. CRISPR-PCR

CRR1 was amplified using C1f04 (5' – CGATCAACCTGTTTTTCAGTAGGT – 3') and C1r09 (5' – CCGCCGAGACAACCGGCTATCC – 3') primers according to Rezzonico *et al.* (2011). Reactions were performed in a final volume of 25 µL containing 1× PCR Buffer, 1.5 mM $MgCl_2$, 0.2 mM of each dNTP (Solis Biodyne, Estonia), 0.4 µM C1f04, 0.4 µM of C1r09, 1.5 U Taq DNA polymerase and 5 µL of genomic DNA. Except for dNTP, all reagents were obtained from Invitrogen (United Kingdom). Amplification was conducted with initial denaturation at 95 °C for 15 min, followed by 35 cycles of 95 °C for 30 s, 60 °C for 30 s and a final extension of 72 °C for 3 min. PCR reactions were performed in Biometra T Professional Thermocycler (Biometra, Germany). PCR products were separated by 1.5% agarose gel electrophoresis in 1× SGTB (w/v) at 24 V cm^{-1} for 60 min. Agarose gels were stained and visualized as described in 2.2.1.

2.2.3. Genomic fingerprintings

PCR fingerprinting profiles were obtained by PCR amplification of genomic repeated sequences to assess the genetic variations among *E. amylovora* isolates. For these analysis, rep-PCR according to Louws *et al.* (1994), and MSP-PCR according to Ryskov *et al.* (1988) were performed as described in Table 2.2. All rep-PCR and MSP-PCR reactions were performed in a final volume of 25 µL. Except for dNTP (Solis Biodyne, Estonia), all reagents were obtained from Invitrogen (United Kingdom). PCR reactions were performed in Biometra T Professional Thermocycler (Biometra, Germany).

Table 2.3 - rep- and MSP-PCR reagents and amplification conditions.

BOX-PCR	
Reagents + Genomic DNA	**Amplification conditions**
1× PCR Buffer	initial denaturation at 94 °C during 7 min
1.5 mM $MgCl_2$	30 cycles: 94 °C for 1 min 53 °C for 1 min 72 °C for 7 min
0.2 mM of each dNTPs	
Primer: 0.2 mM of BOXA1R (5'-CTACGGCAAGGCGACGCTGACG - 3')	
2 U Taq DNA polymerase	
2 µL of genomic DNA	final extension of 72 °C for 15 min
ERIC-PCR	
Reagents + Genomic DNA	**Amplification conditions**
1× PCR Buffer	initial denaturation at 95 °C during 7 min
1.5 mM $MgCl_2$	35 cycles: 94 °C for 1 min 52 °C for 1 min 65 °C for 7 min
0.2 mM of each dNTPs	
Primer: 1.2 mM of ERIC2 (5'- AAGTAAGTGACTGGGGTGAGCG - 3')	
0.5 U Taq DNA polymerase	
5 µL of genomic DNA	65 °C for 15 min

Table 2.4 - Continued.

REP-PCR	
Reagents + Genomic DNA	**Amplification conditions**
1× PCR Buffer	initial denaturation at 95 °C during 7 min
1.5 mM $MgCl_2$	30 cycles: 94 °C for 1 min 44 °C for 1 min 65 °C for 8 min
0.2 mM of each dNTPs	
Primers: 1.2 mM REP1R (5' - IIIICGICGICATCIGGC - 3') and 1.2 mM of REP2I (5' - ICGICTTATCIGGCCTAC - 3')	
0.5 U Taq DNA polymerase	
5 µL of genomic DNA	65 °C for 15 min
MSP-PCR	
Reagents + Genomic DNA	**Amplification conditions**
1× PCR Buffer	initial denaturation at 94°C during 5 min
3 mM $MgCl_2$	40 cycles: 94 °C for 1 min 55 °C for 1 min, 72 °C for 2 min
0.2 mM of each dNTPs	
Primer: 0.8 mM csM13 (5' - GAG GGT GGC GGT TCT - 3')	
2 U Taq DNA polymerase	
5 µL of genomic DNA	72 °C for 6 min

After amplification, 10 µl PCR products were separated by agarose gel electrophoresis: for MSP-PCR (1.5% agarose in TBE 0.5×) at 3 V cm^{-1} for 3h; for BOX-PCR (2.0% agarose in TBE 0.5×) at 3 V cm^{-1} for 7h; for ERIC-PCR (2.0% agarose in TBE 0.5×) and REP-PCR (2.0% agarose in TBE 0.5×) at 2 V cm^{-1} for 6h. Agarose gels were stained and visualized as described in 2.2.1.

Fingerprinting profiles were analysed with BioNumerics software version 6.6 (Applied Maths, Belgium). For cluster analysis, Pearson's correlation coefficient to generate the similarity matrix and unweighted pair group method with arithmetic mean (UPGMA) as clustering method were used.

The reproducibility cut-off level was determined by the mean value of the reproducibility obtained for BOX-PCR. For this purpose, approximately 30% of the isolates were randomly chosen to be analysed in duplicate.

2.3. Biological assays to assess pathogenicity and virulence of *Erwinia amylovora* isolates

Fruitlets of *Pyrus communis* cv. "Rocha" obtained from Quinta Nova, Alcobaça were used to study the pathogenicity and virulence of a set of *E. amylovora* isolates (Table 2.1). Fruitlets were surface disinfected with 70% ethanol (v/v), punctured with a sterile needle and inoculated at the incision site with 10 µL of bacterial suspension in 1× PBS or with 10 µL of 1× PBS for the negative control, respectively. Four fruitlets per isolate, as well as for the negative control, were used. After inoculation, fruitlets were kept in a sterile hermetic plastic container at 18 °C/ 24 °C for 6 d. Relative humidity was maintained by a sterile filter paper moistened with sterile distilled water. Horizontal (H) and vertical (V) length of the lesion produced by each isolate was recorded 6 days after inoculation (DAI) (adapted from EPPO standard PM7/20 (EPPO, 2004)) and the presence of bacterial exudate (oozing) was recorded 6 and 12 DAI. Koch's postulates were fulfilled by re-isolation of the bacterium on nutrient agar (NA) medium and further confirmation by conventional PCR according to Obradovic *et al.* (2007) modified by Gottsberger (EPPO,2013).

Statistical analyses

Lesion size (mm) was estimated as the mean of the H and V length of necrotic tissue minus the length of the necrotic tissue caused by the needle wound measured in the negative control. For bacterial exudate, it was considered a positive result when more than 50% of the replicates had oozing, a negative result when more than 50% of the replicates had no oozing and a variable result when 50% of replicates had oozing.

Dixon's Q test was performed to identify and remove outliers among the lesion size estimated in each set of replicates prior to calculating the mean and standard error (SE) of the mean. Based on lesion size, three virulence categories were defined, namely low (L), medium (M) and high (H).

To test the association between CRISPR-PCR genotypes and virulence categories, one-tailed Fisher's exact test was applied. Following the use of two-by-two tables to perform Fisher's exact test (Zar, 2014), the medium and high virulence categories were grouped together to meet the assumptions of the statistical tests. A p-value < 0.05 was considered significant.

Statistical treatments were performed with Microsoft Office Excel v16.0 for Office 365 (Microsoft, USA) and GraphPad Prism v8.2 (GraphPad Software, USA).

2.4. Flow cytometry analyses

2.4.1. Basic principles of flow cytometry

FCM is a powerful technique for analysis of physiological state of individual cells, which in recent years has been successfully applied in studies of microorganisms (Wang *et al.*, 2010; Kennedy & Wilkinson, 2017).

On the basis of the principle of hydrodynamic focusing, the flow cytometer fluidics system transports particles in a fluid stream, one cell at a time at high speed, to a quartz flow cell, where laser beam and cells interact. This interaction generates optical signals of variable intensities, associated with light scattering and fluorescence emission, which are ultimately correlated to structural and/or functional cell parameters (Adan *et al.*, 2017). Light scattering is the deflection of incident light by the cells, in a direct or orthogonal direction, as they pass through the laser. When light is scattered in a direct direction, with a wavelength analogous to that of incident light, it is referred to as forward scattering (FSC) and provides a rough measure of cell size. When light is scattered in an orthogonal direction, it is referred to as side scatter (SSC), which is commonly associated with cell complexity or granularity (Díaz *et al.*, 2010; Adan *et al.*, 2017). However, other factors may influence the scattering signals, such as refracting differences and optical configuration of flow cytometer. Nevertheless, FSC and SSC parameters allow to distinguish cells with distinct morphological and physiological characteristics (Müller & Nebe-von-Caron, 2010).

Flow cytometer comprises three main systems, namely fluidic, optical and electronic (fig. 2.1). The fluidic system ensures that the cells suspended in a fluid (buffer or water) will be directed to the interrogation point, where cells cross the laser and are analysed. The optical system contains the light sources and consists of one or more lasers, and a set of lenses and optical filters that direct the light to specific detectors (FL1 to FL4), which detect light signals at different wavelengths. The electronic system is responsible for transforming analog data into digital data, which are analysed on a computer using an appropriate software (Adan *et al.*, 2017).

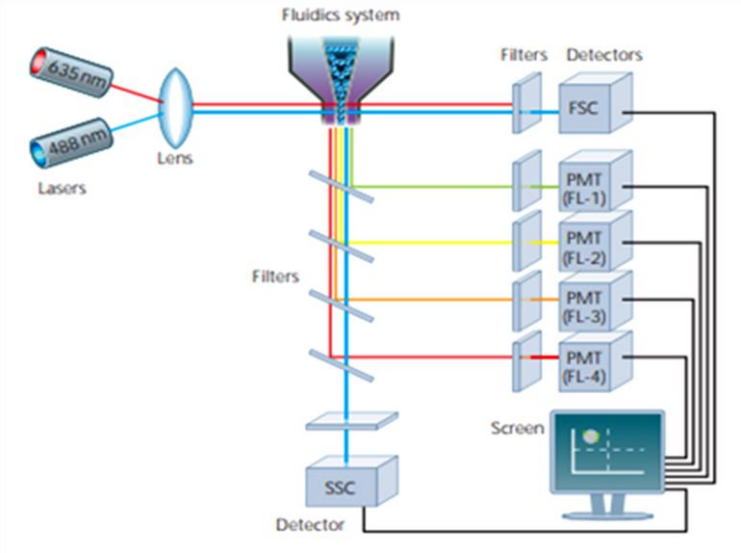

Figure 2.1 - The three main systems of flow cytometry (fluidics, optical and electrical) (figure source: Rahman, 2006).

Fluorescence detection (by FL1 to FL4 detectors) allows the assessment of the natural autofluorescence of cells and any cellular properties with which a fluorescence dye may be associated. Fluorophores are molecules capable of changing from a ground state to an excited state after light absorption. These molecules can return to ground state in two ways, namely from heat loss or from light emission. The light emission can be altered according to chemical reactions, binding events, and environmental alterations (Fu & Finney, 2018). Fluorophores are divided in two extensive categories, namely fluorescence dyes used for labelling other probes, such as antibodies, and dyes that fluoresce according to cell properties, such as membrane potential, membrane permeability, enzyme activity and pH gradients (Díaz *et al.*, 2010).

Cellular viability

Multiparametric measurements associated with various fluorophores allow different physiological stages to be detected in cellular and population level: metabolically active cells with intact membranes (living cells) or with compromised membranes (injured cells); metabolically inactive cells, with intact membranes (dormant, persistent cells or VBNC), or with damaged membranes (dead cells) (Nebe-von-Caron *et al.*, 1998; Díaz *et al.*, 2010).

FCM viability assays rely on the availability of suitable fluorescent probes, which are selected according to their target specificity (e.g. nucleic acids, enzymatic activities or membrane probes) and optical properties (i.e. fluorescence excitation and emission spectra). The binding of several viability probes to their specific targets is conditioned by membrane integrity, which means impermeable fluorophores are excluded by intact cell membranes while permeable fluorophores can cross them (Díaz *et al.*, 2010; Fu & Finney, 2018).

One of the most used methods to assess viability by FCM is based on a dual staining with two fluorophores, Syto9 and propidium iodide (PI) (LIVE/DEAD BacLight Bacterial Viability Kit – L34856 ThermoFisher). Both dyes intercalate with nucleic acids resulting in an enhanced fluorescence. Syto9 can enter the cells regardless of their membrane integrity and emit green fluorescence, allowing the total number of cells to be counted. PI is used as a counterstain and as an identifier of dead cells because it can only enter cells with disrupted membranes and emit a red fluorescence. When both dyes are present, PI exhibits a stronger affinity for nucleic acids than Syto9, allowing differentiation between live and

dead cells based on the relative green and red fluorescence (Berney *et al.*, 2007; Nebe-von-Caron *et al.*, 2000; Díaz *et al.*, 2010).

Another aspect of bacterial viability/vitality is the maintenance of cell membrane potential. In bacteria, the membrane potential reflects the state of energy metabolism and simultaneously the physical and functional integrity of the membrane. Bacteria normally maintain an electrical potential gradient (membrane potential, $\Delta\Psi$) of over 100 mV across the cytoplasmic membrane, with the interior side negative. FCM using probes that present alterations of the transmembrane distribution, depending on the potential, which are accompanied by changes in fluorescence, can measure membrane potential variations (Shapiro, 2000).

The oxonol derivative Bis-(1,3-dibutylbarbituric acid) trimethine oxonol ($DIBAC_4(3)$) is an anionic dye that can enter depolarised cells where it binds to intracellular proteins presenting an enhanced green fluorescence and a red spectral shift. This slow-response potential-sensitive probe enables the distinction between non-viable or dead cells (with a depolarized membrane) and metabolic active cells (with a polarized membrane) (Rezaeinejad & Ivanov, 2009; Díaz *et al.*, 2010; Sträuber & Müller, 2010).

IFCM can also be combined with the viability assessment, for which the samples are first incubated with a specific antibody tagged with a fluorescent dye to identify the bacteria, and then stained with viability dyes. One of the most used fluorophores for bacterial identification is the fluorescein isothiocyanate (FITC), a fluorescein derivative with green fluorescence (Aoki *et al.*, 2010; Babu *et al.*, 2013; Odell & Cook, 2013).

Data acquisition and analysis

FCM analysis of cells suspensions was performed using a Cyflow Space (Sysmex-Partec, Germany) flow cytometer with the True Volumetric Absolute Counting (TVAC) capability and equipped with a blue solid-state laser (20 mw at 488 nm). The TVAC mechanical device allows the cells concentration determination based on the analysis of a fixed volume (200 µL) as defined by the distance between two platinum electrodes reaching into the sample tube with a given diameter. The equipment is equipped with the following optical filters and detectors: 536/40 nm (FL1 green fluorescence), 575 nm (FL2 orange fluorescence) and 610/30 nm (FL3 red fluorescence).

At acquirement, gains were set to a specific and adequate value kept for all analysis. A logarithmic amplification of the incoming signal was applied to measure a broader dynamic range of signals in one histogram. The signal used to detect the presence of cells in the field of view of the cytometer, called trigger signal, was set on FSC to limit the background signals. Flow rate was adjusted to keep total acquired events between 1000 to 1500 events per second. Except for total cell counting, a fixed number of events (25000) were acquired for each sample to allow the samples to be correctly compared.

For data acquirement, Partec FlowMax software was used while data analyses were performed with FlowJo™ v10.6.1 (Becton Dickinson & Company, USA).

Optical signals are detected, recorded and processed by different integrated systems in the flow cytometer, and the acquired data may be graphically visualized while a sample is being analysed. FCM data is usually represented in monoparametric histograms (single parameter frequency distributions) where the x-axis represents the parameter's signal value in channel numbers and the y-axis represents the number of events per channel number (fig.2.2 A and B). Each event placed in the channel corresponds to its signal value and one parameter histogram represents the scattering or fluorescence intensity versus the number of particles or cells (y-axis). Two parameter plots are graphs that display two measurement parameters, one on the x-axis and one on the y-axis and the cell count as a density (dot) plot (Díaz *et al.*, 2010). Pseudo-colo*u*r dot-plots are bivariate density plots in which one dot corresponds to one event or cell. Different colours represent differences in cell density and not

variation on their emission spectra. Blue and green areas have a low cell density, yellow areas have mid-range cell density and orange and red areas present high cells density (fig 2.2 C).

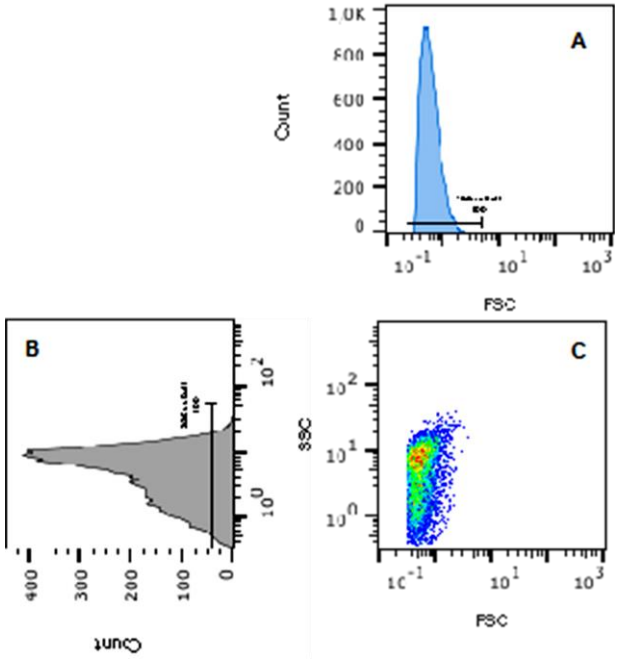

Figure 2.2 - Flow cytometry data illustration. A, B. Monoparametric histogram. C. Pseudo-colour dot-plot.

One of the first steps for the analysis of FCM data is the appropriate gating strategy, in which graphic regions are defined so that the populations of cells that are restricted by them can be properly studied in relation to the different parameters whose analysis is intended. Gates can be of different types: a) range, usually defined in monoparametric histograms (fig. 2.3 A, B D, E and F); b) polygonal regions (fig. 2.3 C and G), for example in FSC *vs* SSC graphs (fig.2.3 C); c) a gate can be set to remove debris and other events of non-interest while preserving cells based on size and complexity; a quadrant gate (fig. 2.3 H) divides two-parameter plots into four regions to discriminate populations as negative, single positive or double positive.

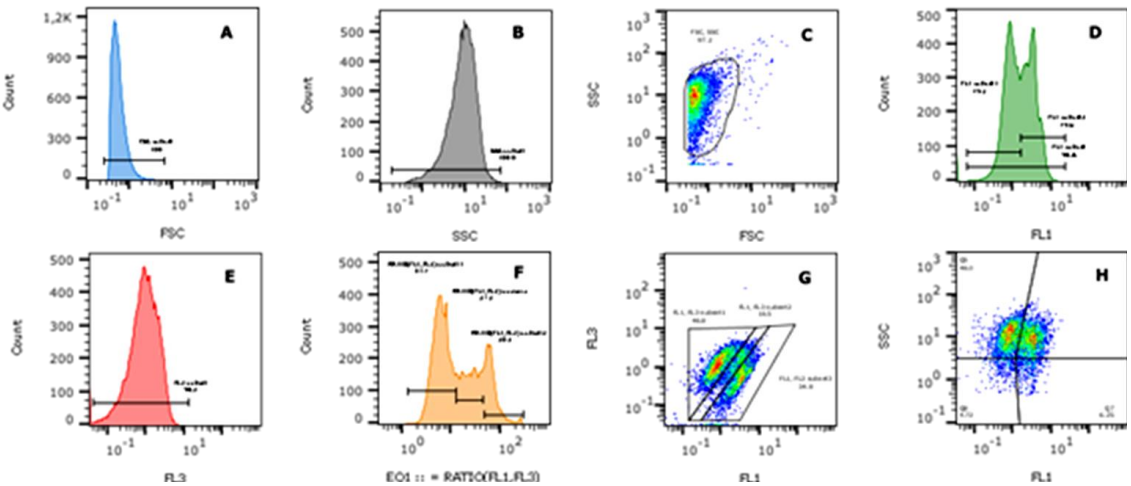

Figure 2.3 - Example of flow cytometry data analysis. A, B, D, E, F. Histograms. A. FSC. B. SSC. D. Green fluorescence (FL1). E. Red fluorescence (FL3). F. Ratio of green fluorescence to red fluorescence (EQ1 = FL1/ FL3). C, G, H. Pseudo-colour dot-plots. C. FSC × SSC (population of interest). G. Green (FL1) × red (FL3) fluorescence. H. Green fluorescence (FL1) × SSC.

Sample measurements were obtained of gated cells from three replicas using FlowJo™ v10.6.1 software (Becton Dickinson & Company, USA) and Microsoft Office Excel v16.0 for Office 365 (Microsoft, USA). Green and red fluorescence intensities were expressed as geometric means. Correlation between the expected and observed viability (%), as well as the observed viability (%) of Syto9 and DIBAC4(3), were performed by a linear correlation analysis.

2.4.2. Viability assessment optimization for pure culture analysis

All staining protocols were performed with 1.5 mL of cell suspensions and 1 µL of each fluorophore stock solution (3.34 mM Syto9, 20 mM PI and 10 mg mL^{-1} $DIBAC_4(3)$) and incubated in the dark at room temperature for 10 min (Syto9 + PI) or 30 min ($DIBAC_4(3)$). As controls, suspensions of *E. amylovora*, *S. cohnii* and *A. veronii* without staining were used. No autofluorescence emission was detected.

To validate the method, the fluorophores were tested in suspensions with different proportions of live cells (LC, untreated) and heat-treated cells (KC, incubated at 60ºC for 30 min), namely 100% LC, 75% LC|25% KC, 50% LC|50% KC, 25% LC|75% KC and 100% KC.

Assessment of cellular viability was based on green fluorescence (FL1) for Syto9 or $DIBAC_4(3)$, and red fluorescence (FL3) for PI.

2.4.3. Detection of *Erwinia amylovora* by immune-flow cytometry

A volume of 980 µL of *E. amylovora* 885 was incubated with 2.5 µL of the primary monoclonal antibody (mAb) Ea7A IVIA for *E. amylovora* (PLANT PRINT Diagnòstics S.L., Spain) at room temperature for 30 min in the dark (Gorris, 1996b). Then, cells were spun down at 14 000 rpm for 15 min, washed and resuspended in 1× PBS (Invitrogen, UK). Samples were conjugated with 10 µL of goat anti-mouse fluorescein isothiocyanate (GAM-FITC) secondary antibody (PLANT PRINT Diagnòstics S.L., Spain) at room temperature for 30 min in the dark. In samples with mixed dyes (mAb + FITC + PI), PI was added 20 minutes after the addition of FITC. The suspension was incubated at room temperature for 10 min in the dark. The same procedure was applied in a *S. cohnii* suspension used as a negative control.

Detection of *E. amylovora* was based on green fluorescence (FL1) for FITC.

2.4.4. Detection and cell viability of *Erwinia amylovora* in artificially infected *Pyrus communis* fruitlets

Pieces of *Pyrus communis* cv. "Rocha" fruitlets infected with the isolates *E. amylovora* 365 and *E. amylovora* 412 (see 2.3) were excised from the transition zone (between the necrotic and healthy tissues) and placed in plastic bags. Samples were macerated for 5 min in antioxidant maceration buffer (AMB) to avoid oxidation (Gorris *et al.*, 2006). Samples were crushed in the plastic bags with a hammer. Macerates were stored at -20 °C with approximately 30% glycerol (v/v) until further use. The same procedure was performed in fruitlets inoculated with 1× PBS to serve as negative control.

Supernatant was collected by centrifugation at 1 500 rpm at 15 °C for 15 minutes and washed two times with 1× PBS (Invitrogen, UK). For detection and cell viability assessment of *E. amylovora*, the procedures described in 2.4.2 and 2.4.3 were performed, respectively. *Erwinia amylovora* 885 was used as positive control.

Detection and cell viability assessment of *E. amylovora* was based on green fluorescence (FL1) for FITC and red fluorescence (FL3) for PI, respectively.

2.5. Dissertation workflow

A schematic overview of the workflow used in the present study is presented in fig. 2.4.

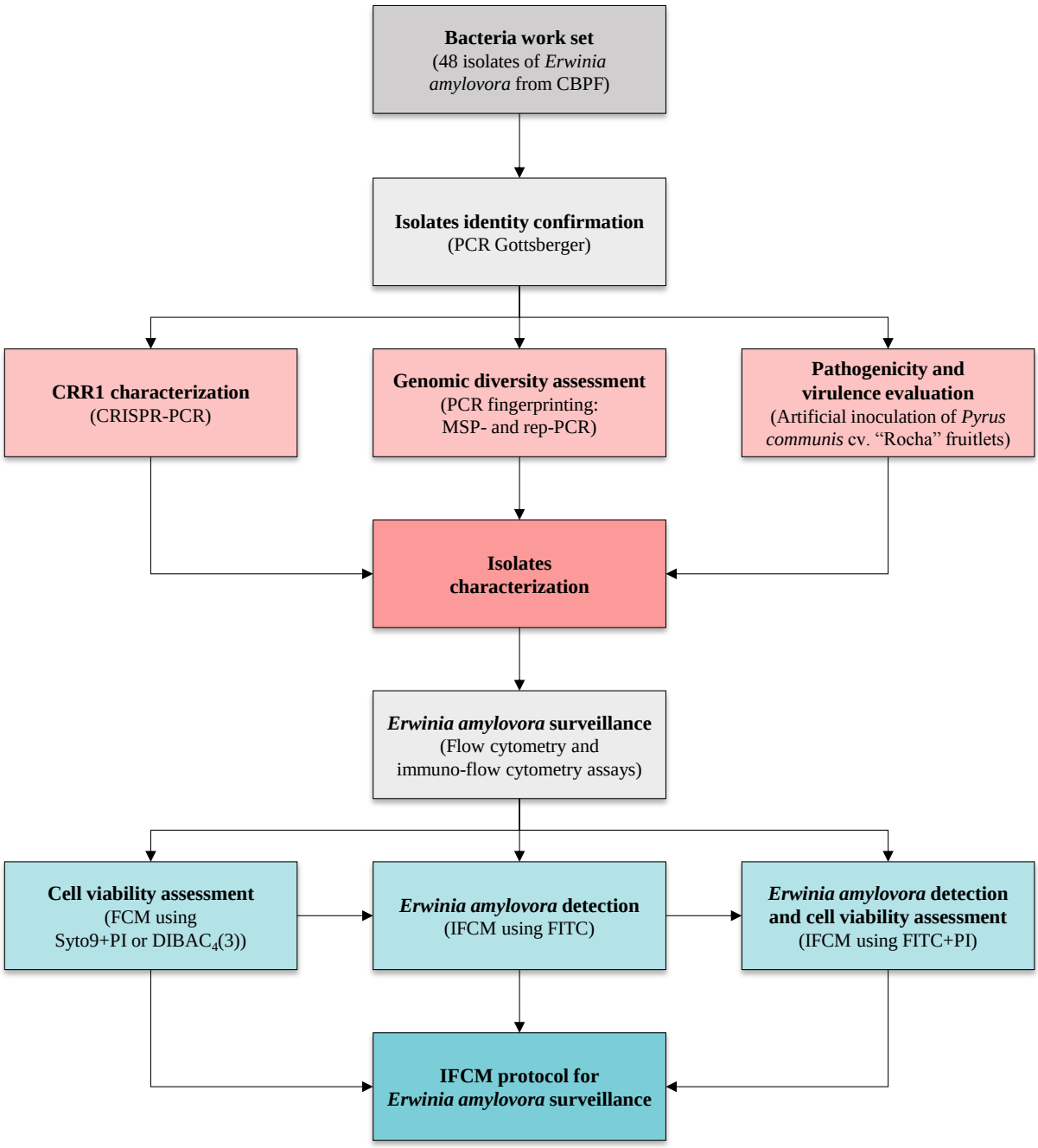

Figure 2.4 – Workflow of the study.

3. Results and Discussion

3.1. Molecular identification and characterization of *Erwinia amylovora* isolates

3.1.1. *Erwinia amylovora* detection and identification

All isolates presented an amplicon with 458 bp (Obradovic *et al.* (2007) modified by Gottsberger (EPPO, 2013)), confirming their identity as *E. amylovora* (fig. 3.1).

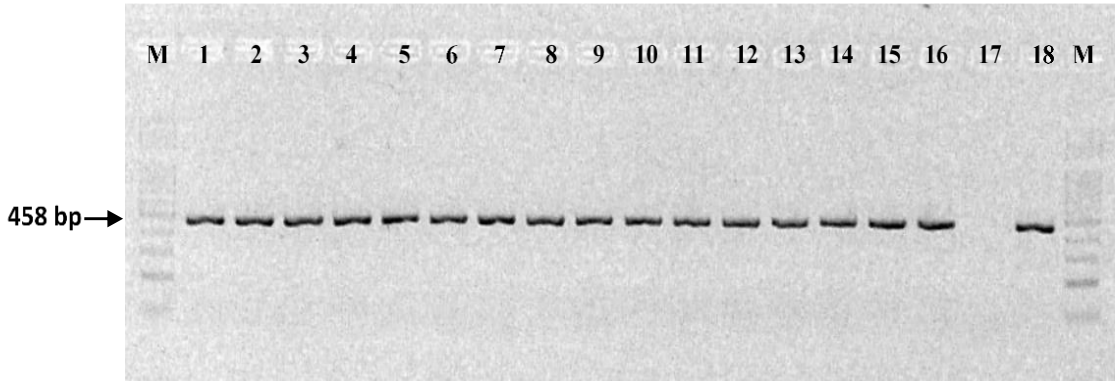

Figure 3.1 - Molecular identification of a set of the *Erwinia amylovora* isolates tested. (M) molecular size marker (100 bp DNA ladder). (1-16) *Erwinia amylovora* 142, 361, 364, 373, 393, 411, 412, 849, 850, 851, 853, 855, 857, 884, 904, 905, respectively. (17) negative control (negative amplification control, NAC). (18) positive control (positive amplification control, PAC) (*Erwinia amylovora* 885).

3.1.2. CRISPR-PCR

Isolates were characterized according to their CRISPR-PCR genotype. Amplification of CRR1 displayed the presence of two strains according to their CRR1 genotype, one with an amplification product with 272 bp and other with a 211 bp product (fig. 3.2 and Supplementary Table 1**)**. These two products were denominated as genotype A and D as previously defined by Rezzonico *et al.* (2011, 2014). Moreover, this analysis provided additional data about CRISPR-PCR genotypes distribution through Europe. It is important to mention that contrary to sequencing, the applied methodology can only discriminate between genotypes A and D. Thus, those terms are mentioned whether the isolates possess an original or derived genotype A or D.

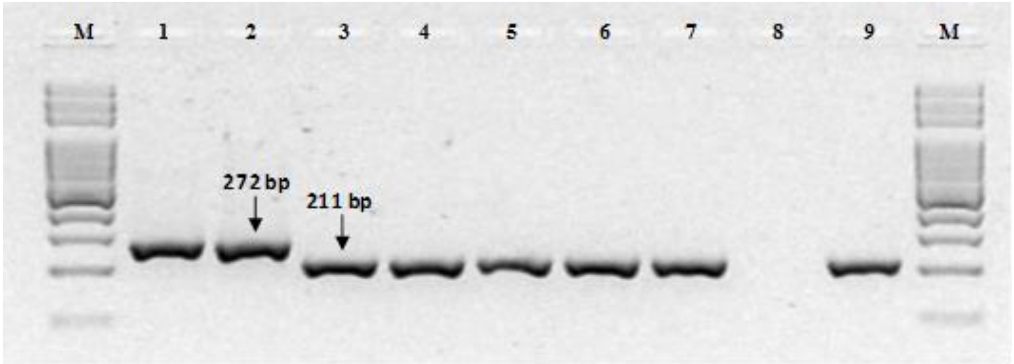

Figure 3.2 - Visualization of CRISPR repeat region 1 products of a set of the *Erwinia amylovora* isolates tested. (M) molecular size marker (100 bp DNA ladder). (1-7) *Erwinia amylovora* 855, 857, 884, 885, 904, 905, 1307, respectively. (8) negative control (NAC). (9) positive control (PAC) (*Erwinia amylovora* 885).

All isolates tested presented a genotype A or a genotype D. However, their distribution within each country was variable (fig. 3.3), with six countries being represented by a single genotype and two

countries presenting both. Out of the 48 isolates tested, 27 presented a genotype A and 21 a genotype D, with an almost identical representation within the tested set of isolates.

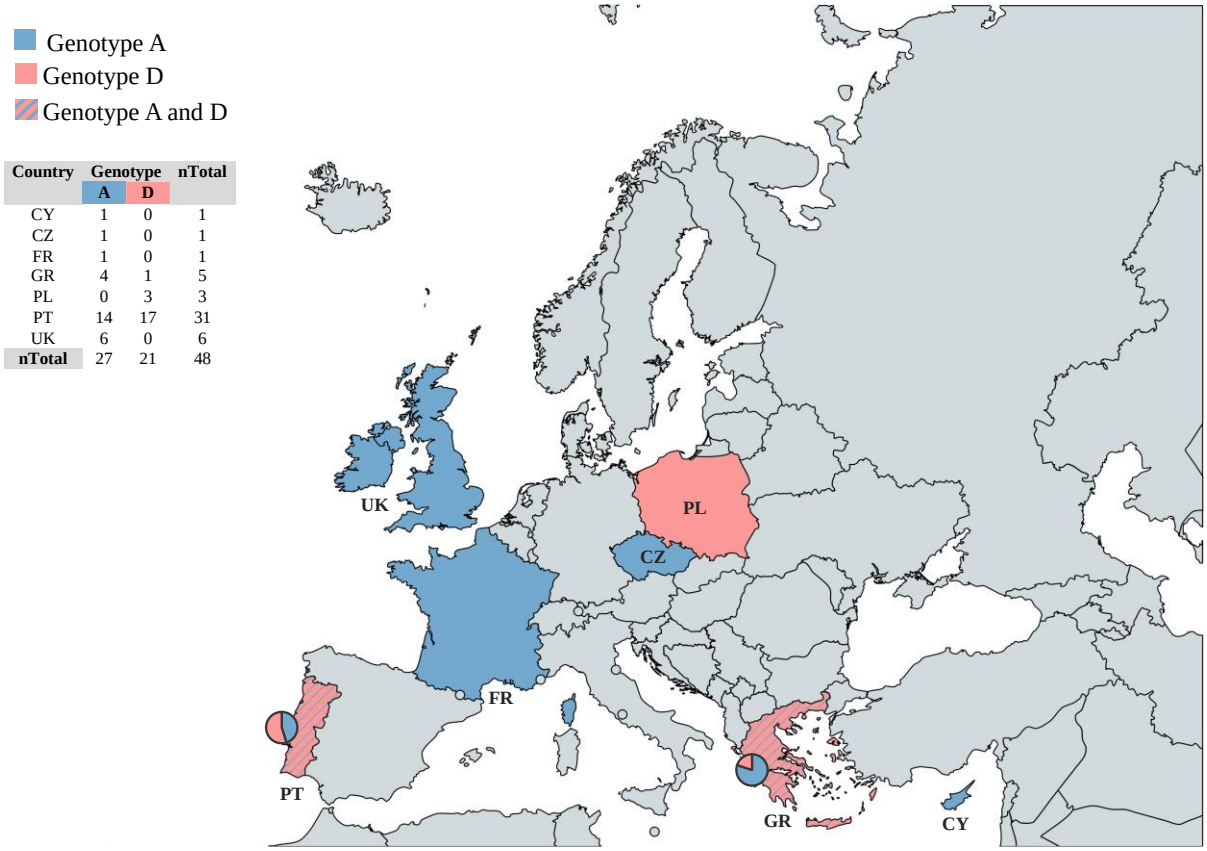

Country	Genotype		nTotal
	A	D	
CY	1	0	1
CZ	1	0	1
FR	1	0	1
GR	4	1	5
PL	0	3	3
PT	14	17	31
UK	6	0	6
nTotal	27	21	48

Figure 3.3 - Distribution of CRISPR-PCR genotypes A and D for the set of *Erwinia amylovora* isolates tested in each European country (data obtained in the present study). Pie-charts representing the number of isolates of each genotype were added to countries where more than one CRISPR-PCR genotype was detected. (CY) Cyprus. (CZ) Czech Republic. (FR) France. (GR) Greece. (PL) Poland. (PT) Portugal. (UK) United Kingdom. n = number of isolates. Figure source: created with a template from mapchart.net.

Thirty-one Portuguese isolates collected between 2010 to 2017 were examined, with a very similar predominance of both genotypes. Fourteen isolates belonged to genotype A and 17 to genotype D. The distribution of the isolates within A or D genotype varied among the years according to the schematic timeline presented in fig. 3.4. In 2010, 2011, 2015 and 2017 both genotypes were detected, while in 2012 and 2014 only genotype A was present. The presence of both genotypes was also detected in previous studies (Rezzonico, 2014; Kurz, 2018). Although the introduction of fire blight in the Portuguese territory occurred relatively recently in comparison to other European countries, the presence of isolates belonging to either one of the genotypes was detected since 2010. This means that there were at least two distinct introductions of *E. amylovora* in Portugal. Whether these introductions occurred simultaneously or at different moments is unknown.

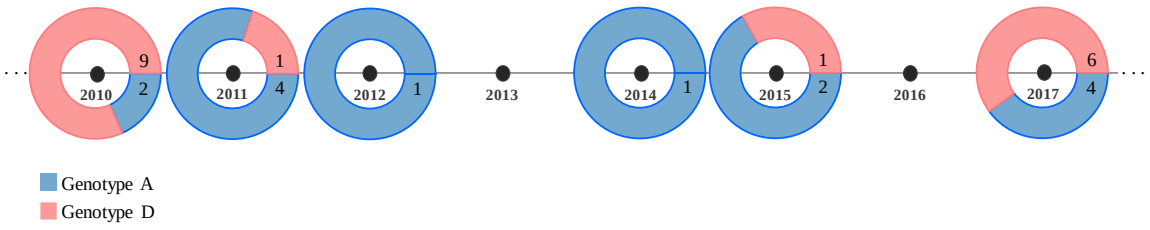

Figure 3.4 - Absolute frequency of CRISPR-PCR genotypes A and D of the 31 *Erwinia amylovora* Portuguese isolates according to their year of isolation.

Multiple occurrences and outbreaks were reported across the country since 2010 until 2017, mostly in Oeste, Centro and Alentejo regions (Cruz, 2010; EPPO Global Database, 2019). From the 31 Portuguese isolates tested, thirteen are from unknown origin. For the remaining 18 isolates, according to the obtained results, genotypes A and D are present in Alentejo, Centro and Oeste regions (fig. 3.5 and Supplementary Table 1). Three isolates from Alentejo region (Campo Maior and Ferreira do Alentejo) isolated in 2010 and 2012 presented genotype A. Two isolates from Centro region (Guarda and Viseu) isolated in 2011 presented genotype A or D. Thirteen isolates from Oeste region (Alcobaça, Bombarral and Alcântara) isolated in 2010 and 2017 were analysed, two presented genotype A and 11 genotype D. Summarily, genotype A was prevalent in Alentejo region, genotype D was prevalent in Oeste region and both genotypes had an equal predominance in Centro region.

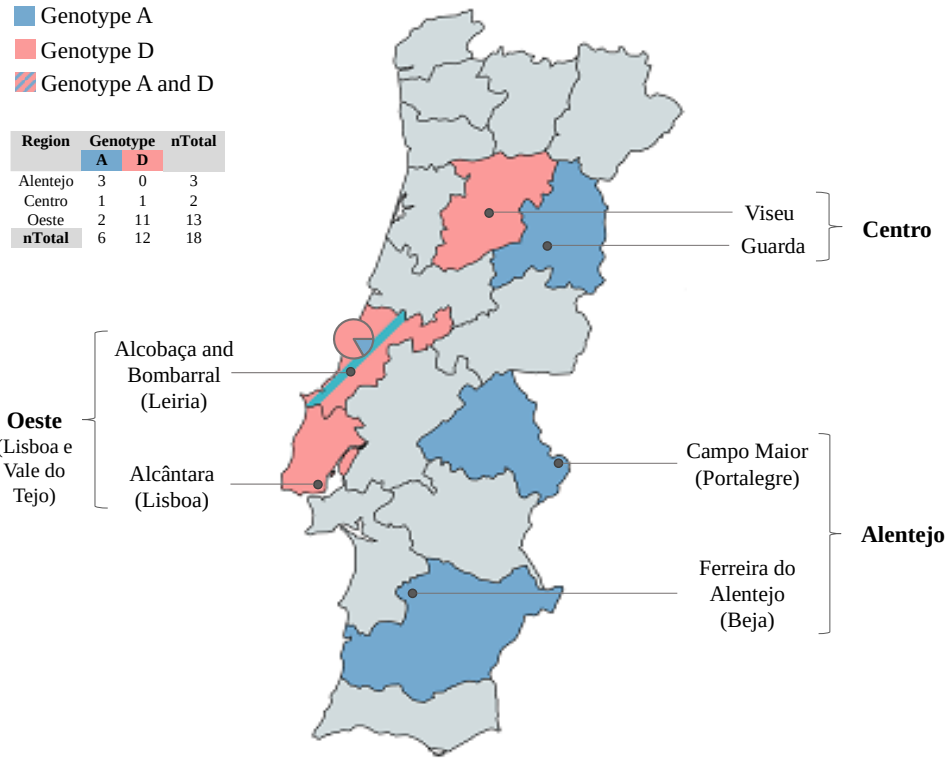

Figure 3.5 - Distribution of CRISPR-PCR genotypes A and D for the 18 *Erwinia amylovora* isolates throughout Portuguese regions (Alentejo, Centro and Alentejo). A pie-chart representing the number of isolates of each genotype was added to cities where more than one CRISPR-PCR genotype was detected. n = number of isolates. Figure source: created with a template from mapchart.net.

For the remaining European isolates tested, the presence of both genotypes was also detected. The isolates from Cyprus, Czech Republic, France and UK presented genotype A, while isolates from Poland presented genotype D. Besides Portugal, Greece was the only country that displayed both genotypes, four isolates presented genotype A and one genotype D (Supplementary Table 1).

Combining the results here obtained with data from previous studies (Rezzonico & Duffy, 2011; Rezzonico, 2014; Kurz, 2018), the distribution map of both genotypes clearly show that genotype A and genotype D are well established in most of the European territory (fig. 3.6), even in Portugal, where the disease was detected long after the onset of the disease in Europe (EPPO Global Database, 2019). In northern Europe, genotype A prevails over genotype D, except for Sweden. Southern Europe countries, except Portugal, presented a mix of both genotypes, however, genotype A prevails over genotype D. In eastern and western Europe, both genotypes are present, but genotype D is prevalent.

Genotype A exhibited a wider geographical distribution in comparison to genotype D, which may indicate that this genotype is more widely distributed throughout Europe. This differential distribution

in space and time of both genotypes could be enhanced by the fact that the first outbreak in Europe of genotype A occurred in 1958 in UK, twenty-one years prior to the first outbreak of genotype D in 1979 in Poland (Rezzonico, 2014).

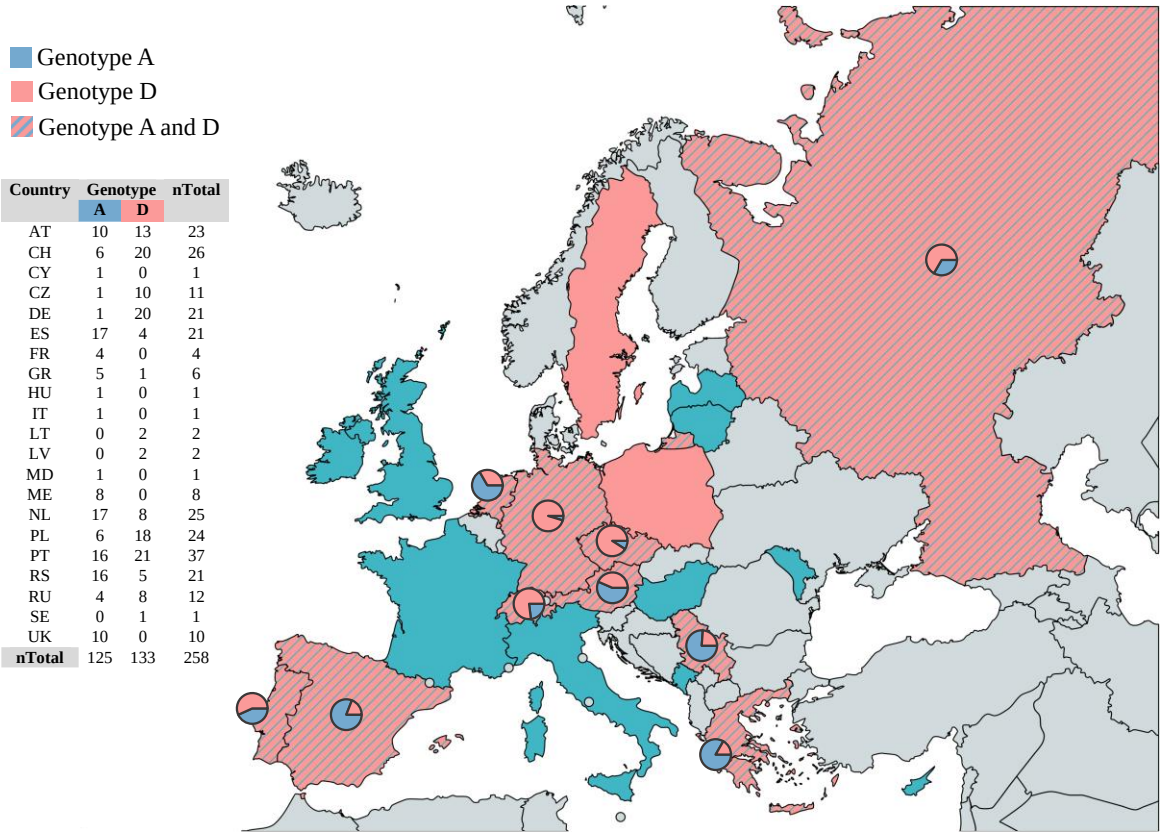

Country	Genotype		nTotal
	A	D	
AT	10	13	23
CH	6	20	26
CY	1	0	1
CZ	1	10	11
DE	1	20	21
ES	17	4	21
FR	4	0	4
GR	5	1	6
HU	1	0	1
IT	1	0	1
LT	0	2	2
LV	0	2	2
MD	1	0	1
ME	8	0	8
NL	17	8	25
PL	6	18	24
PT	16	21	37
RS	16	5	21
RU	4	8	12
SE	0	1	1
UK	10	0	10
nTotal	125	133	258

Figure 3.6 - Distribution of CRISPR-PCR genotypes A and D in each European country (combined data from the present study, Rezzonico (2014) and Kurz, (2018)). A pie-chart representing the number of isolates of each genotype was added to countries where more than one CRISPR-PCR genotype was detected. (AU) Austria. (CH) Switzerland. (CY) Cyprus. (CZ) Czech Republic. (DE) Germany. (ES) Spain. (FR) France. (GR) Greece. (HU) Hungary. (IT) Italy. (LT) Lithuania. (LV) Latvia. (MD) Moldova. (ME) Montenegro. (NL) Netherlands. (PL) Poland. (PT) Portugal. (RS) Serbia. (RU) Russia. (SE) Sweeden. (UK) United Kingdom. n = number of isolates. Figure source: created with a template from mapchart.net.

The emergence of CRISPR-PCR genotypes A and D among European isolates is in agreement with what had been displayed by previous sequencing of CRR1 and CRR2. Furthermore, according to their CRR1 and CRR2 similarities, *E. amylovora* strains from Amygdaloideae subfamily were clustered in three main CRISPR groups. Group I is formed by strains for diverse geographical origin, namely Europe, Mediterranean, North America and New Zealand, while groups II and III gather exclusively strains from USA (Rezzonico *et al.*, 2011). Within group I, an eastern North American *E. amylovora* was the most related with non-North America strains. This suggests that a similar strain may be responsible for the introduction of fire blight disease worldwide (Rezzonico *et al.*, 2011). The coherence of CRISPR-PCR diversity groups was reinforced by previous studies of PCR ribotyping, since PCR ribotypes 1 and 3 matched CRISPR-PCR groups I and III (McManus & Jones, 1995; Donat *et al.*, 2007; Rezzonico *et al.*, 2011).

Sequencing of CRISPR-PCR genotypes enabled to theorize the events responsible for the appearance and evolution of fire blight dissemination outside North America. According to the hypothesis, there were one or two major introduction events of an eastern North American *E. amylovora* strain in European territory (Rezzonico *et al.*, 2011). *Erwinia amylovora* is a bacterial species native from North America, where it remained restricted to wild hosts until the 19th century. The introduction of apple and pear by the first European colonizers in the late 1600s, introduced new rosaceous species susceptible to

fire blight. The transport of fire blight-infected plant material was crucial for the spread of the disease, which appeared first in New Zealand (1919), UK (1950s) and in the Middle East (1988). The oldest European *E. amylovora* isolates tested herein and in other studies (Rezzonico *et al.*, 2011, 2014) are from UK (1958 and 1959), France (1972) and Germany (1974) and all present genotype A, whereas genotype D appeared for the first time in Poland in 1979. The fact that all isolates from USA tested present genotype A, raises the question whether the two genotypes were the result of two different introductions of north American *E. amylovora*, or if genotype D originated from the deletion of spacer 1029 in genotype A (Rezzonico, 2011, 2014).

As referred, the primers only allowed a distinction between genotype A and genotype D, which are related to the presence or absence of a duplication of the spacer 1029, respectively. Previous studies, in which a greater number of primers were used for DNA amplification and for subsequent DNA sequencing, allowed the distinction between ancestral A or D genotypes and A– or D– derived genotypes (Rezzonico, 2011; Rezzonico, 2014). These derived genotypes result not only from differences in spacer 1029, but also from different patterns of presence and absence in additional spacers (fig. 1.6) (Rezzonico, 2014).

3.1.3. Genomic fingerprinting

The use of fingerprinting methods, such as BOX-, ERIC-, REP- and MSP-PCR, were able to produce detailed genomic profiles.

Forty-eight isolates examined with BOX-PCR exhibited complex genomic fingerprinting patterns with a high number of bands. However, all profiles were visually indistinguishable, revealing a low genetic variability. From the hierarchical analysis of these fingerprinting patterns resulted a dendrogram that displayed a limited genomic variability (Supplementary fig. 1), with a reproducibility of 86.9% ± 6.96% (c.v. = 8.0%). This dendrogram comprised two clusters ($\rho = 0.71$), one including 47 isolates and other with only one isolate (*E. amylovora* 1350). These differences might be related to slight variations in the agarose gel staining and not to differences in the bands *per se*, producing one unique cluster comprising all isolates.

Although Pearson's correlation coefficient is less sensitive to the background generated by rep-PCR electrophoresis (Rademaker & De Bruijn, 1997), the homogeneity between profiles was very high leading to artificial differences. The absence of an outgroup in this analysis emphasised even more these differences. Thus, considering that the differences between profiles are mainly caused by background differences and not by differences between genomic profiles, it can be considered that BOX-PCR by itself presents a low capacity to assess diversity among isolates of *E. amylovora*.

Due to the genomic homogeneity observed with BOX-PCR, nine isolates (*E. amylovora* 142, 361, 411, 412, 1312, 1318, 1348, 1350 and 1352) were selected to perform a composite analysis integrating different genomic fingerprinting methods, namely ERIC-, REP- and MSP-PCR. The selection of the isolates took into consideration the country of isolation, the original host and the CRISPR-PCR genomic profile, comprising the maximum diversity of the whole set of isolates used in order to enhance the possibility to detect differences in their genomic profiles. Since the number of isolates tested was smaller, each experiment was performed on a single gel, which allowed to reduce the occurrence of background differences. Similarly to BOX-PCR, a lack of ability to assess diversity among isolates was also displayed by ERIC-, REP- and MSP-PCR.

Due to the limited genomic variability the use of each marker by itself did not possess enough ability to differentiate *E. amylovora* strains. Thus, a composite dendrogram (fig. 3.7) was produced from the similarity average of BOX-, ERIC-, REP- and MSP-PCR experiments. Although this dendrogram showed the advantage of including more genomic information, it also displayed the inability to differentiate the isolates, exhibiting a minimal of genomic similarity of 90.1% ($\rho = 0.82$).

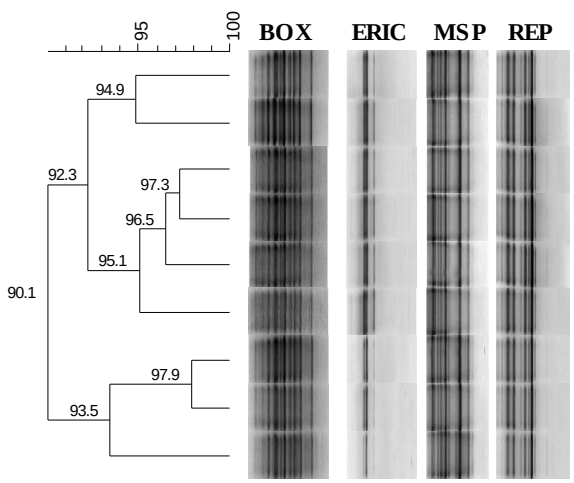

Isolate ID	Host	Year	Country
142	*Crataegus* sp.		France
1350	*Mallus domestica*	2011	Portugal
1318	*Pyrus communis*	2010	Portugal
1348	*M. domestica*	2011	Portugal
1352	*Cydonia oblonga*	2011	Portugal
1312	*P. communis*	2010	Portugal
361	*P. communis*	1984	Greece
412	*P. malus*		Poland
411	*Crataegus* sp.		Poland

Figure 3.7 - Composite dendrogram of BOX-, ERIC-, MSP- and REP-PCR. Genetic similarity between *Erwinia amylovora* isolates was performed based on Pearson's correlation coefficient and unweighted pair group method with arithmetic mean (UPGMA) clustering algorithm (ρ= 0.82). Empty cells, unknown information.

These results were in agreement with previous genetic fingerprinting studies, in which the existence of limited genomic variability between *E. amylovora* isolates had been observed, particularly in strains infecting Amygdaloideae subfamily members, such as *Crataegus* sp., *Cotoneaster* sp., *Cydonia oblonga*, *Malus* sp., *Pyrus* sp. and *Sorbus* sp. (McManus & Jones, 1995; Barionovi, 2006; Donat *et al.*, 2007, Radunović *et al.*, 2017). Similarity coefficients obtained ranged from 96% to 99% among *E. amylovora* strains isolated from fruit-tree crops (McManus & Jones, 1995). This similarity was not restricted to genomic fingerprinting methods and was also consistent with the serological and physiological homogeneity (Vantomme *et al.*, 1982). Comparative genome analysis of *E. amylovora* supports the existence of low intraspecific diversity, particularly among the Amygdaloideae-infecting strains (McManus & Jones, 1995; Smits *et al.*, 2010; Zhao & Qi, 2011; Mann *et al.*, 2013).

All data considered, one may ask "How is that possible that a highly infectious bacteria disseminated around the world can be as homogenous?". To answer this question, it is necessary to take into consideration the evolution and dissemination of *E. amylovora* in the last 250 to 300 years.

E. amylovora was originally associated to indigenous host plants from North America prior to the introduction of apples and pears from the first European settlers in the 17th century. It is hypothesized that the presence of these new hosts may have encouraged a selection of *E. amylovora* genotypes highly virulent for domestic *Malus* sp. and *Pyrus* sp. (Rezzonico, 2011). Horticultural practices, such as vegetative propagation, may have enhanced the dissemination trough clonal host populations highly sensible to fire blight (Rezzonico, 2011). This breeding strategy applied to high-valued pome fruits varieties unable to overcome the disease, led to a restricted exposure of *E. amylovora* to selection pressures and limited genetic recombination events, promoting the lack of diversification among pathogen strains (McManus & Jones, 2011; Rezzonico, 2011; Smits *et al.*, 2011; Mann *et al.*, 2013).

3.2. Biological tests to assess pathogenicity and virulence of *Erwinia amylovora* isolates

The pathogenicity and virulence of *E. amylovora* isolates inoculated in healthy *Pyrus communis* cv. "Rocha" fruitlets were evaluated six DAI. Regarding their pathogenicity, 43 out of the 45 (95.56%) *E. amylovora* isolates were able to induce disease symptoms on the pear fruitlets. The symptoms observed were the typical symptoms of the disease and included formation of necrotic lesions and oozing surrounding the inoculation site (fig. 3.8).

Figure 3.8 - *Pyrus communis* fruitlets cv. "Rocha" 6 days after inoculation (DAI) with the *Erwinia amylovora* isolates tested. A. Pear fruitlets inoculated with 1× PBS (negative control, C^-). B. Pear fruitlets inoculated with *Erwinia amylovora* 1314 showing a black necrotic tissue and no oozing. C. Pear fruitlets inoculated with *Erwinia amylovora* 373 showing a black necrotic tissue and oozing. Scale bars = 10 mm.

The presence of a dark brown to black necrotic tissue surrounding the incision site was induced by all isolates. Regarding oozing, a positive result was induced by 18 isolates and an indeterminate result (50% of replicates had oozing and 50% of replicates had no oozing) was induced by 13 isolates, while 14 isolates were not able to induce oozing. Due to the high undermined results, oozing assessment was also registered at 12 DAI. In consequence, the number of positive results increased for 28 isolates and the indeterminate results decreased to 3 (Supplementary Table 1).

Erwinia amylovora induced an evolutive necrosis, characterized by the appearance of a black coloured tissue as a result of bacterial multiplication through intercellular spaces. Bacterial exudate or oozing, which is composed by bacteria and EPS, is a consequence of this migration through the tissues. Vanneste & Green (2000) associated symptom progression to an absorption of water by EPS and to the increase of physical pressure in intercellular spaces, which may lead to bacterial exudate. Although bacterial exudate is a common sign of fire blight, its presence is not mandatory (EPPO, 2004).

Lesion size was variable, ranging from 0.00 mm to a maximum size of 9.13 mm. *Erwinia amylovora* 142 and *E. amylovora* 544, did not cause any symptoms and were, consequently, classified as non-pathogenic. Three virulence categories were defined considering the heterogeneous results from lesion size, namely L (> 0.00 - 3.33 mm), M (> 3.33 - 6.66 mm) and H (> 6.66 - 9.99 mm) (fig. 3.9).

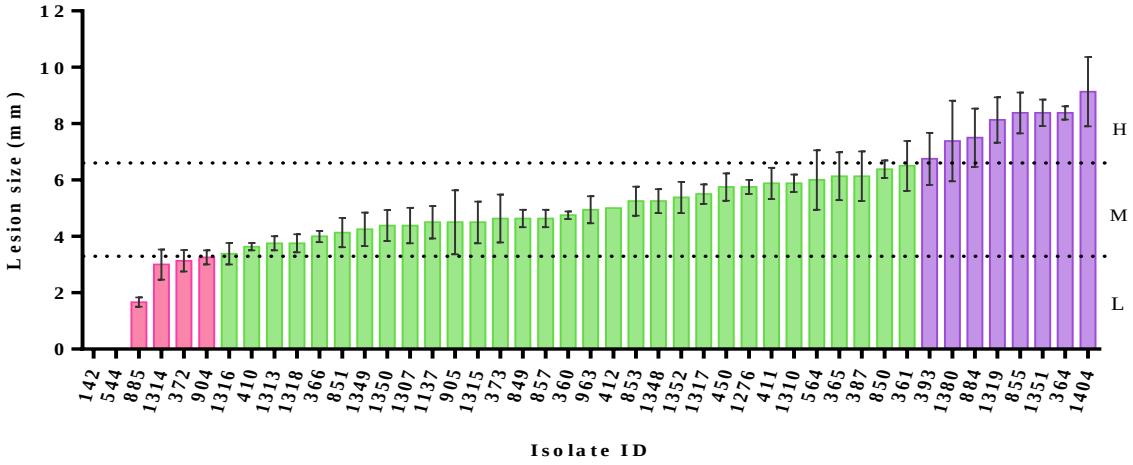

Figure 3.9 - Virulence assessment ± SEM (standard error of the mean) 6 days after inoculation (DAI) of healthy fruitlets of *Pyrus communis* cv. "Rocha" inoculated with the *Erwinia amylovora* isolates tested. The dotted lines define three virulence categories, namely low (L), medium (M) and high (H).

Out of the 45 isolates, 4.44% were non-pathogenic, 8.89% were in the L category, 68.89% were in the M category and 17.78% were in the H category (fig. 3.10). A second measurement of the lesion size at 12 DAI was not possible, since a considerable number of fruitlets were completely necrotized.

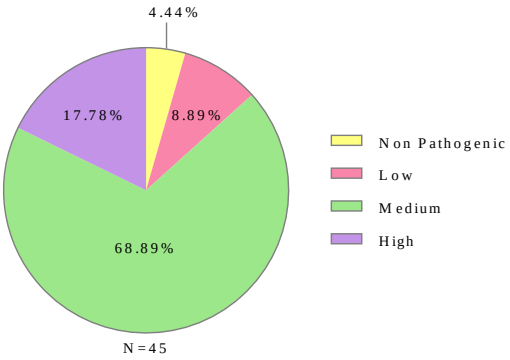

Figure 3.10 - Relative frequency of *Erwinia amylovora* isolates according to their pathogenicity and virulence categories.

A parallel boxplot was used to compare some aspects of the virulence categories at once (fig. 3.11). Low, Medium and High virulence categories displayed a mean of 2.76, 4.95 and 8.00 mm, respectively. The Medium category displayed the higher dispersion regarding the lesion size, whereas the lowest dispersion was observed in the High category (fig. 3.11), meaning that the isolates within the latter category had the lowest virulence variability. None of the virulence categories displayed symmetry and the skewness was different between categories. The medium category displayed a right skewed data set, while the remaining categories had a left skewed data set. This means that within the Low and High virulence categories, isolates with higher lesion sizes are closer together than the isolates with a smaller lesion size. In turn, in the Medium category, isolates with a smaller lesion are more condensed than isolates with a bigger lesion size. No obvious outliers were detected in any category (Zar, 2014).

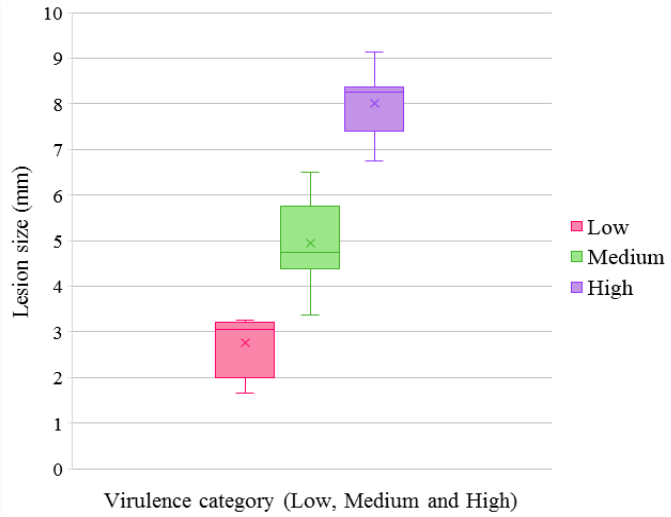

Figure 3.11 - Boxplots showing the distribution of the lesion size (mm) per virulence category. The lower and upper boundaries of each boxplot enclose 25–75% of the data. The line within the boxplots shows the median value, the bar lines above and below the boxplots indicate minimum and maximum values and × indicates the mean value. Low, Medium and High virulence categories boxplots were based on n = 4, n = 31 and n = 8 isolates, respectively.

No considerable differences in lesion size between Portuguese and European isolates were detected (fig. 3.12). The boxplot for the Portuguese isolates is larger in comparison to the boxplot for the European isolates, suggesting a higher virulence variability. Data from European and Portuguese

isolates are skew to the right. One outlier was detected in each region, corresponding to *E. amylovora* 142 and *E. amylovora* 544, respectively.

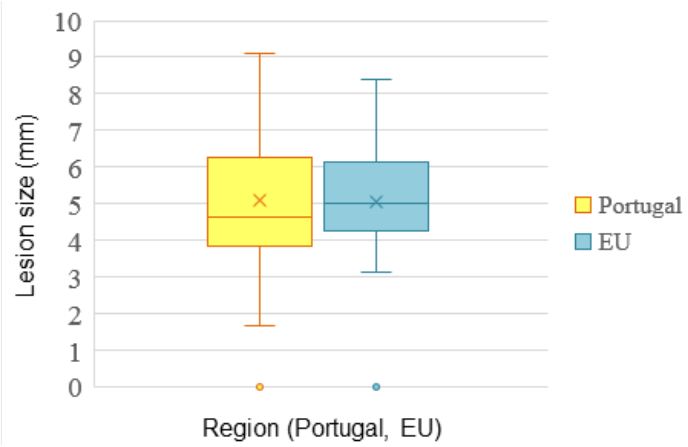

Figure 3.12 - Boxplots showing the distribution of the lesion size (mm) per region. The lower and upper boundaries of each boxplot enclose 25–75% of the data. The line within the boxplots shows the median value, the bar lines above and below the boxplots indicate minimum and maximum values and × indicates the mean value. Lesion size of Portugal and EU were based on n = 28 and n = 17, respectively.

The isolates studied were collected from 6 members of the Amygdaloideae subfamily, including *Crataegus* sp., *Cotoneaster* sp., *Cydonia oblonga*, *Malus* sp., *Pyrus* sp. and *Sorbus* sp. (Table 2.1). Except for *E. amylovora* 142 and *E. amylovora* 544, considered as non-pathogenic, all isolates were able to cause disease on the inoculated fruits, regardless of their original host. These results are not surprising, since generally Amygdaloideae-infecting strains do not evidence host specificity (van der Zwet & Keil, 1979; Mohan & Thomson, 1996, Momol & Aldwinckle, 2000). The adaptation to a wide range of hosts may be related to the relatively small number of type III secretion system (T3SS) effectors identified in *E. amylovora*, which may reflect a co-evolutive adaptation between the pathogen and their hosts (Smits *et al.*, 2010).

The high level of pathogenicity registered herein emphasized the high susceptibility of *P. communis* cv. "Rocha" to fire blight disease. *Pyrus communis* is very susceptible to *E. amylovora*, as it was reported as the least resistant host to fire blight (van der Zeit & Keil, 1979). Moreover, previous studies already highlighted the higher susceptibility of *P. communis* cv. "Rocha" in comparison to other Portuguese *P. communis* and *Malus domestica* varieties (Cruz *et al.*, 2018). The use of a susceptible host is important in pathogenicity assays since it allows eventual differentiation in virulence phenotypes, which is extremely beneficial particularly for genomically homogeneous pathogens.

The infection and pathogenesis of *E.* amylovora is intimately related to the synthesis of numerous virulence factors, which are crucial in the early stages of the disease (Piqué *et al.*, 2015). The production of a loose capsule composed by EPS, such as amylovoran and levan, is an obligatory component to a successful pathogenic process, since these are key elements for surpassing the host immune system, biofilm formation and protection against nutrient loss under dry conditions (Koczan *et al.*, 2009; Ordax *et al.*, 2009; Vrancken *et al.*, 2013). It has been demonstrated that a lack of amylovoran production or a mutation in the amylovoran synthesis (*ams*) genes cluster result in non-pathogenic strains (Bellemann & Geider, 1992; Geider *et al.*, 1993). Although amylovoran is considered one of the main virulence factors responsible for fire blight disease, by itself is not enough for the development of fire blight symptoms (Bernhard *et al.*, 1996). The hypersensitive reaction and pathogenicity (*hrp*) genes encode components of T3SS and effector proteins, such as disease specific A/E (DspA/E) effector (Oh & Beer, 2005; Oh et al., 2005). These components are essential for the pathogenicity and for the success in early stages of the infection. Thus, in their absence, *E. amylovora* pathogenicity is highly compromised (Zhao et al., 2005; Pester et al., 2012). Therefore, the non-pathogenic *E. amylovora* 142 and *E. amylovora* 544

may be related to a loss of pathogenic capacity, due to any of the mentioned mechanisms. However, non-pathogenic strains do not necessarily imply that the bacterium does not have the ability to invade and multiply inside the host. A previous study reported that shoots artificially inoculated with *E. amylovora* can persist as latent infection in symptomless tissues (Crepel *et al.* 1995). Although this hypothesis is a possibility for the non-pathogenic isolates in the present study, a longer inoculation time would be necessary to confirm it.

Virulence is often associated with processes of acquisition/deletion of genes or polymorphisms of virulence-associated genes (Ma *et al.*, 2006; Adhikari *et al.*, 2013). Variations regarding the synthesis and expression of EPS, as well as the T3SS and associated proteins, have a particularly important role in virulence differences between *E. amylovora* strains. Previous studies indicate that the level of virulence is correlated with the amount of amylovoran produced, which means that the greater the expression of amylovoran, the higher the virulence observed. (Maes *et al.*, 2001, Koczan *et al.*, 2009, Wang *et al.* 2009). Levan mutants may cause a slower development of symptoms in the host (Koczan *et al.*, 2009). Genome sequencing of 12 strains of *E. amylovora* revealed a very high similarity in the *ams* genes cluster, but variation in the *hrp* genes cluster (Mann *et al.*, 2013). Moreover, despite the extremely high genomic homogeneity among *E. amylovora*, particularly for the Amygdaloideae-infecting strains, the results obtained reinforce the existence of a differential expression of virulence genes which resulted in a diverse virulence phenotype on the infected *P. communis* cv. "Rocha" fruitlets. A lower expression of some of these factors may result in naturally less virulent isolates, which may make it difficult to overcome the host defences, and possibly may compromise strain pathogenicity.

Noteworthy, all isolates included in the low virulence category belonged to CRISPR genotype D. An association between the two variables was observed (Fisher's exact test; $p = 0.0393$) (Supplementary fig. 3), yet how they can interact is unknown. CRISPR-Cas system has an important role in microbial adaptive immunity against foreign nucleic acids (Horvath & Barrangou, 2010). However, only recently the role of CRISPR in pathogenicity and virulence has started to be explored. For instance, CRISPR-cas9 system seems to be involved in the regulation of virulence associated genes of the pathogen *Campylobacter jejuni* (Shabbir *et al.*, 2018).

3.3. Polyphasic analysis of *Erwinia amylovora* isolates

The diversity of *E. amylovora* isolates was assessed through a polyphasic analysis based on phenotypic and genotypic characters. The present analysis did not include the genomic fingerprinting results, since they did not allowed strain discrimination. Thus, it was based on phenotypic (i.e. pathogenicity, virulence and oozing) and genomic characters (i.e. CRISPR-PCR) This analysis discriminated the isolates into 11 groups (I, II, III, IV, V, VI, VII, VIII, IX, X and XI) (Table 3.1). Group III comprised the higher number of isolates ($n = 13$), followed by groups VIII and VII ($n = 7$ and $n = 6$, respectively) that differ in oozing. Groups II, V and IX comprised only one isolate each.

Table 3.1 - Diversity of *Erwinia amylovora* isolates based on phenotypic (pathogenicity, virulence and oozing) and genomic (CRISPR-PCR) characters. Additional data regarding host species was taken into consideration to further discriminate the isolates into groups (I, II, III, IV, V, VI, VII, VIII, IX and X).

Characteristics				**Host species**												**n**	**Group**
Pathogenicity	**CRISPR-PCR**	**Virulence**	**Oozing**	*Pyrus communis*	*P. malus*	*P. pyrifolia*	*P. amigdaligormis*	*Mallus domestica*	Pomme tree	*Cydonia oblonga*	*Sorbus* sp.	*Crataegus* sp.	*Cotoneaster salicifolius*	*Cotoneaster* sp.	Unknown		
Y	A	H	Y	2									1		2	5	**I**
			N	1												1	**II**
		M	Y	3			1	2	1	1		1	1	1	2	13	**III**
			V							1	2					3	**IV**
			N												1	1	**V**
	D	H	Y												3	3	**VI**
		M	Y	3		1						1			1	6	**VII**
			N	3	1			2				1				7	**VIII**
		L	Y	1												1	**IX**
			N	2											1	3	**X**
N	A	NA	NA						1			1				2	**XI**
Total				15	1	1	1	4	2	2	2	4	2	1	10	45	11

n = number of isolates, Y = yes, N = no, V = variable, H = high, M = medium, L = low, NA = not applicable.

The combined analysis of phenotypic and genotypic data allowed the detection of a higher level of diversity among *E. amylovora* isolates when compared to the individual analysis of each character. However, it was not possible to establish any association between the hosts from which the isolates were obtained, and their corresponding groups formed in the present analysis. For example, the isolates from *P. communis* are distributed over several groups, which suggests that isolates of *E. amylovora* obtained from the same host species present both phenotypic and genotypic variability. This may be related with the lack of host specificity that Amygdaloideae-infecting strains generally display. Interestingly, both isolates collected from *Sorbus* sp. are included in group IV, however the number of isolates is too small to establish any association.

3.4. Flow cytometry

3.4.1. Viability assessment optimization for pure culture analysis

In order to validate the method for the assessment of *E. amylovora* viability by FCM, protocols were optimised using pure cultures. Cultures were grown to exponential phase, and harvested cells were centrifuged at 4 000 rpm for 15 min at room temperature; the cells were washed twice and resuspended in 1× PBS buffer, and the cell concentrations were determined by cytometry (TVAC). For optimization of viability staining, the sample concentrations were adjusted prior to staining by dilution with 1× PBS to obtain cell concentrations in a range of 5×10^5 to 1×10^6 cfu mL^{-1}. Mixtures of live (untreated) and dead (heat-treated) cells were prepared with defined ratios (100%, 75%, 50%, 25% and 0% viability); therefore, cells suspensions both from viable and dead cells were adjusted to a fixed cell concentration.

Membrane integrity – Syto9 + PI

Regardless of whether the cells are untreated or heat-treated, the cell population under study (FCS *vs* SSC) was homogeneous and showed well defined scattering signals (fig. 3.13 A and B).

Simultaneous staining of bacterial cells with Syto9 and PI resulted in a characteristic and reproducible viability pattern in plots; the red (FL3) *vs.* green (FL1) fluorescence dot plots and the fluorescence ratio histogram (FL1/FL3) clearly differentiate viable cells with intact membranes (fig. 3.13 A), from dead cells with permeable membranes (fig. 3.13 B).

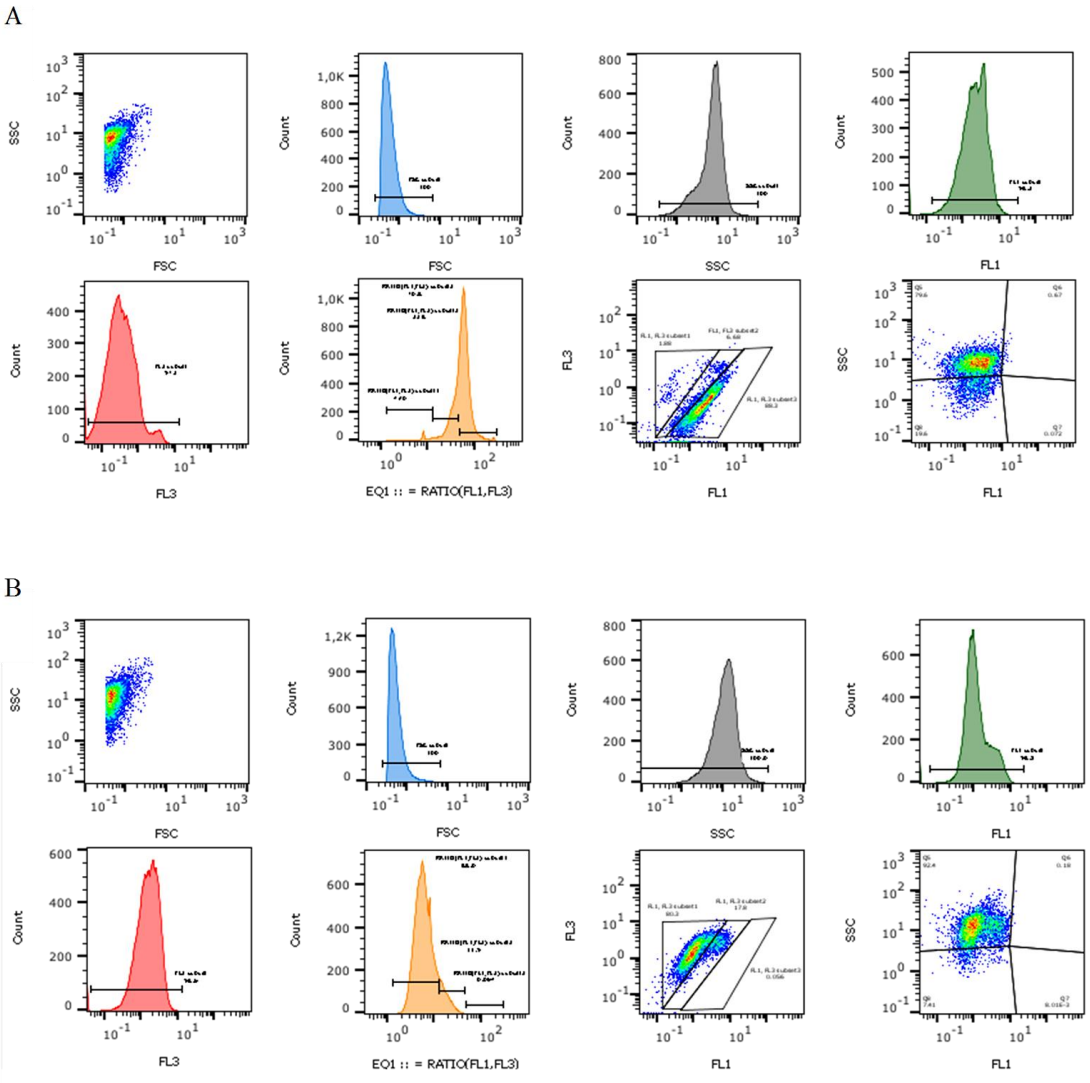

Figure 3.13 - Example of flow cytometry data acquisition of *Erwinia amylovora* 885 using Syto9 and PI. A. Live cells (untreated, LC). B. Dead cells (heat-treated, KC).

Figure 3.14 presents a comparative analysis of the results obtained in the assessment of the viability in the different mixtures of viable cells and dead cells previously defined.

A maximum value of green fluorescence intensity was detected in 100% live cells (LC) samples. As the percentage of LC decreased, a progressive right-to-left deviation of green fluorescence occurred, reaching a minimal value in the presence of 100% heat-treated cells (killed cells, KC) (fig. 3.14 A). The emission of red fluorescence had a minimum value in the presence of 100% LC, and a progressive right-deviation was observed with the decrease of LC, reaching a maximum peak in 100% KC (fig. 3.14 B). Differences in green (Syto9) and red (PI) fluorescence have become more evident by analysing the fluorescence ratio (FL1/FL3), which allows a clear differentiation of subpopulations (fig. 3.14 C).

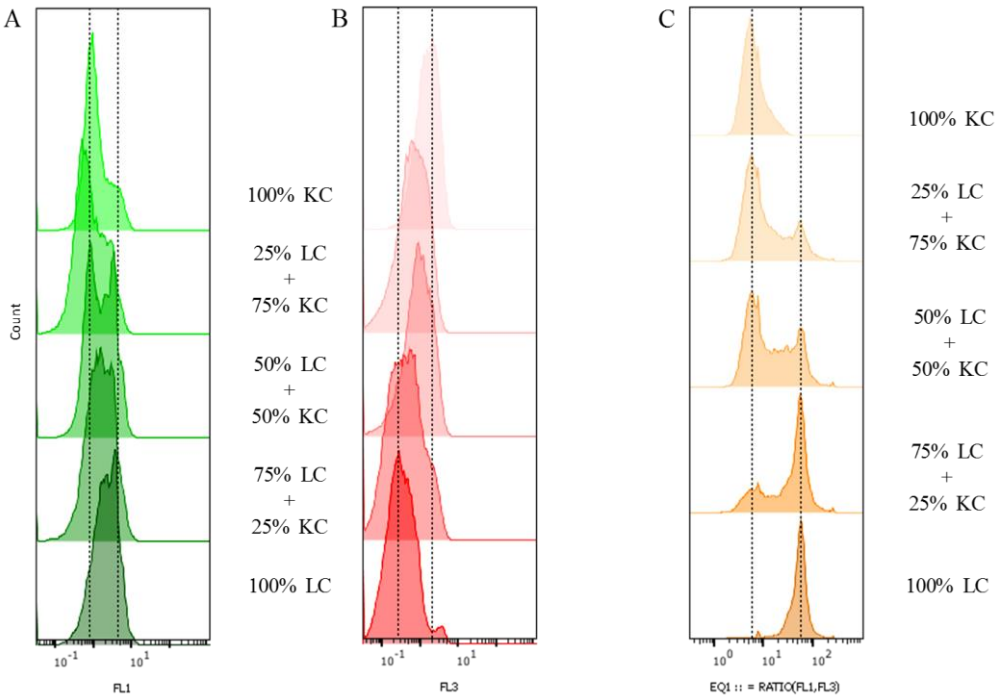

Figure 3.14 - Flow cytometry comparison of different proportions of live cells (LC) and heat-treated cells (KC) of *Erwinia amylovora* 885 using Syto9 and PI. A. Syto9 fluorescence histogram (FL1). B. PI fluorescence histogram (FL3). C. Ratio of Syto9 to PI fluorescence (EQ1 = FL1/ FL3).

Fluorescence deviations observed in different untreated and treated cells mixtures can be explained by the affinity of both fluorophores for their target. Syto9 is a green membrane-permeable nucleic acid stain, which means that theoretically it can enter and stain equally cells with an intact or damaged membrane. However its fluorescence may change in the presence or absence of PI (Nebe-von-Caron *et al.*, 2000; Stocks, 2004; Díaz *et al.*, 2010). PI is a red membrane-impermeable nucleic acid stain, which enters in cells with compromised or damaged membranes, such as injured and dead cells (Díaz *et al.*, 2010). Viable cells exhibited high green fluorescence and low red fluorescence, whereas injured or killed cells showed high red fluorescence and low green fluorescence (Jung *et al.*, 2008; Díaz *et al.*, 2010). Nevertheless, when Syto9 and PI are simultaneously present within a cell, the fluorophores can interact resulting in Syto9 signal quenching and PI signal enhancement. As PI possesses a stronger affinity to nucleic acids than Syto9 (association constants respectively at 3.7×10^5/M and 1.8×10^5/M), a decrease of green fluorescence and an increase of red fluorescence emission can be observed (Stocks, 2004). Moreover, the emission spectrum of Syto9 overlies the excitation spectrum of PI, insomuch that a potential fluorescence resonant energy transfer (FRET) may occur, which is characterized by energy allocation from Syto9 to PI. The occurrence of FRET between the fluorophores used might suggest that the stains can be simultaneously present on the DNA molecule (Stocks, 2004).

Remarkably, although PI is a membrane impermeable stain, red fluorescence emission was higher in LC samples than in control samples (i.e. without stains). If LC have intact cellular membranes through which PI should not be able to enter due to its chemical properties, how is this possible?

This paradoxical effect can be mainly explained by two reasons: a) unbound PI has a strong background signal (Stiefel *et al.*, 2015), and b) certain cell physiology status leading to membrane permeability change, such as cell division and wall synthesis, may contribute to PI entrance in the cell and, consequently, to disturbances in red fluorescence emission (Ruger *et al.*, 2012; Stiefel *et al.*, 2015). This last scenario raises a problem, since it can suggest that living cells may be considered dead cells, over- or underestimating cell viability.

The results gathered by Syto9 (FL1) × PI (FL3) dot-plots (fig. 3.15), enabled the visualization of the distribution of *E. amylovora* subpopulations, as well as their relative population density, according to their cytoplasmic membrane integrity. As a result of the differential green and red fluorescence emission, three subpopulations were defined, namely a subpopulation of viable cells (LC on the right gate), a subpopulation of injured cells (on the middle gate) and a subpopulation of dead cells (KC on the left gate). The relative density of each subpopulation varied according to the LC/KC ratio. In 100% LC samples, a higher population density at the right gate and a lower cell density at the left gate were observed. However, as the percentage of KC increased, a progressive shift of population density from right to the left occurred.

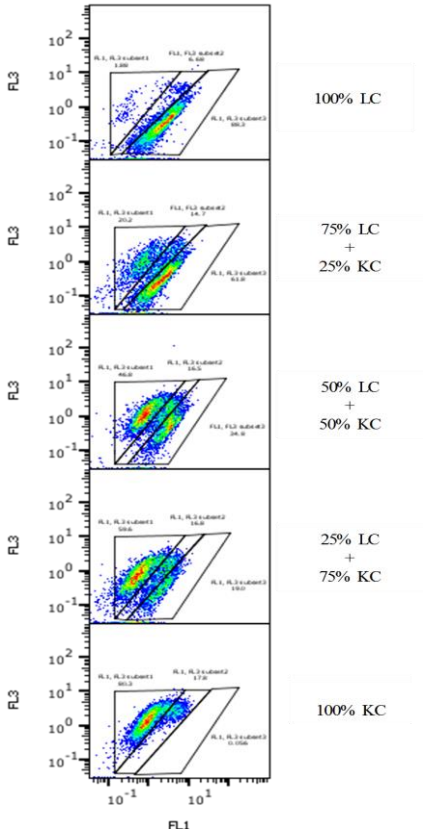

Figure 3.15 - Pseudo-colour dot-plots Syto9 (FL1) × PI (FL3) in different ratios of live cells (LC) and heat-treated cells (KC) of *Erwinia amylovora* 885. Blue and green areas represent low cell density, yellow areas represent a mid-range cell density and orange and red areas represent high cell density.

Although untreated cells were considered 100% viable, about 22% of the cells were damaged and about 4.5% were dead (table 3.2). In 100% KC samples, about 12.5% of cells could be considered injured (table 3.2 and fig. 3.16), which seems to suggest the existence of cells resistant to the heat treatment process. This may be due to the fact that the temperature (60 ºC) or the incubation time used were not sufficient. It was not possible to raise the temperature due to the occurrence of cell lysis at higher temperatures (data not shown). This pattern strongly suggests that injured cells correspond to intermediate states of viability, which are characterized by different intracellular concentrations of Syto9 and PI that can evolve into viable cells or dead cells, depending on external conditions; these cells were considered as a subpopulation on their own, with distinct physiological characteristics.

Table 3.2 - Expected and observed cellular viability (%) for the ratio (FL1/FL3). These values were calculated for live, damaged and dead cells in each sample examined. Each value of the observed viability corresponds to the mean (± standard deviation) of n = 3.

Sample	Expected viability (%)	Observed viability | FL1/FL3 (%)		
		Dead cells	Damaged cells	Live cells
100% LC	100	4.54 ± 0.55	22.6 ± 0.15	70,8 ± 0.85
75% LC + 25% KC	75	22.53 ± 0.68	27.3 ± 0.20	48.6 ± 0.90
50% LC + 50% KC	50	51.83 ± 1.40	27.1 ± 1.40	20.4 ± 0.06
25% LC + 75% KC	25	63.43 ± 0.84	20.1 ± 1.12	16.2 ± 1.46
100% KC	0	87.37 ± 2.03	12.5 ± 2.01	0.09 ± 0.03

As shown in table 3.2 and figure 3.16, the percentage of injured cells has remained relatively constant (≈ 20 – 27%) in all mixtures, being slightly lower in the sample of 100% dead cells (12%). For data obtained from the validation experiments, the % of experimentally determined live and dead cells was used to generate a scatter plot against the expected proportions as derived from the different LC/KC adjusted ratios. The scatter plot was analysed using a linear regression analysis. A good correlation was observed between the expected and determined viability when using Syto9 and PI for LC (R^2 = 0.95) and KC (R^2 = 0.99) (Supplementary fig. 4).

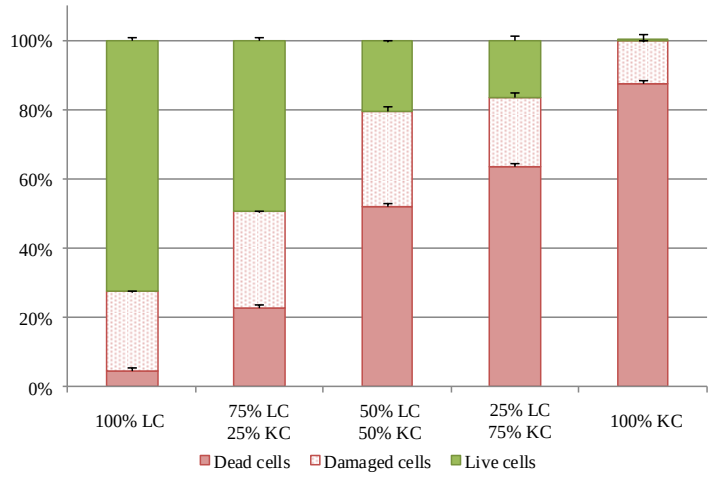

Figure 3.16 - Stacked bar chart highlighting the observed cellular viability (%) (± standard deviation) for the ratio (FL1/FL3) in each sample.

Membrane potential – $DIBAC_4(3)$

Cellular viability was also assessed using $DIBAC_4(3)$, a slow-response and membrane potential-dependent fluorophore that enters depolarized cells and binds to intracellular proteins positively charged (Rezaeinejad & Ivanov, 2009; Díaz *et al.*, 2010). As a result of this sensitivity to membrane potential, distinct intensity of green fluorescence enabled the differentiation between metabolically active (LC) and metabolically inactive (KC) cells (fig. 3.17). A lower intensity of green fluorescence associated with viable cells was observed, as they were energized and had polarized membranes. As the proportion of dead cells increased, a left-to-right fluorescence shift was observed due to an increase in the depolarization of the membranes, resulting in the entrance of $DIBAC_4(3)$ into the cells and, consequently, in an enhancement of green fluorescence intensity. In 100% LC and mixed ratios LC/KC, two distinct fluorescence intensity peaks were evident.

The untreated cells (100% LC) (fig. 3.17) showed a small peak of higher fluorescence intensity, which may represent that in this initial population some cells could be partially depolarized.

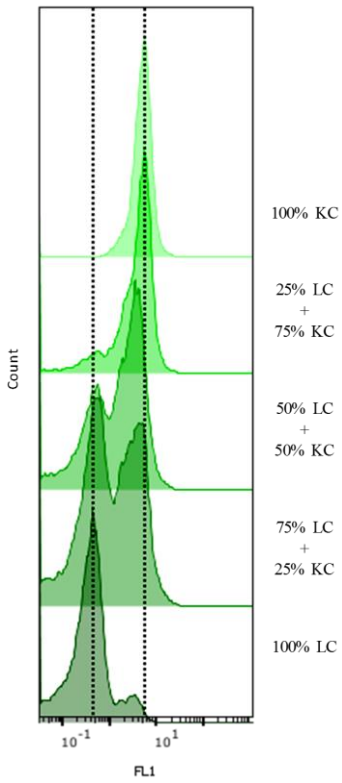

Figure 3.17 - FCM comparison of different proportions of *Erwinia amylovora* 885 live cells (LC) and heat-treated cells (KC) using $DIBAC_4(3)$. Green fluorescence histogram (FL1).

Figure 3.18 presents a comparative illustration of the results obtained with *E. amylovora* 885 cells in suspension, with different LC/KC ratios, for cell vitality evaluation. In the graphs it was possible to visualize the distribution of *E. amylovora* subpopulations and their relative density according to their metabolic activity/membrane potential. As expected, in the 100% LC sample, a higher population density was observed on the left gate (fig. 3.18 A), due to the polarized membrane that prevent the entry of $DIBAC_4(3)$. A small population was also detected at the right gate, revealing the presence of some depolarized cells. As verified with Syto9 and PI, these results suggest that, although this sample had a theoretical value of 100% energised cells, a small percentage of depolarized cells was present. With the increase of dead cells, a shift in the population density from the left to the right gate was observed.

Although $DIBAC_4(3)$ emits green fluorescence, it can also cause a red spectral shift with membrane depolarization, and for this reason the analysis of FL1 × FL3 dot-plots was performed (fig. 3.18 B). Besides the above-mentioned increase in green fluorescence, with the membrane depolarization, a slight increase in red fluorescence was also observed in the presence of dead cells. Any of these dot-plots can be used to differentiate *E. amylovora* subpopulations relatively to the membrane potential.

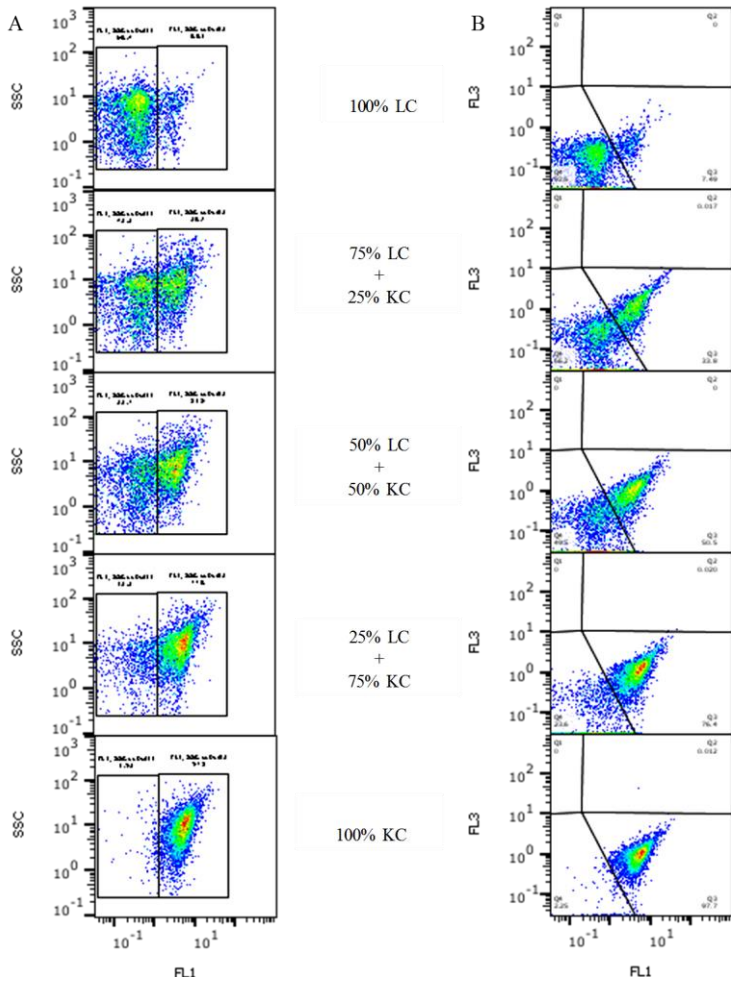

Figure 3.18 - Pseudo-colour dot-plots correspondents to different ratios of live (LC) and dead (KC) cells of *Erwinia amylovora* 885 stained with DIBAC$_4$(3). A. Green fluorescence (FL1) × SSC. B. Green fluorescence (FL1) × Red fluorescence (FL3). Blue and green areas represent low cell density, yellow areas represent a mid-range cell density and orange and red areas represent high cell density.

A linear correlation was observed between the expected and observed viability when using DIBAC$_4$(3) (R^2 = 0.99) (fig. 3.19).

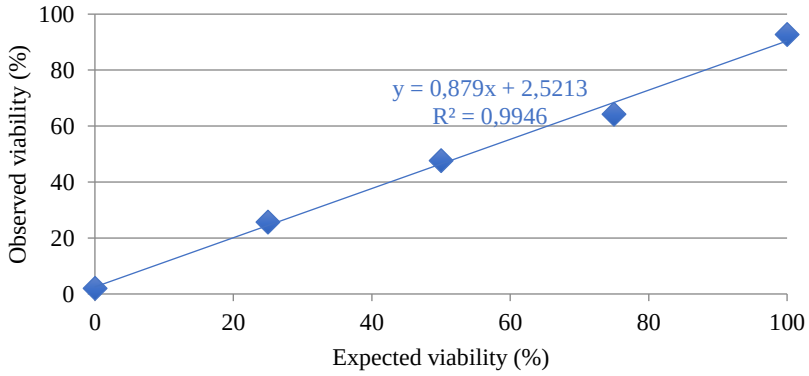

Figure 3.19 - Correlation between the expected and observed viability (%) using DIBAC$_4$(3) for FL1 × FL3 dot-plot of *Erwinia amylovora* 885 determined by flow cytometry.

A linear correlation was observed between the expected and observed viability when using DIBAC$_4$(3) or Syto9 (R^2 = 0.97) in *E. amylovora* 885 dead cells (fig. 3.20), which means that both

fluorophores are suitable to assess *E. amylovora* viability. Thus, the choice between the two fluorophores will depend on the purpose of the study.

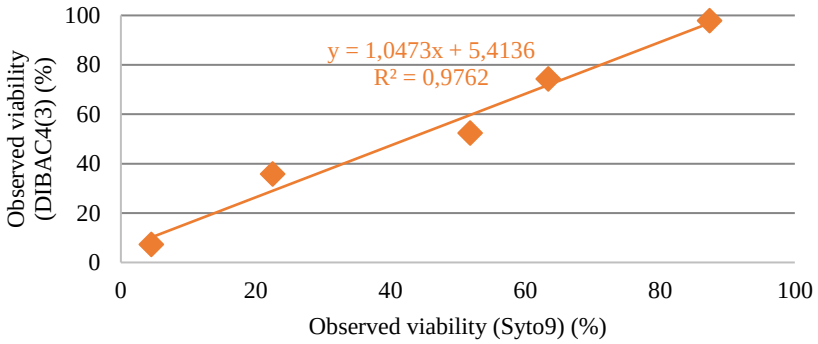

Figure 3.20 - Correlation between the observed viability (%) using $DIBAC_4(3)$ or Syto9 in *Erwinia amylovora* 885 dead cells determined by flow cytometry.

3.4.2. Cellular viability assessment of *Erwinia amylovora* in mixed samples

The previous FCM assays were successful in the characterization of cell viability of a pure culture of *E. amylovora*. However, this can be compromised in the analysis of environmental samples, where microbial communities are commonly associated. For this reason, it was appropriate to evaluate and compare responses of *E. amylovora* cells to fluorophores in mixed samples. For this purpose, besides *E. amylovora*, two other bacteria were analysed, namely *Aeromonas veronii* (Gram-negative) and *Staphylococcus cohnii* (Gram-positive).

Although Syto9 and PI are general nucleic acid stains used for viability assays, it has been reported that the response of bacteria to these stains is not always the same. Stiefel *et al.* (2010) observed that Syto9 entrance is more difficult in live Gram-negative bacteria than in Gram-positive bacteria, due to the presence of the external membrane. Thus, since the response of bacteria to fluorophores is not linear, the present study explored whether these differences would allow to distinguish *E. amylovora* from other bacteria in mixed sample.

Figures 3.21 and 3.22 summarize the homogeneity of the responses of untreated cells of *E. amylovora* and *A. veronii* (both Gram-negative cells) to Syto9 and PI. The observed green and red fluorescence values (fig. 3.21 A and B) were close, insomuch that when assessing the ratio of FL1 to FL3 in a mixed sample with both bacteria, the fluorescence peaks were overlapping (fig. 3.21 C). As expected, due to the overlapping of fluorescence emission peaks, in the FL1 × FL3 and ratio (FL1/FL3) × SSC dot-plots (fig. 3.22) the two populations were undistinguishable.

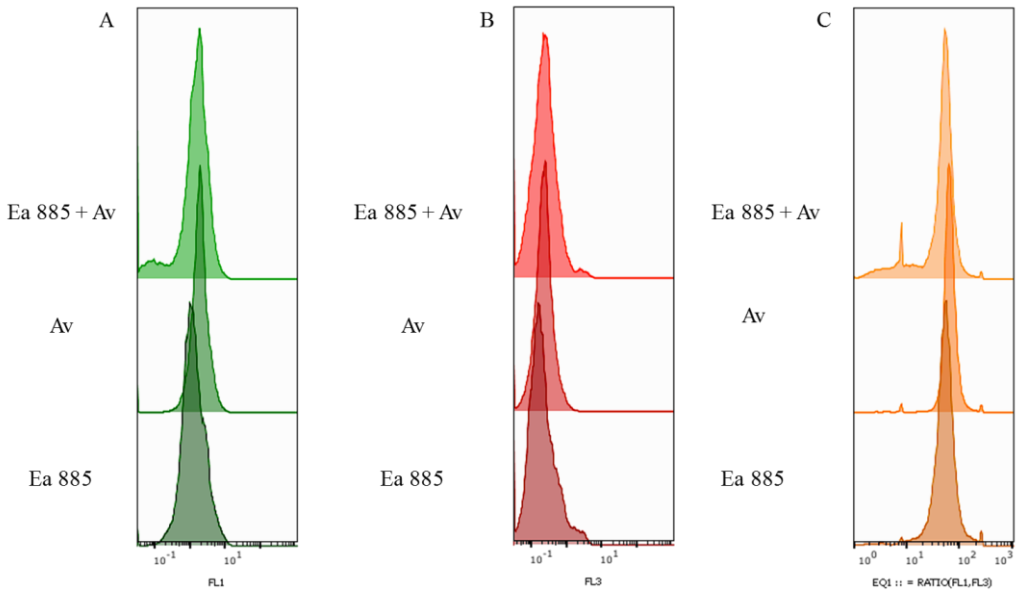

Figure 3.21 - Green and red fluorescence of *Erwinia amylovora* 885 (Ea 885) and *Aeromonas veronii* (Av) untreated cells (LC) using Syto9 and PI. A. Syto9 fluorescence histogram (FL1). B. PI fluorescence histogram (FL3). C. Ratio of Syto9 to PI fluorescence (EQ1 = FL1/ FL3).

Cells of *E. amylovora* and *A. veronii* heat-treated and stained with Syto9 and PI were also analysed by FCM. Figure 3.22 represents the comparison between the isolated response of each bacteria in pure cultures and their combined response when in mixed samples. In general, green fluorescence decreased on *E. amylovora* and *A. veronii* KC, however a second peak with higher intensity of green fluorescence was observed in *A. veronii* cells, suggesting the presence of LC in the sample (fig. 3.23 A); the red fluorescence increased in *E. amylovora* and *A. veronii* (fig. 3.23 B), but the presence of a subpopulation of *A. veronii* viable or injured cells was confirmed in ratio (FL1/FL3) histogram (fig. 3.23 C).

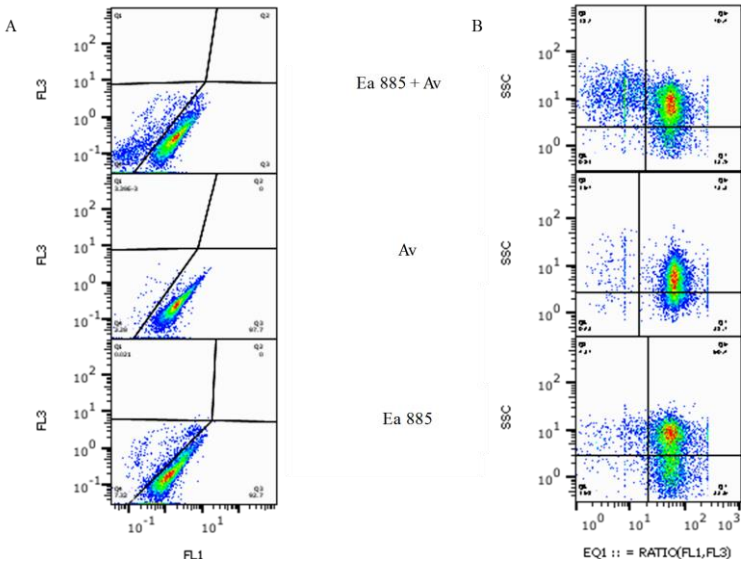

Figure 3.22 - Pseudo-colour dot-plots untreated cells of *Erwinia amylovora* 885 (Ea 885) and *Aeromonas veronii* (Av). A. Syto9 (FL1) × PI (FL3). B. Ratio of Syto9 to PI fluorescence (EQ1 = FL1/ FL3) × SSC.

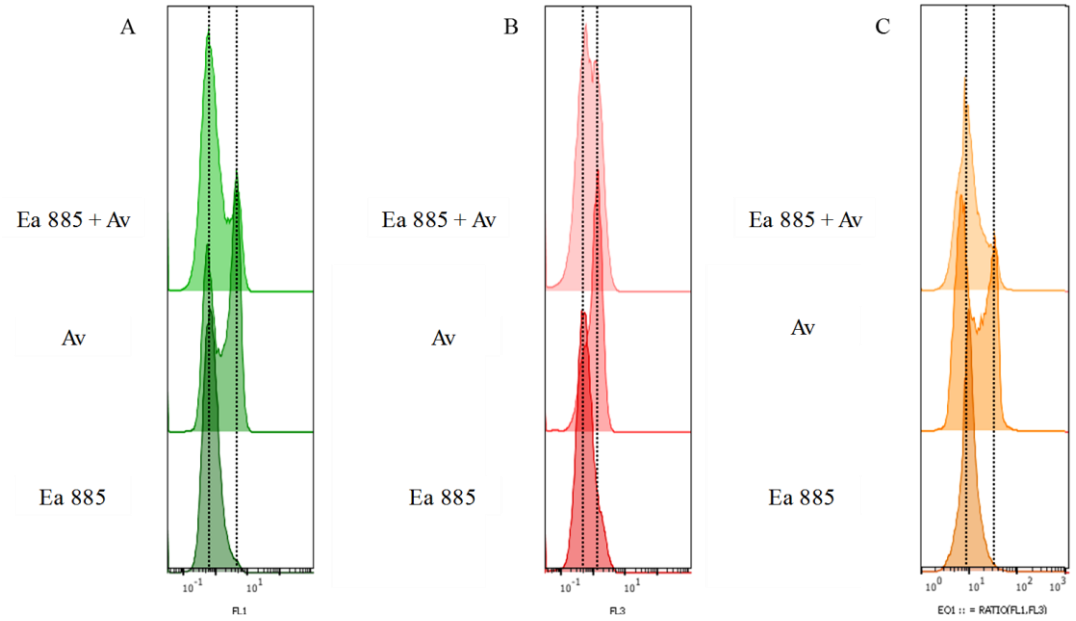

Figure 3.23 - Green and red fluorescence of *Erwinia amylovora* 885 (Ea 885) and *Aeromonas veronii* (Av) heat treated cells (KC) using Syto9 and PI. A. Syto9 fluorescence histogram (FL1). B. PI fluorescence histogram (FL3). C. Ratio of Syto9 to PI fluorescence (EQ1 = FL1/ FL3).

As expected, due to the similar fluorescence, in FL1 × FL3 and ratio (FL1/FL3) × SSC dot-plots (fig. 3.24 A and B) the two bacteria were undistinguishable. However, it was possible to differentiate a small subpopulation of *A. veronii* from the remaining dead cells. These results confirmed the presence of a dead cells population (on the left gate) and a population of living or injured cells (on the right gate), suggesting that the temperature (60 ºC) used in the heat-treatment process was not sufficient to kill *A. veronii* cells, and that this bacterium was more resistant to high temperatures when compared with *E. amylovora*.

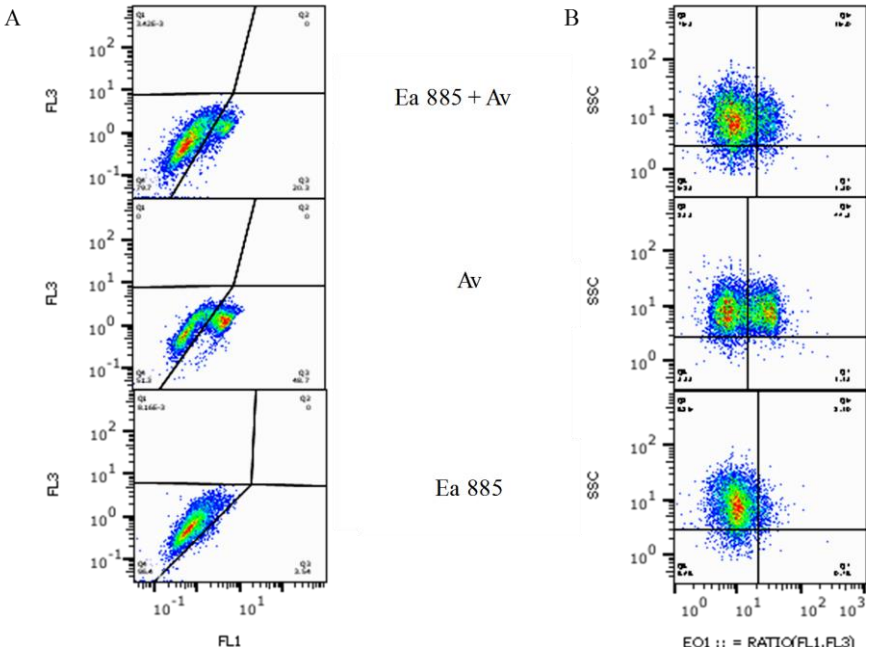

Figure 3.24 - Pseudo-colour dot-plots of heat-treated cells (KC) of *Erwinia amylovora* 885 (Ea 885) and *Aeromonas veronii* (Av). A. Syto9 (FL1) × PI (FL3). B. Ratio of Syto9 to PI fluorescence (EQ1 = FL1/ FL3) × SSC.

Interestingly, despite the similarity observed in the cytometric profiles when comparing untreated cells of *S. cohnii* (Gram-positive) and *E. amylovora* (fig. 3.25), the former has presented a slightly higher red fluorescence (fig. 3.25 B). Thus, it was possible to discriminate the two bacterial populations in the mixed sample by analysing the FL1/FL3 histogram (fig. 3.25 C), FL1 × FL3 and (FL1/FL3) × SSC dot-plots (fig. 3.26). In the dot-plot FL1 × FL3, *S. cohnii* population was found in quadrant Q4 due to the higher red fluorescence, while *E. amylovora* was found in quadrant Q3 (fig. 3.26 A). In the dot-plot (FL1/FL3) × SSC, the population of *E. amylovora* was delimited on the right side of the vertical gate (fig. 3.26 B), which corresponds to the highest ratio values due to the lower red fluorescence.

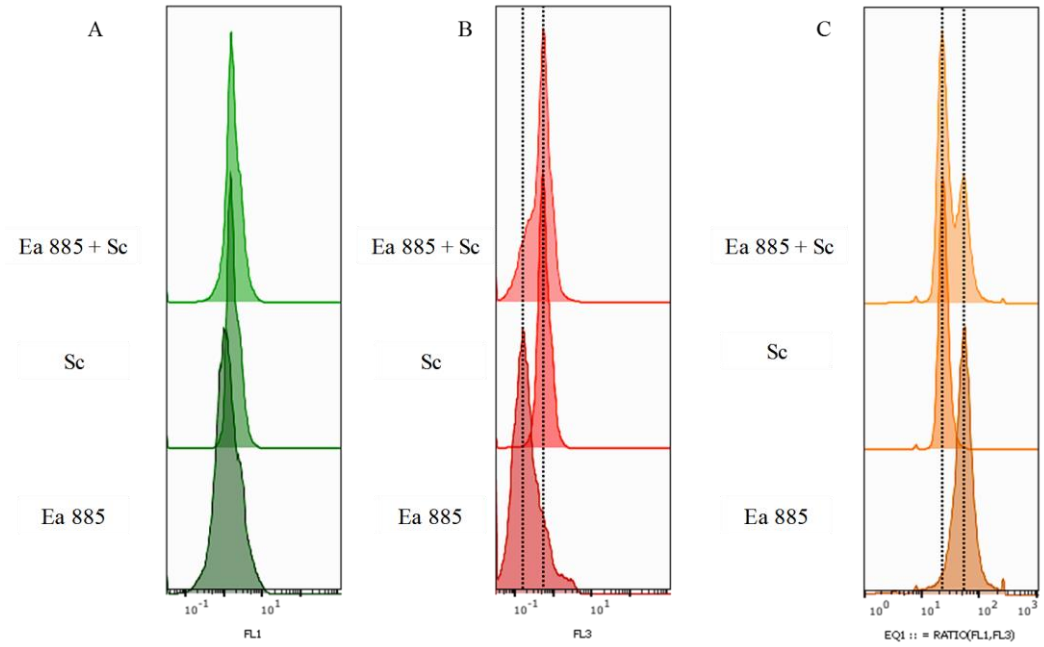

Figure 3.25 - Green and red fluorescence of *Erwinia amylovora* 885 (Ea 885) and *Staphylococcus cohnii* (Sc) untreated cells (LC) using Syto9 and PI. A. Syto9 fluorescence histogram (FL1). B. PI fluorescence histogram (FL1). C. Ratio of Syto9 to PI fluorescence (EQ1 = FL1/ FL3).

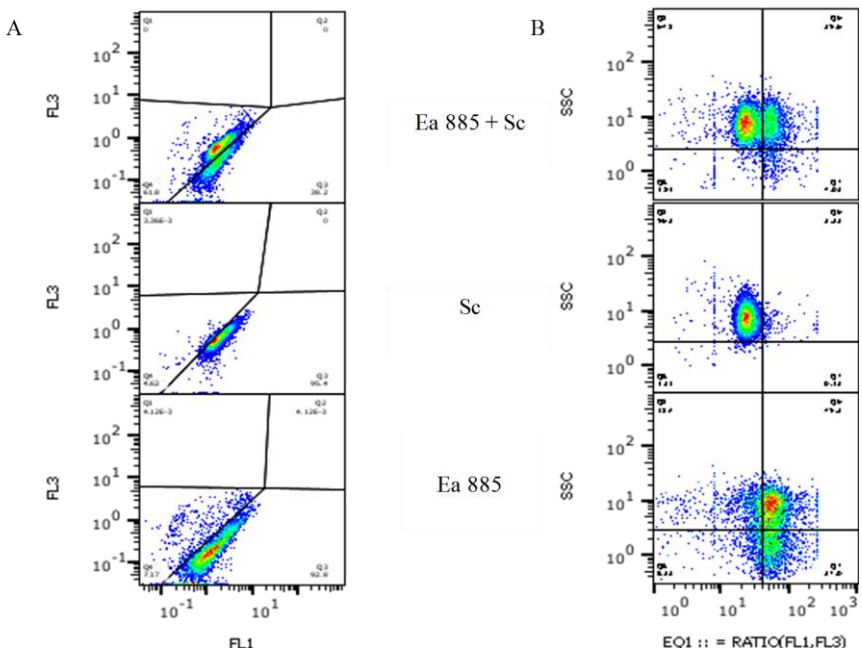

Figure 3.26 - Pseudo-colour dot-plots untreated cells (LC) of *Erwinia amylovora* 885 (Ea 885) and *Staphylococcus cohnii* (Sc). A. Syto9 (FL1) × PI (FL3); B. Ratio of Syto9 to PI fluorescence (EQ1 = FL1/ FL3) × SSC.

For heat-treated cells (KC), an increase in red fluorescence and a decrease in green fluorescence were observed in *E. amylovora*, due to the competition between fluorophores, as previously discussed (see 3.4.1.). For *S. cohnii* KC, green fluorescence slightly increased while red fluorescence remained unchangeable in comparison to LC samples (fig. 3.27 A and B). Since red fluorescence stayed relatively constant, the ratio (FL1/FL3) value was higher for *S. cohnii* than for *E. amylovora* (fig. 3.27 C).

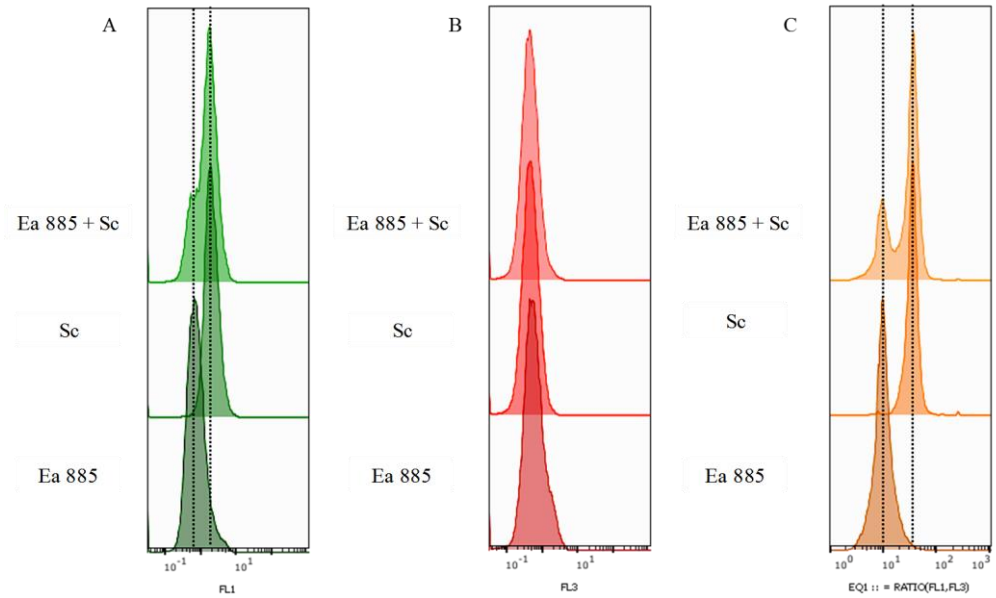

Figure 3.27 - Green and red fluorescence of *Erwinia amylovora* 885 (Ea 885) and *Staphylococcus cohnii* (Sc) heat-treated cells (KC) using Syto9 and PI. A. STYO 9 fluorescence histogram (FL1). B. PI fluorescence histogram (FL3). C. Ratio of Syto9 to PI fluorescence (EQ1 = FL1/ FL3).

Consequently, in the dot-plots FL1 × FL3 and ratio (FL1/FL3) × SSC (fig. 3.28), it was possible to differentiate the two bacterial populations. At FL1 × FL3 dot-plot, *S. cohnii* population was found in quadrant Q3, due to the higher green fluorescence emission, while *E. amylovora* was found in

quadrant Q4 (fig. 3.28 A). In the ratio (FL1/FL3) × SSC dot-plot, *E. amylovora* was on the right side of the vertical gate, due to a higher ratio value, while *S. cohnii* was on the left side (fig. 3.28 B).

These results suggest that the different responses of the bacteria to fluorophores, may interfere in the assessment of the cellular viability of *E. amylovora* in environmental samples. In the present study, it was possible to differentiate between *E. amylovora* and *S. cohnii*, but *E. amylovora* and *A. veronii* behaved in a very similar way in response to the fluorophores used, which made it very difficult to distinguish them.

Cell viability by itself does not always have the ability to distinguish *E. amylovora* population from other bacteria. Considering that in environmental samples the number of bacteria species present may be high, and that the cell viability status of bacteria in the same ecological niche may be similar, this is a limiting factor for the detection and cell viability assessment of *E. amylovora*.

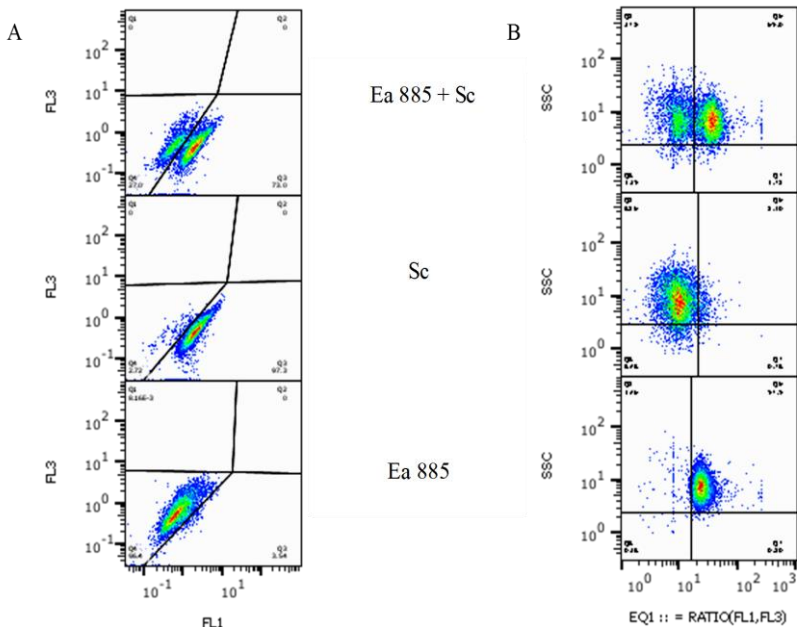

Figure 3.28 - Pseudo-colour dot-plots between different ratios of heat-treated cells (KC) of *Erwinia amylovora* 885 (Ea 885) and *Staphylococcus cohnii* (Sc). A. Syto9 (FL1) × PI (FL3). B. Ratio of Syto9 to PI fluorescence (EQ1 = FL1/ FL3) × SSC.

The ability to differentiate specific bacteria species in mixed samples is extremely difficult using only the fluorescent staining approach. An alternative method for species differentiation in mixed samples is to combine viability staining with specific antibody labelling.

3.4.3. Detection of *Erwinia amylovora* by immuno-flow cytometry

The association of FCM with monoclonal or polyclonal antibodies against specific cellular antigens could enable to identify cell populations within a background mixture of bacteria in a sample matrix (Kennedy & Wilkinson, 2017). In the present study, light scatter signals were used to identify the cell population of interest, while the measurement of fluorescence intensity provided specific information on each individual cell or labelled target cells.

The FSC and SSC signals obtained with *E. amylovora* and *S. cohnii* were very similar (fig. 3.29 A), although some heterogeneity in SSC was observed, namely in *S. cohnii* (fig. 3.29 B). In mixed samples, FSC and SSC signals are not enough to discriminate between the two bacterial populations. The use of a monoclonal primary antibody conjugated with FITC, allowed the visualization of a high green fluorescence corresponding to *E. amylovora* and a low green fluorescence corresponding to *S. cohnii*

(fig. 3.29 C). Thus, in mixed samples the existence of two distinct green fluorescence intensity peaks enabled the differentiation between *E. amylovora* and *S. cohnii*.

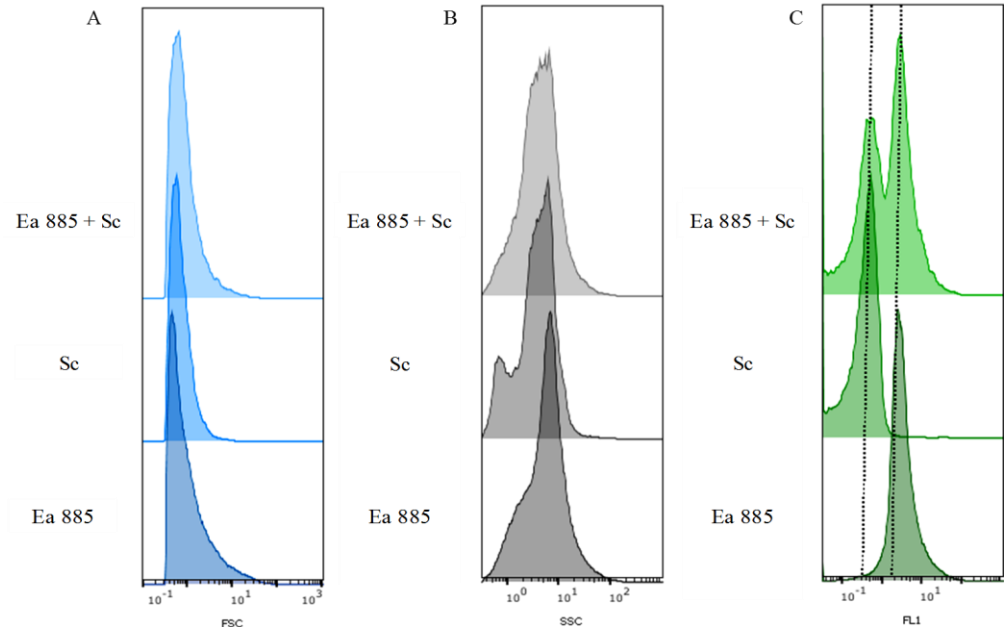

Figure 3.29 - Scattering signals and fluorescence emission of *Erwinia amylovora* 885 (Ea 885) and *Staphylococcus cohnii* (Sc) live cells (LC). A. FSC histogram. B. SSC histogram. C. FITC green fluorescence histogram (FL1).

In FL1 × SSC dot-plots (fig. 3.30) it was possible to define a separation between the two bacterial populations: *S. cohnii* population located in Q4 gate, while *E. amylovora* population was mainly located in Q3 gate.

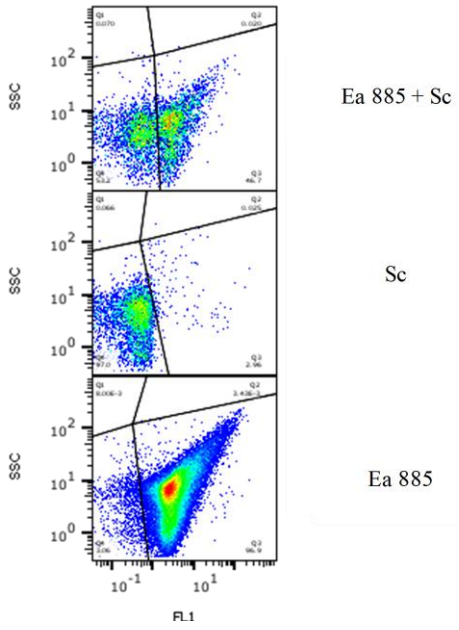

Figure 3.30 - Pseudo-colour dot-plot of *Erwinia amylovora* 885 (Ea 885) and *Staphylococcus cohnii* (Sc). FITC (FL1) × SSC.

Although the immunofluorescence had enabled the detection of *E. amylovora* population, an unexpected low emission of green fluorescence was observed in *S. cohnii*. This may be related with the occurrence of a non-specific binding process. For these analyses, an indirect immunofluorescence (IIF) method was applied, in which an unconjugated antibody (primary antibody) was first added to each sample. Then, a labelled secondary antibody was used to detect the primary antibody that was already

bounded to the target antigen. According to manufactures (Abcam, 2019; ThermoFisher, 2019), one of the drawbacks of IIF compared to direct immunofluorescence is a higher probability of a non-specific binding, particularly related to the secondary antibody.

The higher green fluorescence emission in *E. amylovora* results from a signal amplification caused by the binding of several FITC-labelled antibodies (secondary antibodies) to the Ea7A IVIA antibody (primary antibody). Concerning the non-specific binding, the green fluorescence detected in *S. cohnii* results from the binding of part of the secondary antibody to a target in *S. cohnii*, which culminates in background fluorescence. Although it cannot be totally excluded, a cross reaction between the primary antibody and *S. cohnii* seems unlikely, due to its specificity demonstrated in serological tests (Gorris, 1996b). Ea7A IVIA is a monoclonal antibody that demonstrated specificity to *E. amylovora* EPS. No cross-reaction with any species of epiphytic microflora of members of Rosaceae family or with other phytopathogenic bacteria was detected in serological tests (Gorris, 1996b).

The present IFCM assay has allowed to discriminate *E. amylovora* present in a mixed sample. Therefore, the next step would be to implement this protocol to detect *E. amylovora* in biological material, while simultaneously assessing its cellular viability with the use of fluorophores.

3.4.4. Detection and cell viability assessment of *Erwinia amylovora* on artificially infected *Pyrus communis* fruitlets

The FCM immunoassays have validated the previously established protocols, allowing the detection of *E. amylovora* in *P. communis* fruitlets artificially infected with *E. amylovora* 365 (P365) and 412 (P412). As can be seen in fig. 3.31, P365- and P412-infected fruitlets samples showed well-defined green fluorescence, characteristic of FITC-labelled antibodies (fig. 3.31 A2 and C2, respectively). However, when infected fruitlets samples were compared with pure culture cells (Ea 885), the former was found to have a lower FITC fluorescence intensity (fig. 3.31 A1, 2 and C1, 2). These differences in FITC fluorescence allowed the discrimination of Ea 885 cells from bacteria isolated from artificially infected *P. communis* fruitlets in mixed samples (fig. 3.31 A1, 2, 3 and C1, 2, 3).

The differences on FITC fluorescence may be related with the dimensions of the EPS surrounding the cells. According to Schollmeyer *et al*. (2012), the size of amylovoran surrounding *E. amylovora* cells can be heterogeneous depending on bacteria growth and isolation process. In fact, cells growth conditions, cells metabolism and EPS breakage may affect EPS chain length. Thus, variations of EPS size may have implications in the fluorescence emission observed in the present analysis due to these factors:

a) Longer EPS chains may present a higher quantity of antibody-binding sites, resulting in higher fluorescence intensity, whereas shorter EPS chains may present a lower quantity of antibody-binding sites, resulting in a lower fluorescence intensity. When extracting *E. amylovora* from the artificially infected *P. communis* fruitlets, samples underwent a maceration process, which could possibly lead to EPS breakage and its consequent depletion in the samples. According to this hypothesis, the possible presence of longer EPS chains in Ea 885 may explain the higher fluorescence emission in comparison to P365 e P412, which EPS chains may have been broken and partial lost during the isolation process.
b) Bacterial adaptation to distinct growth conditions may generate variation in the length of EPS. Ea 885 grew under *in vitro* conditions in a culture medium that provided its growth nutritional requirements. P365 and P 412 grew under *in planta* conditions, where bacteria rely on their ability to surpass the host defence mechanisms as well as to acquire nutrients from the host. According to this hypothesis, these constraints may lead bacteria to produce shorter EPS to act more quickly, which in consequence lead to the detection of a lower fluorescence emission.

In the flow cytometric immunoassays, PI was used to assess the viability of cells detected with FITC-labelled antibodies, since there is no overlap in the emission spectra of these fluorophores. As shown in fig. 3.31, Ea 885 heat-treated cells labelled with FITC and PI showed almost no variation in green fluorescence (fig. 3.31 A1, 4 and C1, 4). However, a clear decrease in the FL1/FL3 ratio was observed due to increased red fluorescence of PI (fig. 3.31 B1, 4 and D1, 4). When these cells were added to the artificially infected P365 and P412 samples, the differentiation of the subpopulations became less clear (fig 3.31 B3, 5 and D3, 5, respectively). This may be related with the overlap between the FL1/FL3 ratio of the P365 or P412 infected samples, and the ratio corresponding to the heat-treated Ea 885 cells that was shifted to the left (fig. 3.31 B2, 5 and D2, 5).

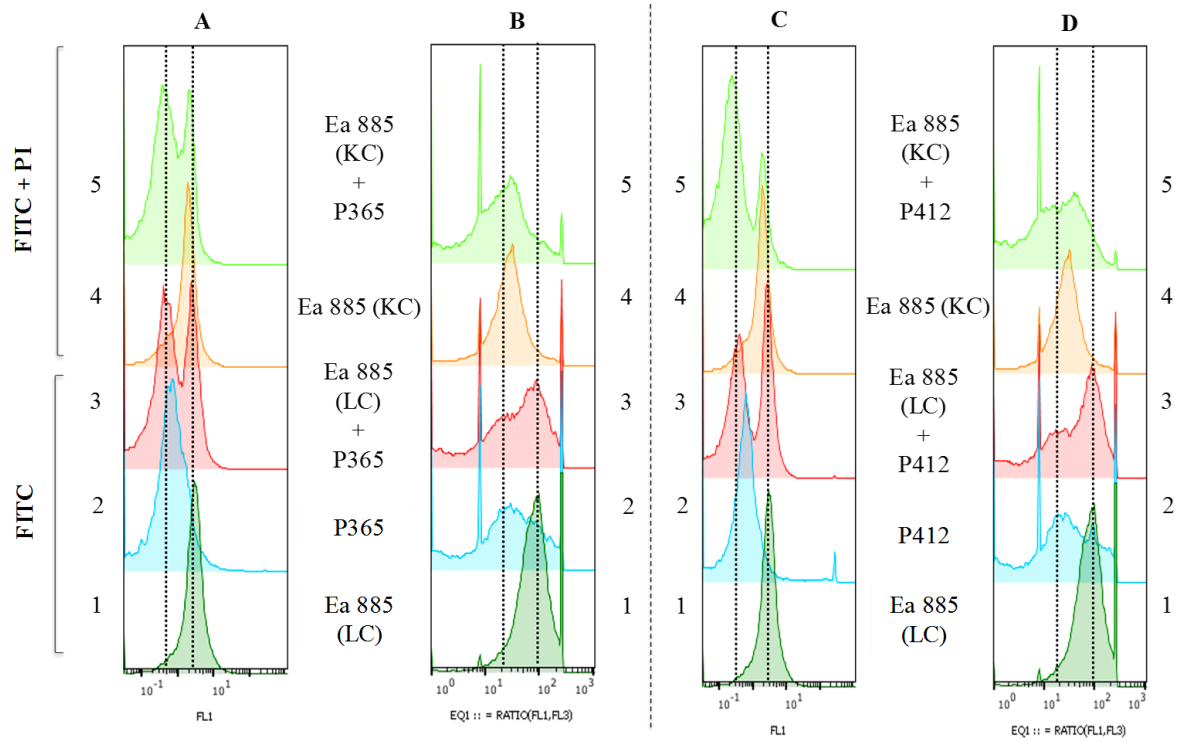

Figure 3.31 - Green fluorescence (FL1) and FL1/FL3 ratio of *Erwinia amylovora* Ea 885, and artificially infected samples P365 and P412 using FITC alone or combined with PI. A, C. FITC histogram (FL1). B, D. FL1 /FL3 fluorescence ratio.

It should be noted that the populations P365 and P412 were more heterogeneous when compared with Ea 885, presenting a greater variability, which was graphically translated by wider histogram bases (fig. 3.31 B4, B5 and D4, D5). This may be related with the process by which the biological material was collected. Pieces of pear fruitlets infected with P365 and P412 were excised from the transition zone, located between the necrosis and healthy tissues. This procedure can lead to the appearance of cells with different physiological states in the same sample: dead cells (from necrotic tissue remains), injured cells and live cells (responsible for disease's progression in healthy tissues).

At FL1 × FL3 dot-plots (fig. 3.32), the differentiation of bacterial populations was also observed. Ea 885 population was mainly located in quadrant Q3, due to the higher green fluorescence, while P365 and P412 were mainly located in quadrant Q4. Nevertheless, some P365 and P412 cells were also located in quadrant Q3, which is in line with the higher variability observed in these samples. In mixed samples (in the absence and presence of PI), it was also possible to distinguish the two bacterial subpopulations (fig. 3.32 A3, 5 and B3, 5).

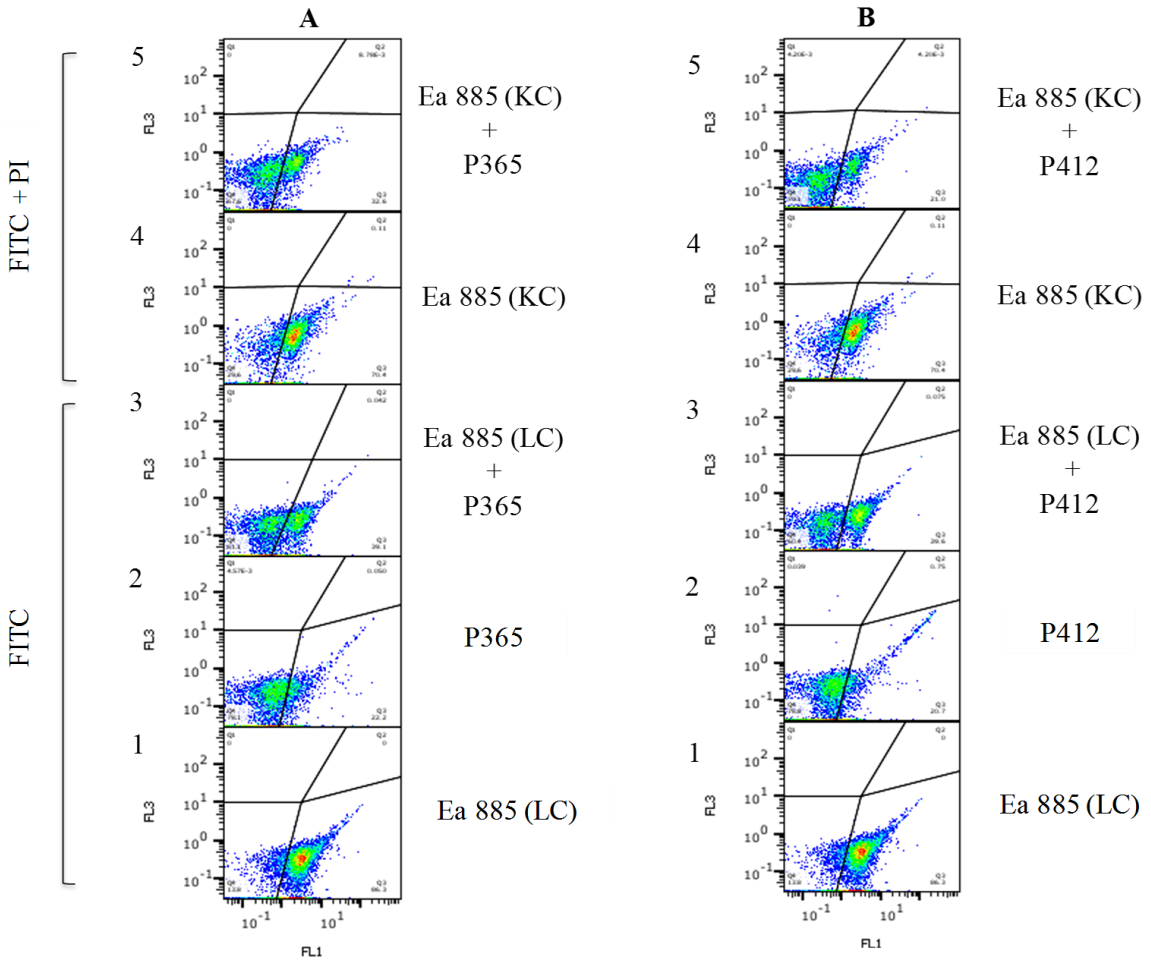

Figure 3.32 - Pseudo-colour dot-plots of *Erwinia amylovora* Ea 885, and artificially infected samples P365 and P412 using FITC alone or combined with PI. A. Ea 885 and P365 FITC (FL1) pseudo-colour dot-plots. B. Ea 885 and P412 FITC (FL1) pseudo-colour dot-plots.

4. Global Discussion and Final Remarks

Molecular characterisation

The use of different molecular techniques, including CRISPR-, rep- and MSP-PCR has reinforced the high genomic homogeneity of *Erwinia amylovora*.

CRISPR-PCR was a simple and fast method that enabled the distinction of Portuguese and European *E. amylovora* isolates in two strains, namely strains with genotype A and strains with genotype D. As both genotypes have shown to be spread almost equitably throughout Europe, discrimination using only one spacer is not enough to trace further geographical associations between Portuguese and European isolates. To overcome this limitation, the amplification and subsequent sequencing of a greater number of spacers needs to be performed. Moreover, a greater number of isolates needs to be analysed to provide a more detailed and accurate overview on the geographical distribution of both genotypes.

Genomic fingerprints obtained with BOX-, ERIC-, REP- and MSP-PCR displayed complex yet very homogenous genomic profiles among *E. amylovora* Amygdaloideae-infecting isolates, revealing a low degree of genetic variability. Therefore, none of the techniques had an adequate discriminatory capacity to assess *E. amylovora* isolates infraspecific diversity.

Alternatively, Multiple-Locus VNTR (variable number of tandem repeats) Analysis (MLVA) can be used in future epidemiological studies to characterize *E. amylovora*, since this method was able to distinguish 227 haplotypes within 833 worldwide *E. amylovora* isolates (Bühlmann *et al.*, 2013).

Biological assays

Biological assays consisted in the observation of fire blight symptoms, such as necrotic lesion and oozing, induced in artificially infected plant material. A greater variability was observed among *E. amylovora* isolates through the biological assays when compared with the molecular methods used. Apart from two non-pathogenic isolates, a wide phenotypic diversity resulting from the lesion sizes led to the grouping of isolates into three virulence categories, namely low, medium, and high. A correlation between the low virulence category and the CRISPR genotype D was observed.

Further studies should focus on understanding the genetic background that causes differential expression of virulence genes in this highly genomic homogenous species. In addition, further studies need to be conducted to unveil a possible explanation for the correlation mentioned above.

Polyphasic analysis

The implementation of the polyphasic analysis allowed to integrate genotypic and phenotypic data, resulting in the distribution of *E. amylovora* isolates in one of eleven groups. The compilation of these data resulted in a greater discrimination capacity than when each method was analysed by itself. In the future, whenever additional findings from other studies are collected, data should be added to this database to obtain more detailed information about the isolates.

Flow cytometry analysis

In the present dissertation, FC and IFCM protocols were developed, validated, and successfully applied for the detection and cell viability assessment of *E. amylovora* present in artificially infected *P. communis* fruitlets.

In the viability assays using a *E.amylovora* pure culture, Syto9 in combination with PI, and $DIBAC_4(3)$ were suitable to assess membrane integrity and membrane potential, respectively. The use

of Syto9 and PI enabled to distinguish three populations of *E. amylovora* including live, injured and dead cells.

Despite the existence of non-specific bindings, flow cytometric immunoassays allowed the discrimination of *E. amylovora* in mixed samples. Regarding the detection and cell viability of *E. amylovora* in infected plant material, the association of a labelled monoclonal antibody with PI showed the presence of a heterogeneous *E. amylovora* population. The reason behind FITC heterogeneity is unknown, although differences in EPS may be a plausible explanation; as for PI, it revealed that different populations of *E. amylovora* can be found during the infection process according to their viability.

Future studies should include: (i) double staining assays with $DIBAC_4(3)$ and PI to simultaneously evaluate cell membrane potential and integrity; (ii) a IFCM analysis between the same strain of *E. amylovora* grown under *in vitro* and *in planta* conditions to test if different growth conditions play a role in the fluorescence intensity detected; (iii) optimization of the established IFCM protocol by using a direct immunofluorescence method to test if a reduction of non-specific bindings occurs; (v) apply the IFCM protocol in naturally infected plant material.

Nevertheless, this dissertation highlights the potential of FCM and IFCM as a promising alternative tool to study *E. amylovora*. Although FCM is a more costly method, when protocols are well defined its high-speed sample processing and multi-parametric analysis offer considerable diagnostic advantages in comparison to traditional techniques. Moreover, its ability to distinguish different viability states can be used to obtain information concerning the physiological states in the same population of *E. amylovora*. This can pave the way to valuable discoveries and data regarding *E. amylovora* unclear life cycle, which can be of extreme importance in the implementation of prophylactic measures to control fire blight.

References

Abcam, (2019). Direct vs indirect immunofluorescence. In: Abcam. Accessed on the 2nd of December 2019. Retrieved from https://www.abcam.com/secondary-antibodies/direct-vs-indirect-immunofluorescence.

Adan A, Alizada G, Kiraz Y, Baran Y, Nalbant A. (2017). Flow cytometry: basic principles and applications. Crit Rev Biotechnol 37(2): 163-176.

Adhikari BN, Hamilton JP, Zerillo MM, Tisserat N, Lévesque CA, Buell CR. (2013). Comparative genomics reveals insight into virulence strategies of plant pathogenic oomycetes. PLoS One 8: e75072.

Alvarez-Barrientos A, Arroyo J, Canton R, Nombela C, Sanchez-Perez M. (2000). Applications of flow cytometry to clinical microbiology. Clin Microbiol Rev 13: 167–195.

Aoki V, Sousa JX Jr., Fukumori LM, Perigo AM, Freitas EL, Oliveira ZN. (2010) Direct and indirect immunofluorescence. An Bras Dermatol 85(4): 490–500.

Babu RSA, Chandrasekar P, Lalith P, Reddy CKS, Kumar KK, Reddy BVR. (2013). Immunofluorescence and its application in dermatopathology with oral manifestations. Rev J Orofac Sci 5: 2–8.

Barionovi D, Giorgi S, Stoeger AR, Ruppitsch W, Scortichini M. (2006). Characterization of *Erwinia amylovora* strains from different host plants using repetitive-sequences PCR analysis, and restriction fragment length polymorphism and short-sequence DNA repeats of plasmid pEA29. J Appl Microbiol 100: 1084–1094.

Baker KF. (1971) Fire blight of pome fruits: the genesis of the concept that bacteria can be pathogenic to plants. Hilgardia 40: 603–633.

Bellemann P, Geider K. (1992). Localization of transposon insertions in pathogenicity mutants of *Erwinia amylovora* and their biochemical characterization. J Gen Microbiol 138: 931–940.

Bergervoet JHW, van der Wolf JM., Peters J. (2007). Detection and Viability Assessment of Plant Pathogenic Microorganisms using Flow Cytometry. In Doležel J, Greilhuber J. and Suda J.(eds), Flow Cytometry with Plant Cells: Analysis of Genes, Chromosomes and Genomes. Wiley-VCH Verlag GmbH & Co. KGaA, Weinheim, Germany.

Berney M, Hammes F, Bosshard F, Weilenmann HU, Egli T. (2007). Assessment and interpretation of bacterial viability by using the LIVE/DEAD BacLight Kit in combination with flow cytometry. Appl. Environ. Microbiol 73: 3283–3290.

Bernhard F, Schullerus D, Bellemann P, Nimtz M, Coplin DL, Geider K. (1996). Genetic transfer of amylovoran and stewartan synthesis between *Erwinia amylovora* and *Erwinia stewartii*. Microbiology 142: 1087–1096.

Billing E. (2000). Fire blight Risk Assessment Systems and Models. In: Vanneste J (ed), Fire blight, the disease and its causative agent *Erwinia amylovora*. CABI publishing, Wallingford, UK: 293-318.

Bogs J, Geider K. (2000). Molecular analysis of sucrose metabolism of *Erwinia amylovora* and influence on bacterial virulence. J Bacteriol. 182: 5351–5358.

Bonn WG, van der Zwet T. (2000). Distribution and economic importance of fire blight. In: Vanneste J (ed), Fire blight, the disease and its causative agent *Erwinia amylovora*. CABI publishing, Wallingford, UK:37-53.

Bugert, P. and Geider, K. (1995) Molecular analysis of the ams operon required for exopolysaccharide synthesis of Erwinia amylovora. Mol Microbiol 15: 917–933.

Bühlmann A, Dreo T, Rezzonico F, Pothier JF, Smits THM, Ravnikar M, Frey JE, Duffy B. (2014). Phylogeography and population structure of the biologically invasive phytopathogen *Erwinia amylovora* inferred using minisatellites. Environ Microbiol 16: 2112-2125.

Cabrefiga J, Montesinos E. (2017). Lysozyme enhances the bactericidal effect of BP100 peptide against *Erwinia amylovora*, the causal agent of fire blight of rosaceous plants. BMC Microbiol 17: 39.

Campbell JA. (1920). The orchard: the outbreak of fire blight. New Zeal J Agr 20: 181–182.

Chitarra LG, Langerak CJ, Bergervoet JHW, Van den Bulk RW. (2002). Detection of the plant pathogenic bacterium *Xanthomonas campestris* pv. campestris in seed extracts of *Brassica* sp. Applying fluorescent antibodies and flow cytometry. Cytometry 47: 118-126.

Cockayne AH. (1921). Fire blight and its control: the hawthorn question. New Zeal J Agr 23: 30–36.

Crepel C, Geenen J, Maes M (1995). The latent survival of *Erwinia amylovora* in hibernating shoots. Acta Horti 411: 21–25.

Crosse JE, Bennett M, Garrett CME. (1958). Fire blight of pear in England. Nature (London) 182: 1530.

Cui Y, Li Y, Gorgé O, Platonov ME, Yan Y, Guo Z, Pourcel C, Dentovskaya SV, Balakhonov SV, Wang X, Song Y, Anisimov AP, Vergnaud G, Yang R. (2008). Insight into microevolution of *Yersinia pestis* by clustered regularly interspaced short palindromic repeats. PLoS One 3:e2652.

Cruz L. (2010). Fogo Bacteriano – *Erwinia amylovora*. Boletim técnico. INRB/UIPP (BT-05).

Cruz L, Sousa R. (2013). Agente causal: detecção e identificação, caracterização fenética e filogenética. in: Cadernos Técnicos nº2 Fogo Bacteriano – *Erwinia amylovora*. Eds. Sustinia, Agricultura Sutentável, Lisboa, Portugal. pp. 9.

Cruz L, Cruz J, Sousa R. (2018). Studies on differential susceptibility of "Rocha" pear clones and Portuguese varieties of pear and apple to fire blight – tools for the sustainability of fruit chain production. Rev Ciênc Agrár 41: 92-96.

Davey HM (2011). Life, death, and in-between: meanings and methods in microbiology. Appl Environ Microbiol 77: 5571–5576.

Dewdney MM, Biggs AR, Turechek WW. (2007). A Statistical Comparison of the Blossom Blight Forecasts of MARYBLYT and Cougarblight with Receiver Operating Characteristic Curve Analysis. Phytopathology 97(9): 1164-76.

Díaz M, Herrero M, García LA, Quirós C. (2010). Application of flow cytometry to industrial microbial bioprocesses. Biochem Eng J 48: 385–407.

Donat V, Biosca EG, Peñalver J, López MM. (2007) Exploring diversity among Spanish strains of *Erwinia amylovora* and possible infections sources. J Appl Microbiol 103: 1639– 1649.

El-Helaly, AF, Abo-El-Dahab MK, El-Goorani MA. (1964). The occurrence of the fire blight disease of pear in Egypt. Phytopathol Mediterr 3: 156–163.

EPPO. (1997). *Erwinia amylovora*. Quarantine Pests for Europe. 2nd edition. CABI, Wallingford, UK: 1001–1007.

EPPO. (2004). Data sheets on quarantine pests – *Erwinia amylovora*.

EPPO. (2004). Diagnostic protocols for regulated pests - *Erwinia amylovora*. PM 7/20 OEPP/EPPO Bullettin 34: 159-171.

EPPO. (2010). ELISA tests for plant pathogenic bacteria. PM 7/101 (1). OEPP/EPPO Bulletin 40: 369-372

EPPO. (2013). Diagnostic protocols for regulated pests - *Erwinia amylovora*. PM 7/20 (2) OEPP/EPPO Bullettin 34: 159-171.

EPPO, (2019). EPPO Global Database (available online). Accessed on the 1st of October 2019. Retrieve from: https://gd.eppo.int

Fang Y, Ramasamy RP. (2015). Current and prospective methods for plant disease detection. Biosensors 5: 537–561.

Fricke W, Mammel M, McDermott P, Tartera C, White D, Leclerc J, Ravel J, Cebula T. (2011). Comparative genomics of 28 *Salmonella enterica* isolates: evidence for CRISPR-mediated adaptive sublineage evolution. J. Bacteriol 193: 3556–3568.

Fu Y, Finney NS. (2018). Small-Molecule Fluorescent Probes and Their Design. RSC Adv 8(51): 29051-29061

Geier G, Geider K. (1993). Characterization and influence on virulence of the levansucrase gene from the fire blight pathogen *Erwinia amylovora*. Physiol Mol Plant Pathol 42: 387–404.

Geier G. (2000). Exopolyssaccharides of *Erwinia amylovora*: Structure, Biosynthesis, Regulation, Role in Pathogenicity of Amylovoran and Levan. In: Vanneste J (ed), Fire blight, the disease and its causative agent *Erwinia amylovora*. CABI publishing, Wallingford, UK: 117-140.

Gorris MT, Cambra M, Llop P, Lecomte P, Chartier R, Paulin JP, Lóopez MM. (1996a). A sensitive and specific detection of *Erwinia amylovora* based on the ELISA-DASI enrichment method with monoclonal antibodies. Acta Hortic 411: 41–45.

Gorris MT, Cambra E, Paulin JP, Chartier R, Cambra M, López MM. (1996b). Production and characterization of monoclonal antibodies specific for *Erwinia amylovora* and their use in different serological techniques. Acta Hortic 411: 47–51.

Gusberti M, Klemm U, Meier MS, Maurhofer M. (2015). Fire blight control: the struggle goes on. A comparison of different fire blight control methods in Switzerland with respect to biosafety, efficacy and durability. Int J Environ Res Public Health 12: 11422-11447.

Harkins KR, Harrigan K. (2004). Labeling of bacterial pathogens for flow cytometric detection and enumeration. Curr Protoc Cytom 11: 11-17.

Hauben L, Swings J. (2005). *Erwinia*. In Bergey's Manual of Systematics of Archaea and Bacteria. 2nd edn. vol. 2, part B: Springer, New York: 670–679.

Hiett KL, Seal BS. (2009). Use of repetitive element palindromic PCR (rep-PCR) for the epidemiologic discrimination of food-borne pathogens. Methods Mol Biol 551: 49-58.

Horan PK, Slezak SE, Poste G. (1986). Improved flow cytometric analysis of leukocyte subsets: Simultaneous identification of five cell subsets using two color immunofluorescence. Proc Natl Acad Sci USA 83: 8361-8365.

Horvath P, Barrangou R. (2010). CRISPR/Cas, the immune system of bacteria and archaea. Science 327: 167-170.

Hummer KE, Janick J. (2009). Rosaceae: taxonomy, economic importance, genomics. In: Genetics and Genomics of Rosaceae. Springer, USA, New York,USA: 1–17.

Jock S, Donat V, López MM, Bazzi C, Geider K. (2002) Following spread of fire blight in Western, Central and Southern Europe by molecular differentiation of *Erwinia amylovora* strains with PFGE analysis. Environ Microbiol 4: 106–114.

Jock S, Geider K. (2004). Molecular differentiation of *Erwinia amylovora* strains from North America and of two Asian pear pathogens by analyses of PFGE patterns and hrpN genes. Environ Microbiol 6: 480–490.

Jonhson KB, Stockwell VO. (2000). Biological Control of Fire blight. In: Vanneste J (ed), Fire blight, the disease and its causative agent *Erwinia amylovora*. CABI publishing, Wallingford, UK: 319-328.

Jung WK, Koo HC, Kim W, Shin S, Kim SH, Park YH. (2008). Antibacterial activity and mechanism of action of the silver ion in *Staphylococcus aureus* and *Escherichia coli*. Appl Environ Microbiol 74: 2171–2178.

King EO, Ward MK, Raney DE. (1954). Two simple media for the demonstratoin of pyocyanin and fluorescein. J Lab Clin Med 44: 301-307.

Kennedy D, Wilkinson MG. (2017) Application of Flow Cytometry to the Detection of Pathogenic Bacteria. Curr Issues Mol Biol 23: 21−38.

Koczan JM, McGrath MJ, Zhao YF, Sundin GW. (2009). Contribution of *Erwinia amylovora* exopolysaccharides amylovoran and levan to biofilm formation: implications in pathogenicity. Phytopathology 99: 1237–1244.

Kumar SS, Ghosh AR. (2019). Assessment of bacterial viability: a comprehensive review on recent advances and challenges. Microbiology 165(6): 593–610.

Kurz M. (2018). Molecular Analysis of the Distribution of two Ancestral Populations of *Erwinia amylovora* in Europe using CRISPR Data. Wadenswil. ZHAW IUNR.

Lapage S, Shelton J, Mitchell T. (1970). Methods in Microbiology'. Vol. 3A., Academic Press, London.

López MM, Bertolini E, Olmos A, Caruso P, Gorris MT, Llop P, Penyalver R, Cambra M. (2003). Innovative tools for detection of plant pathogenic viruses and bacteria. Int Microbiol 6: 233-243.

López MM, Ordax M, Peñalver J, Roselló M, Gorris M, Cambra M, Marco-Noales E, Biosca E, Palacio-Bielsa A, Llop P. (2009). El fuego bacteriano de las rosáceas (*Erwinia amylovora*). Capítulo 2 - *Erwinia amylovora*: Características generales. Métodos de diagnóstico de la enfermedad e identificación de *E. amylovora*. Ministerio de Medio Ambiente y Medio Rural y Marino.

Louws FJ, Fullbright DW, Stephens CT, De Bruijn FJ. (1994). Specific genomic fingerprinting of phytopathogenic *Xanthomonas* and *Pseudomonas* pathovars and strains generated with repetitive sequences and PCR. Appl Environ Microbiol 60: 2286-2295.

Luz JP. (2013). Bioecologia e ciclo de vida. In: Cadernos Técnicos nº2 Fogo Bacteriano – *Erwinia amylovora*. Eds. Sustinia, Agricultura Sutentável, Lisboa, Portugal.

Ma W, Dong FF, Stavrinides J, Guttman DS. (2006). Type III effector diversification via both pathoadaptation and horizontal transfer in response to a coevolutionary arms race. PLoS Genet 2: e209.

Maes M, Orye K, Bobev S, Devreese B, Van Beeumen J, De Bruyn A, Busson R, Herdewijn P, Morreel K, Messens E. (2001). Influence of amylovoran production on virulence of *Erwinia amylovora* and a different amylovoran structure in *E. amylovora* isolates from Rubus. Eur J Plant Pathol 107: 839–844.

Mann RA, Smits THM, Bühlmann A, Blom J, Goesmann A, Frey JE, Plummer KM, Beer SV, Luck J, Duffy B, Rodoni B. (2013). Comparative genomics of 12 strains of *Erwinia amylovora* identifies a pan-genome with a large con- served core. PLoS One 8: e55644.

Martin F, Costa G, Delaruelle C, Diez J. (1998). Genomic fingerprinting of ectomycorrhizal fungi by microsatellite-primed PCR. In: Varma A (ed), Mycorrhiza Manual. Springer-Verlag, Berlim: 463-474.

Martin B, Humbert O, Camara M, Guenzi E, Walker J, Mitchell T, Andrew P, Prudhomme M, Alloing G, Hakenbeck R. (1992). A highly conserved repeated DNA element located in the chromosome of Streptococcus pneumoniae. Nucleic Acids Res 20: 3479.

McGhee G, Sundin G. (2012). Erwinia amylovora CRISPR elements pro- vide new tools for evaluating strain diversity and for microbial source tracking. PLoS One 7: e41706.

McManus PS, Jones AL. (1995). Genetic fingerprinting of *Erwinia amylovora* strains isolated from tree-fruit crops and *Rubus* spp. Phytopathology 85: 1547–1553.

McManus PS, Stockwell VO, Sundin GW, Jones AL. (2002). Antibiotic use in plant agriculture. Annu Rev Phytopathol 40 443–465.

Meijneke CAR. (1972) Perevuur en zijn verspreiding. Gewasbescherming 3: 128–136.

Mohan SK, Thomson S. (1996). An outbreak of fire blight in plums. Acta Hortic 411: 73–76.

Momol MT, Aldwincke HS. (2000). Genetic Diversity and Host Range of *Erwinia amylovora*. In: Vanneste J (ed), Fire blight, the disease and its causative agent *Erwinia amylovora*. CABI publishing, Wallingford, UK: 55-72.

Müller S, Nebe-von-Caron G. (2010). Functional single-cell analyses: flow cytometry and cell sorting of microbial populations and communities. FEMS Microbiol Rev 34: 554–587.

Nebe-von Caron G, Stephens P, Badley RA. (1998). Assesment of bacterial viability status by flow cytometry and single cell sorting, J Appl Microbiol 84: 988–998.

Nebe-von-Caron G, Stephens PJ, Hewitt CJ, Powell JR, Badley RA. (2000). Analysis of bacterial function by multi-colour fluorescence flow cytometry and single cell sorting. J Microbiol. Methods 42: 97–114.

Netherlands Plant Protection Service. (1966). A Case of Fire blight in The Netherlands. European and Mediterranean Plant Protection Organization, Report 286, Wageningen.

Odell ID, Cook D. (2013). Immunofluorescence techniques. J Invest Dermatol 133: e4.

Obradovic D, Balaz J, Kevresan S. (2007). Detection of *Erwinia amylovora* by novel chromosomal polymerase chain reaction primers. Mikrobiologiia 76: 844–852

Oh CS, Beer SV. (2005). Molecular genetics of *Erwinia amylovora* involved in the development of fire blight. FEMS Microbiol Lett 253: 185–192.

Oh CH, Kim JF, Beer SV. (2005). The Hrp pathogenicity island of *Erwinia amylovora* and identification of three novel genes required for systemic infection. Mol Plant Pathol 6: 125-138.

Ordax M, Marco-Noales E, López MM, Biosca EG. (2006). Survival strategy of *Erwinia amylovora* against copper: induction of the viable but-nonculturable state. Appl Environ Microbiol 72: 3482-3488.

Ordax M, Biosca EG, Wimalajeewa SC, López MM, Marco-Noales E. (2009). Survival of *Erwinia amylovora* in mature apple fruit calyces through the viable but nonculturable (VBNC) state. J Appl Microbiol 107(1): 106-16.

Palacio-Bielsa A, Roselló M, Llop P, López MM. (2011). *Erwinia* spp. from pome fruit trees: similarities and differences among pathogenic and non- pathogenic species. Trees Struct Funct 26: 13-29.

Pester D, Milčevičová R, Schaffer J, Wilhelm E, Blümel S. (2012). *Erwinia amylovora* expresses fast and simultaneously hrp/dsp virulence genes during flower infection on apple trees. PLoS ONE 7: e32583.

Pinto SS. (2012). Plano de ação nacional para o controlo do fogo bacteriano - Relatório 2012. Lisboa: Direcção Geral de Alimentação e Veterinária – Direcção de Serviços de Sanidade Vegetal.

Pirc M, Ravnikar M, Tomlinson J, Dreo T. (2009). Improved fire blight diagnostics using quantitative real-time PCR detection of *Erwinia amylovora* chromosomal DNA. Plant Pathol 58: 872– 881.

Piqué N, Miñana-Galbis D, Merino S, Tomás JM. (2015). Virulence factors of *Erwinia amylovora*: a review. Int J Mol Sci 16: 12836–12854.

Prates A, Cavaco M. (2013). Métodos culturais, biológicos e químicos. Estratégias integradas. In: Cadernos Técnicos nº2 Fogo Bacteriano – *Erwinia amylovora*. Eds. Sustinia, Agricultura Sutentável, Lisboa, Portugal. pp: 24-31.

Potter D, Eriksson T, Evans RC, Oh SH, Smedmark JEE, Morgan DR, Kerr M, Robertson KR, Arsenault MP, Dickinson TA, Campbell CS. (2007). Phylogeny and classification of Rosaceae. Plant Syst Evol 266: 5–43.

Psallidas PG, Tsiantos J. (2000). Chemical Control of Fire blight. In: Vanneste J (ed), Fire blight, the disease and its causative agent *Erwinia amylovora*. CABI publishing, Wallingford, UK: 199-234.

Rademaker JLW, De Bruijn FJ. (1997). Characterization and classification of microbes by rep-PCR genomic fingerprinting and computer-assisted pattern analysis. In: Caetano-Anollés G and Gresshoff PM (ed.), DNA markers: protocols, applications and overviews. John Wiley and Sons, Inc., New York: 151-171.

Radunović D, Gavrilović V, Gašić K, Paunović M, Stojšin V, Grahovac M. (2017). Molecular characterization of *Erwinia amylovora* strains originated from pome fruit and indigenous plant in Montenegro. J Plant Pathol 99(1): 197-203.

Rahman M. (2006). Introduction to Flow Cytometry. AbD Serotec 1-33.

Rezaeinejad S, Ivanov V. (2011). Heterogeneity of *Escherichia coli* population by respiratory activity and membrane potential of cells during growth and long-term starvation. Microbiol Res 166: 129 – 135.

Rezzonico F, Smits T, Duffy B. (2011). Diversity, evolution and functionality of CRISPR regions in the fire blight pathogen *Erwinia amylovora*. Appl Environ Microbiol 77: 3819–3829.

Rezzonico F. (2014). Diversity analysis in *Erwinia amylovora* isolates from Central Asia. Phytfire final meeting. Urgup, Turkey. Retrieved from: http://www.phytfire.org/Euphresco2014_WP6_Rezzonico.pdf.

Rico A, Ortiz-Barredo A, Ritter E, Murillo J. (2004). Genetic characterization of *Erwinia amylovora* strains by amplified fragment length polymorphism. J Appl Microbiol 96: 302-310.

Rico A, Führer ME, Ortiz-Barredo A, Murillo J. (2008). Polymerase chain reaction fingerprinting of *Erwinia amylovora* has a limited phylogenetic value but allows the design of highly specific molecular markers. Phytopathology 98: 260-269.

Ruger M, Bensch G, Tungler R, Reichl U. (2012). A flow cytometric method for viability assessment of *Staphylococcus aureus* and *Burkholderia cepacia* in mixed culture. Cytom Part A. 81(12): 1055-66.

Ryskov AP, Jincharadze AG, Pronysak MI, Ivanov PL, Limborska SA. (1988). M13 phage DNA as a universal marker for DNA fingerprinting of animals, plants and microorganisms. FEBS Lett 233: 388-392.

Santander RD, Biosca EG. (2017). *Erwinia amylovora* psychrotrophic adaptations: evidence of pathogenic potential and survival at temperate and low environmental temperatures. PeerJ 5: e3931.

Schollmeyer M, Langlotz C, Huber A, Coplin DL, Geider K. (2012). Variations in the molecular masses of the capsular exopolysaccharides amylovoran, pyrifolan and stewartan. Int J Biol Macromol 50: 518-522.

Shabbir MAB, Tang Y, Xu Z, Lin M, Cheng G, Dai M, Wang X, Liu Z, Yuan Z, Hao H. (2018). The Involvement of the cas9 Gene in Virulence of *Campylobacter jejuni*. Front Cell Infect Microbiol 8: 285.

Shapiro HM. (2000). Membrane potential estimation by flow cytometry. Methods 21: 271-279.

Shariat N, Dudley EG. (2014). CRISPRs: molecular signatures used for pathogen subtyping. Appl Environ Microbiol 80: 430-439.

Smits TH, Rezzonico F, Kamber T, Blom J, Goesmann A, Frey JE, Duffy B. (2010). Complete genome sequence of the fire blight pathogen *Erwinia amylovora* CFBP1430 and comparison to other *Erwinia* spp. Mol Plant Microbe Interact 23: 384-393.

Smits TH, Rezzonico F, Duffy B. (2011). Evolutionary insights from *Erwinia amylovora* genomics. J. Biotechnol. 155: 34-39.

Steiner PW. (2000). Integrated Orchard and Nursery Management for the Control of Fire Blight. CABI publishing, Wallingford, UK: 9-36.

Stiefel P, Schmidt-Emrich S, Maniura-Weber K, Ren Q. (2015). Critical aspects of using bacterial cell viability assays with the fluorophores SYTO9 and propidium iodide. BMC Microbiol 15: 36.

Stocks SM. (2004). Mechanism and use of the commercially available viability stain, BacLight. Cytom A 61: 189–195.

Sträuber H, Müller S. (2010). Viability states of bacteria–specific mechanisms of selected probes. Cytom A 77: 623–634.

ThermoFisher. (2019). Immunolabelling. In: ThermoFisher. Accessed on the 2nd of December 2019. Retrieved from https://www.thermofisher.com/pt/en/home/life-science/cell-analysis/cell-analysis-learning-center/molecular-probes-school-of-fluorescence/imaging-basics/labeling-your-samples/immunolabeling.html.

Thomson SH. (2000). Epidemiology of fire blight. In: Vanneste J (ed), Fire blight, the disease and its causative agent *Erwinia amylovora*. CABI publishing, Wallingford, UK: 339-358.

Vanneste JL. (1995) *Erwinia amylovora*. In: Singh US, Singh RP and Kohmoto K (eds) Pathogenesis and Host Specificity in Plant Diseases: Histopathological, Biochemical, Genetic and Molecular Bases, Vol. 1. Oxford and London: Pergammon Press: 21–46.

Vanneste JL, Yu J. (1996). Biological control of fire blight using *Erwinia herbicola* Eh252 and *Pseudomonas fluorescens* A506 separately or in combination. Acta Hortic 411: 351–353.

Vanneste JL, Eden-Green S. (2000). Migration of *Erwinia amylovora* in Host Plant Tissues. In: Vanneste J (ed), Fire blight, the disease and its causative agent *Erwinia amylovora*. CABI publishing, Wallingford, UK: 73-74.

Vantomme R, Swings J, Goor M, Kersters K, De Ley J. (1982). Phytopathological, serological, biochemical and protein electrophorectic characterization of *Erwinia amylovora* strains isolated in Belgium. Phytopathol Z 103: 349 - 369

van der Zwet T. (1994) The various means of dissemination of the fire blight bacterium *E. amylovora*. European and Mediterranean Plant Protection Organization Bulletin 24: 209–214

van der Zwet T, Keil HL. (1979). Fire blight, a bacterial disease of Rosaceous plants. Agriculture Handbook, Science and Education Administration USDA. USA, Beltsville: 10-19.

Vrancken K, Holtappels M, Schoofs H, Deckers T, Valcke R. (2013). Pathogenicity and infection strategies of the fire blight pathogen *Erwinia amylovora* in Rosaceae: State of the art. Microbiology (UK) 159: 823–32.

Wang D, Korban SS, Zhao Y. (2010a). Molecular signature of differential virulence in natural isolates of *Erwinia amylovora*. Phytopathology 100: 192–198.

Wang Y, Hammes F, De Roy K, Verstraete W, Boon N. (2010b). Past, present and future applications of flow cytometry in aquatic microbiology. Trends Biotechnol 28: e:416e424.

Winslow C, Broadhurst J, Buchanan RE, Krumwiede CJ, Rogers LA, Smith GH. (1920). The families and genera of the Bacteria. Final report of the Committee of the Society of American Bacteriologists on characterization and classification of bacterial types. J Bacteriol 5: 191–229.

Xiang Y, Huang CH, Hu Y, Wen J, Li S, Yi T, Chen H, Xiang J, Ma H. (2017) Evolution of Rosaceae fruit types based on nuclear phylogeny in the context of geological times and genome duplication. Mol Biol Evol 34: 262– 281.

Zar JH. (2014). Biostatistical analysis: Pearson new international edition. 5th edition. Pearson, Harlow, England, UK.

Zhao Y, Qi M. (2011). Comparative genomics of *Erwinia amylovora* and related *Erwinia* species — what do we learn?. Genes 2: 627–639.

Zhao Y, Blumer S, Sundin G. (2005). Identification of *Erwinia amylovora* genes induced during infection of immature pear tissue. J Bacteriol 187: 8088–8103.

Appendix A. Media and solutions

Media

Nutrient Agar medium (NA) (pH = 6.8) (1 L) **(**Lapage *et al.*, 1970)
- 23 g of Nutrient Agar;
- 1 L of distilled water;
- Sterilize by autoclaving (15 min at 121 °C).

King medium B (KMB) (pH = 7.2 ± 0.2) (1 L) (King *et al.*, 1954)
- 20 g of Peptone Protease;
- 10 mL of Glycerol;
- 1.5 g of $MgSO_4.7H_2O$;
- 1.5 g of K_2HPO_4;
- 15 g of Bacteriological agar;
- 1 L of distilled water;
- Sterilize by autoclaving (15 min at 121 °C).

Solutions

Antioxidant Maceration Buffer (AMB) (pH = 7) (1 L) (Gorris *et al.*, 1996b)
- 20 g of Polyvinylpyrrolidone (PVP-10);
- 10 g of Mannitol;
- 960 mL of distilled water
- Sterilize by autoclaving (15 min at 121 °C).
- Add by filtration in the previous solution 1.76 g of Ascorbic Acid diluted in 20 mL distillate water;
- Add by filtration in the previous solution 3 g of Reduced Glutathione diluted in 20 mL distillate water.

Phosphate-Buffered Saline (PBS) 10 mM (pH = 7.2) (1 L) (EPPO,2013)
- 2.9 g of $Na_2HPO_4.12H_2O$;
- 0.2 g of KH_2PO_4
- 0.2 g of KCl;
- 8.0 g of NaCl;
- 1 L of distilled water;
- Sterilize by autoclaving (15 min at 121 °C).

Appendix B. Supplementary Tables and Figures

Supplementary Table 1 - Results of CRISPR repeat region 1 amplification, pathogenicity and virulence evaluation of *Erwinia amylovora* isolates.

CPBF Isolate ID	Country, region	CRISPR genotype (A-272 bp; D-211 bp)	Pathogenicity and virulence evaluation		
			Lesion size (mm)	Presence of exudate 6 DAI	12 DAI
142	France	A	0,00	N	N
360	Cyprus	A	4,75	Y	Y
361	Greece	A	6,50	V	Y
364	Greece	A	8,38	Y	Y
365	Greece	A	6,13	Y	Y
366	Greece	A	4,00	Y	Y
372	Greece	D	3,13	Y	Y
373	Czech Republic	A	4,63	Y	Y
387	Ireland	A	6,13	Y	Y
393	Ireland	A	6,75	Y	Y
410	Poland	D	3,63	N	N
411	Poland	D	5,88	Y	Y
412	Poland	D	5,00	N	N
450	Ireland	A	5,75	V	Y
544	Portugal	A	0,00	N	N
564	Portugal	A	6,00	Y	Y
593	Portugal	D	NA	NA	NA
849	Portugal	A	4,63	Y	Y
850	Portugal	D	6,38	Y	Y
851	Portugal	D	4,13	Y	Y
853	Portugal	A	5,25	N	N
855	Portugal, Oeste	A	8,38	Y	Y
857	Portugal	A	4,63	V	Y
884	Portugal	D	7,50	V	Y
885	Portugal	D	1,67	N	N
904	Portugal, Oeste	D	3,25	N	N
905	Portugal, Oeste	D	4,50	V	Y
963^{T}	United Kingdom	A	4,95	Y	Y
1137	Ireland	A	4,50	V	V
1276	Ireland	A	5,75	V	V
1307	Portugal, Oeste	D	4,38	Y	Y
1310	Portugal, Oeste	D	5,88	V	Y
1311	Portugal, Oeste	A	NA	NA	NA
1312	Portugal, Oeste	A	NA	NA	NA

Supplementary Table 1 – Continued.

CPBF Isolate ID	Country, region	CRISPR genotype (A-272 bp; D-211 bp)	Pathogenicity and virulence evaluation		
			Lesion size (mm)	Presence of exudate 6 DAI	12 DAI
1313	Portugal, Oeste	D	3,75	N	N
1314	Portugal, Oeste	D	3,00	N	N
1315	Portugal, Oeste	D	4,50	Y	Y
1316	Portugal, Oeste	D	3,38	N	N
1317	Portugal, Oeste	D	5,50	N	N
1318	Portugal, Oeste	D	3,75	N	N
1319	Portugal	D	8,13	V	Y
1348	Portugal, Centro	D	5,25	N	N
1349	Portugal, Centro	A	4,25	Y	Y
1350	Portugal, Alentejo	A	4,38	V	Y
1351	Portugal	A	8,38	N	N
1352	Portugal, Alentejo	A	5,38	V	V
1380	Portugal, Alentejo	A	7,38	V	Y
1404	Portugal	A	9,13	Y	Y

CPBF = Colecção Portuguesa de Bactérias Fitopatogénicas, DAI = days after inoculation, Y = yes, N = no, V = variable, NA = not applicable.

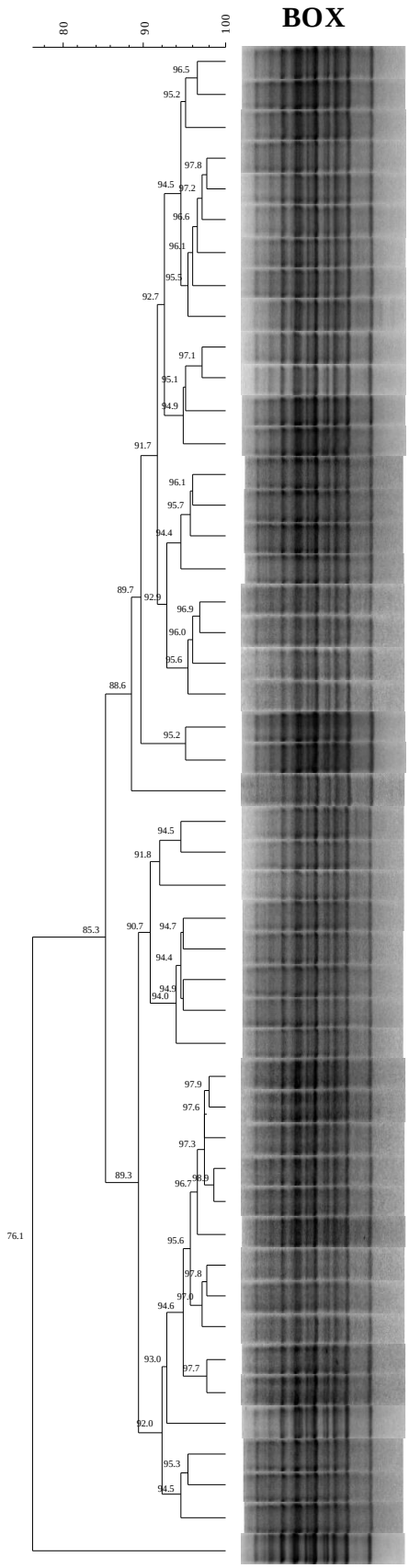

Isolate ID	Host	Year	Country
361	*Pyrus communis*	2011	Greece
364	*P. communis*	2011	Greece
373	*Crataegus* sp.	2011	Czech Republic
387	*Cotoneaster salicifolius*	2011	Ireland
412	*P. malus*		Poland
849		2017	Portugal
393	*C. salicifolius*	2011	Ireland
410	*Crataegus* sp.	2011	Poland
411	*Crataegus* sp.	2011	Poland
850		2017	Portugal
851		2017	Portugal
360	*P. communis*	2010	Cyprus
372	*P. communis*	2011	Greece
1318	*P. communis*	2010	Portugal
1319		2010	Portugal
1348	*Mallus domestica*	2011	Portugal
1317	*P.communis*	2010	Portugal
1312	*P. communis*	2010	Portugal
1313	*M. domestica*	2010	Portugal
1316	*P. communis*	2010	Portugal
1314	*P. communis*	2010	Portugal
365	*P. amydgaliformis*	2011	Greece
366	*P. communis*	2011	Greece
1315	*P. communis*	2010	Portugal
450	*Cotoneaster* sp.		Ireland
1137	*Sorbus* sp.		Ireland
1276	*Sorbus* sp.		Ireland
593	*P. communis*	2015	Portugal
1404		2014	Portugal
544		2015	Portugal
1380	*Cydonia oblonga*	2012	Portugal
564		2015	Portugal
884		2017	Portugal
885		2017	Portugal
963	*P. communis*	1959	United Kingdom
904	*P. communis*	2017	Portugal
905	*P. communis*	2017	Portugal
855		2017	Portugal
1307	*P. communis*	2010	Portugal
1310	*P. communis*	2010	Portugal
1311	*P. communis*	2010	Portugal
853		2017	Portugal
857		2017	Portugal
142	*Crataegus* sp.	2011	France
1351	*P. communis*	2011	Portugal
1352	*C. oblonga*	2011	Portugal
1349	*M. domestica*	2011	Portugal
1350	*M. domestica*	2011	Portugal

Supplementary Figure 1 - Dendrogram generated from BOX-PCR fingerprinting of the 48 *Erwinia amylovora* isolates. Genetic similarity between isolates was performed based on Pearson's correlation coefficient index and unweighted pair group method with arithmetic mean (UPGMA) clustering algorithm (ρ = 0.71). Empty cells, unknown information.

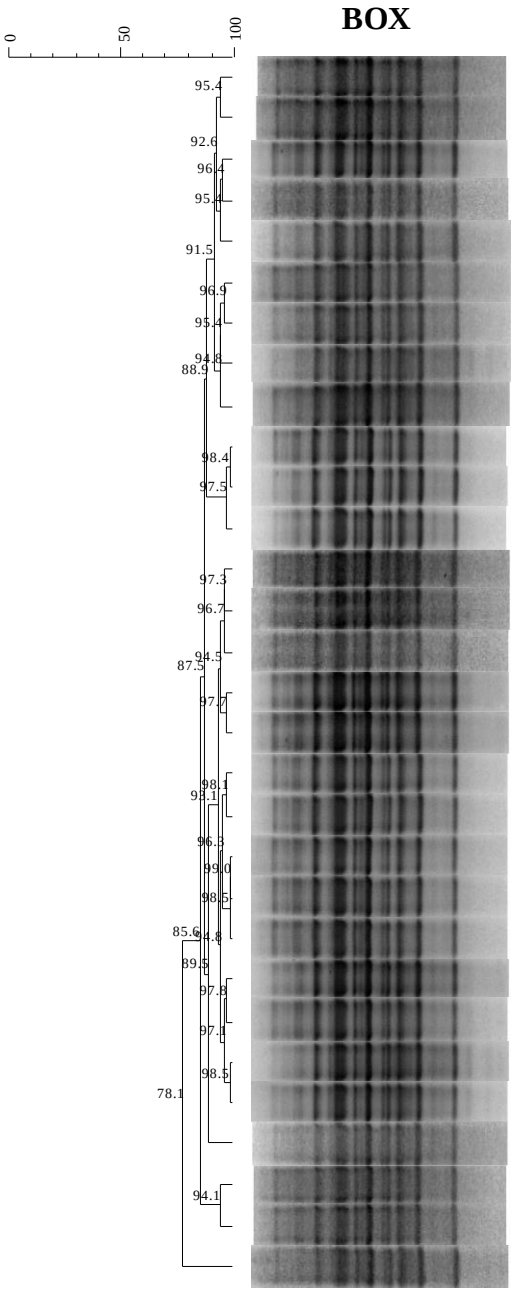

Isolate ID	Host	Year	Country
1318	*Pyrus communis*	2010	Portugal
1348	*Mallus domestica*	2011	Portugal
850 R		2017	Portugal
1311	*P. communis*	2010	Portugal
850		2017	Portugal
387	*Cotoneaster salicifolius*	1993	Ireland
393	*C. salicifolius*	2011	Ireland
411	*Crataegus* sp.	2011	Poland
361	*P. communis*	1984	Greece
564 R		2015	Portugal
1404 R		2014	Portugal
1276 R	*Sorbus* sp.	1993	Ireland
855		2017	Portugal
885		2017	Portugal
1307	*P. communis*	2010	Portugal
361 R	*P. communis*	1984	Greece
387 R	*C. salicifolius*	1993	Ireland
1318 R	*P. communis*	2010	Portugal
1348 R	*M. domestica*	2011	Portugal
1307 R	*P. communis*	2010	Portugal
1315 R	*P. communis*	2010	Portugal
1311 R	*P. communis*	2010	Portugal
393 R	*C. salicifolius*	2011	Ireland
855 R		2017	Portugal
411R	*Crataegus* sp.	2011	Poland
885 R		2017	Portugal
1276	*Sorbus* sp.	1993	Ireland
564		2015	Portugal
1404		2014	Portugal
1315	*P. communis*	2010	Portugal

Supplementary Figure 2 - Dendrogram generated from BOX-PCR fingerprinting of a set of the 48 *Erwinia amylovora* isolates and respective replicates. Genetic similarity between isolates was performed based on Pearson's correlation coefficient index and unweighted pair group method with arithmetic mean (UPGMA) clustering algorithm ($\rho = 0.71$). Empty cells, unknown information.

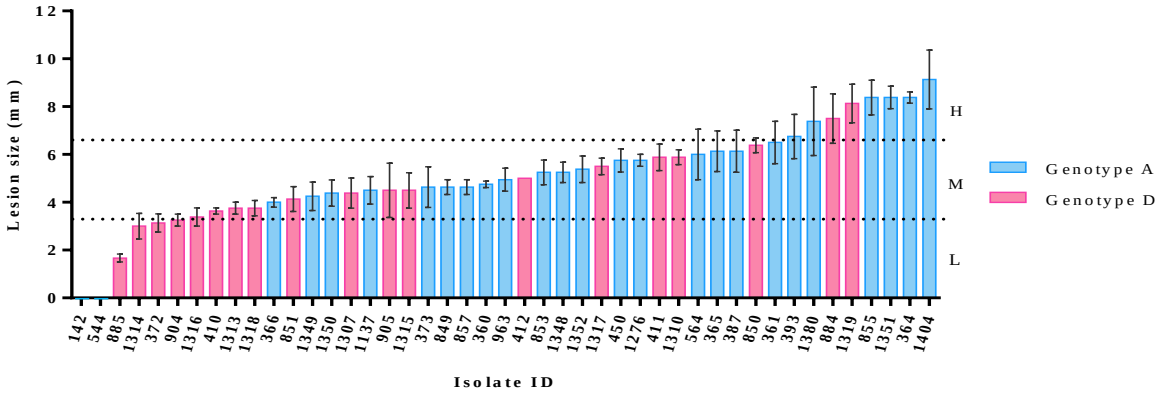

Supplementary Figure 3 - Virulence assessment ± SEM (standard error of the mean) 6 days after inoculation (DAI) of healthy fruitlets of *Pyrus communis* cv. "Rocha" inoculated with *Erwinia amylovora* isolates and their CRISPR-PCR genotype. The dotted lines define three virulence categories, namely low (L), medium (M) and high (H). Bar colour indicates CRISPR-PCR genotype profiles.

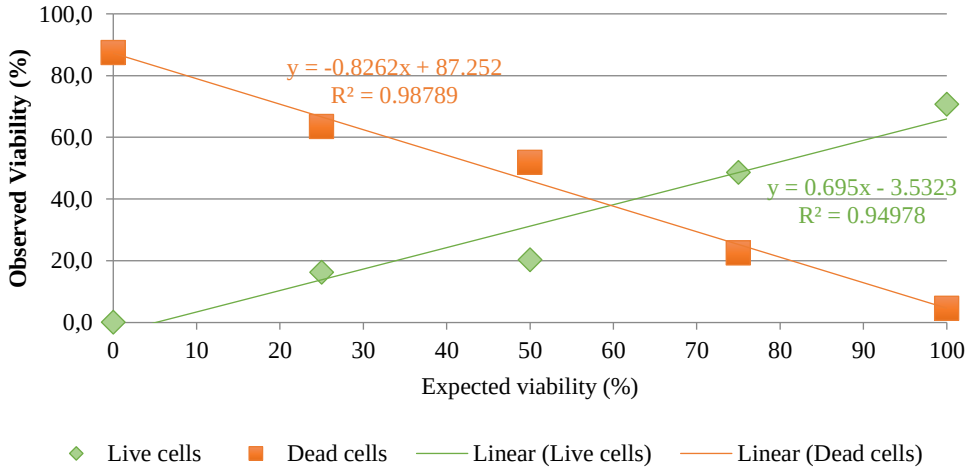

Supplementary Figure 4 - Correlation between the expected and observed viability (%) for Syto9 and PI for FL1 × FL3 dot-plot of *Erwinia amylovora* 885 determined by flow cytometry.